

CHALMERS



Clay Conductivity and Water Saturation Models

*Master's Thesis in the International Master's Programme Applied Environmental
Measurement Techniques*

SHAHZAD AHMED

Department of Civil and Environmental Engineering
Water Environment Technology

CHALMERS UNIVERSITY OF TECHNOLOGY

Göteborg, Sweden 2005

Master's Thesis 2005:67

MASTERS THESIS 2005:67

Clay Conductivity and Water Saturation Models

Shahzad Ahmed

Department of Civil and Environment Engineering
Water Environment Technology
CHALMERS UNIVERSITY OF TECHNOLOGY
Göteborg, Sweden 2005

Clay conductivity and water saturation models

© Shahzad Ahmed, 2005

Master's Thesis 2005:67

Department of Civil and Environment Engineering
Water Environment Technology
Chalmers University of Technology
SE-412 96 Göteborg
Sweden
Telephone +46(0)31-772 1000

Reproservice, Chalmers University of Technology, Göteborg, Sweden 2005

Clay Conductivity and water Saturation Models
SHAHZAD AHMED
Department of Civil and Environmental Engineering,
Institute of Environment & Resources,
Hydrocarbon and Mineral Resources,
Technical University of Denmark, DTU,
Chalmers University of Technology

ABSTRACT

Shales have great influence on the determination of fluid saturations. Clay in the shaly formation also conducts the electrical current in addition to formation water. Waxman and Smits saturation resistivity relationship related the conductivity of shale to CEC of clay. In absence of core CEC measurements, different models were proposed to account the effect of shale conductivity on total conductivity of formation and to predict effective water saturation. In this work CEC of cores samples (obtained from well # 03) was measured and water saturation results obtained by using Waxman and Smits saturation resistivity relationship were compared with water saturation results obtained from other water saturation methods. Water saturation predicted by Waxman and Smits equation is found to be higher than water saturation calculated by using Laminated Sand and Shale Model, Total Shale relation, Volan model, and Normalised Waxman and Smits equation, while lower than water saturation obtained by using Cyber Look program and Archie Model. Differences in water saturation results were attributed to differences in estimation of shale conductivity contribution to total formation conductivity by different water saturation methods.

Key words, water saturation, conductivity, porosity, log, shale, Cation Exchange Capacity (CEC)

ACOKNOWLEDGEMENT

This is a master thesis from Department of Environment and Resources, Technical University of Denmark worked out in the period of 14 Sep. 2003 to 29 May 2004. The project has been supervised by Ida Lyke Fabricius (DTU) and Greg Morrison (Chalmers).

First of all I would be thankful to almighty God who give me wealth of knowledge and make me able to know his miseries in universe.

Grate thanks to my supervisor "Ida Lyke Fabricius" who invited me as guest student in DTU. She is one of best teachers ever in my life. She created determination in my study approach. She always welcomed me, whenever, I knocked her door for seeking guideline about my project work.

Thanks to all my teachers at Chalmers University of Technology Gothenburg, Sweden who taught me. Special thanks to my Program Director "Mr Greg Morison" who allowed me to do project work at DTU (Copenhagen). Many thanks to Mr Sink, who showed his keen interests in completing my lab works. I am also thankful to Hector who cleaned core samples one and half month with patience. I am also thankful to my parents and all my family members who prayed for me and showed patience in bearing my absence from home.

Many thanks to Chief chemist "Abdul Wahid Butt" (O.G.D.L) and Deputy Chief Engineer "Abdur Rashid Wattoo" (O.G.D.L) who encouraged me to study in abroad.

I would like to say special thanks to my brother Amjad Ali (O.G.D.C.L) who always stood beside me and he is key behind my successes in studies. Thanks to my beloved Uzma who constantly encouraged me, during my whole Master studies. She always spared some time for me from her very busy daily life to give me moral support.

Many thanks to Mr Mushtaq for his kind help who trusted on me. My thanks to my class fellow Khalid for his all time help.

Thanks to Mr Ahmed Yar Cheema (DTU) and Adnan Qadir Chemma (DTU) who gave shelter in Copenhagen and for their moral support.

Many thanks to Mr Yousaf Cheema (DTU), who formatted my thesis report with his full devotion.

I am also thankful to Javed Bahtee (DTU) and Irfan Ahmed (Neil's Brock College) who gave me good company in Copenhagen.

In the end thanks to "**MAERSK OIL COMPANY**" for providing log data and core samples for project work.

Table of Contents

1. Introduction	1
1.1 Lithology in Shaly Sands	1
1.2 Lithology in Shale Model	1
1.3 Lithology in Clay Model	2
1.4 Porosity in Shaly Sands	4
1.5 Effective- Porosity from the Shale Model.	4
1.6 Effective-Porosity from Clay Model	5
1.7 Resistivity logging	5
1.8 Water Resistivity	5
1.9 Formation Factor and Porosity	6
1.10 Water Saturation	6
1.11 Water-Saturation Using Shale Model.	8
1.11.1 Laminated Sand-shale simplified Models	8
1.11.2 Dispersed Shale Simplified Model	8
1.11.3 Total Shale Relationship	10
1.12 Water-Saturation Using the Clay Model.	10
1.12.1 Waxman-Smits Model.	10
1.11.2 Dual Water Model	12
2. Material and Methods	17
2.1 Samples Preparation	17
2.2 Conductivity	17
2.3 Grain Density and Porosity	17
2.4 Specific Surface Area	17
2.5 X-Ray Diffraction	18
2.6 Cation Exchange Capacity	18
3. Characterisation of Chalk	19
3.1 x-Ray Diffraction	19
3.1.1 Impurities in Chalk Samples	19
3.2 Specific Surface Area	22
3.3 Cation Exchange Capacity	23
3.4 a, m, B Values	26
3.5 Formation Water R_w and R_{wb}	27
4. Comparison of Water Saturations between Waxman and Smits Saturation Resistivity Relationship and Different Water Saturation Models	28
4.1 Comparison of Water Saturations between Waxman and Smits Saturation Resistivity Relationship and Archie's Water Saturation Equation Model	28
4.2 Comparison of Water Saturations between Waxman and Smits Saturation Resistivity Relationship and Laminated Sand and Shale Model	30
4.3 Comparison of Water Saturations between Waxman and Smits Saturation Resistivity Relationship and Total Shale Relation	32

4.4	Comparison of Water Saturations between Waxman and Smits Saturation Resistivity Relationship and Volan Model	34
4.5	Comparison of Water Saturations Between Waxman and Smits Saturation Resistivity Relationship and Cyber Look Program	36
4.6	Comparison of Water Saturations between Waxman and Smits Saturation Resistivity Relationship and Normalised Waxman And Smits Saturation Equation	38
4.7	Comparison of Water Saturations Between Waxman and Smits Saturation Resistivity Relationship and Dispersed Shale Model	40
5	Inter Comparison of Water Saturation Results Obtained by each method in Well No 3A and 3 P	44
6	Conclusion	55
7	References	56

List of Appendices

A	X-ray Diffraction
B	BET of Chalk Samples
C	BET of IR OF Chalk Samples
D	CEC
E	Core conductivity and Porosity
F	Miscellaneous

1 INTRODUCTION

Physical properties such as density, porosity, resistivity, shale contents of subsurface formations varies with depth. The plots of these properties against depth are called well logs. Well Logs are run to obtain the information such as porosity, resistivity of rock formation in subsurface evaluation. Both porosity and resistivity measurements are used to compute water saturation, S_{wr} in rock formation. From water saturation measurements, quantity of hydrocarbon in formation is estimated. The resistivity and porosity parameters are measured with logging tools. It has been considered that hydrocarbon bearing formation rock have very low or zero conductivity. Conductivity of rock is only due to water present in clean sand formation. Archie proposed water saturation determination for clean water bearing sand formation. Presence of clay or shale increases the conductivity of rock formation and also affects the porosity readings. Therefore, the conductivity measurements obtained from logging data are higher than true resistivity due to extra conductivity caused by shale. The shale contents are usually estimated by gamma-ray log. Different water saturation models have been developed to account the extra conductivity caused by clay. The log derived porosity is corrected by calibrating with core porosity (1). Formations rock matrix consist of sand and shale. Shale can be distributed in the formation in three ways e.g. (i) Laminated shale (ii) Dispersed shale (iii) Structural shale. The way of shale distribution affects log measurement differently. In water saturation determination two approaches are used to model the shale in shaly formation. One is Shale Sand Model and other is Clay Sand Model.

1.1 Lithology in Shaly Sands

In shaly sands, the rock matrix is composed of shale and quartz. In shale model such lithology is described as shale and quartz. In the particular formation shale consists of clay, mica, feldspar, iron oxide and organics. In Clay Model formation rock matrix can be described as clay and sand (2). In clay models, sand comprises quartz, mica, and feldspar.

1.2 Lithology in Shale Model.

To evaluate shaly sand subsurface formation, it is necessary to know much quantity of shale is present in typical formation to estimate the true conductivity and porosity of formation from logging data. Three types of different logs like gamma-ray, spontaneous potential and sonic log can be use to measure the amount of shale (3,4). The gamma-ray log measures the natural radioactivity of formations. In sedimentary formation the log normally reflects the shale content of formations due to tendency of radioactive elements to concentrate in clays and shales. Uranium, Potassium and Thorium are the common radio active elements present in shale and clay. Clean formations exhibit very low radioactivity. Spontaneous Potential curve record the electrical potential (voltage) produced by the interaction of formation connate water, conductivity of drilling fluid and certain-ion-selective rock (shale). Above mentioned techniques use a common method to estimate the quantity of shale given below.

$$V_{sh} = \frac{(Log_{reading} - Log_{min_sh})}{(Log_{max_sh} - Log_{min_sh})} \quad (1)$$

Here, V_{sh} is the estimated shale volume, $Log_{reading}$ is reading of shale indicator log, e.g. gamma ray, spontaneous potential or sonic. Log_{max_sh} is the reading of shale indicator from 100 % log shale section and Log_{min_sh} is the reading of shale indicator across the clean quartz (0.0% shale) sections.

Density log can also be used to determine the amount of shale present in typical sand formation .The density log reading of a formation is the sum of densities of all formation constituents weighted in unit bulk volume of formation and is given by Equation(2)

$$\rho_b = \rho_w S_w + \rho_h \phi(1 - S_w) + \rho_{qtz} (1 - \phi - V_{sh}) + \rho_{sh} V_{sh} \quad (2)$$

Here, $\rho_b, \rho_w, \rho_h, \rho_{qtz}, \rho_{sh}$ corresponds to the formation bulk density, water density, hydrocarbon density, quartz density and shale density respectively. ϕ and S_w corresponds to formation porosity and water saturation respectively. Another method to quantify the shale is the neutron-density cross plot (5). In this method neutron and density logs are plotted on neutron-density cross plot. The clean sand points lie along the quartz sandstone and shaly points fall below that line towards a far point (shale point). Shale volume is estimated by dividing the distance of any point P from the quartz sand stone with distance of shaly point line S from the same line. Actually, these plots are made by assuming 100 % water. Since the density of oil is close to water, therefore these plots can be used with some approximation. Use of such cross plots is difficult if the gas or light hydrocarbons are present in the formation because the gas and light hydrocarbons have very low density as compared to water density. Points correspond to gas bearing section in the formation shift the data point above the quartz sandstone. It is very hard to get reliable results in presence of gas (5,6). Most of above mentioned techniques over estimate shale volume in formation. Gamma ray technique is convenient and practical but it can be inaccurate. Shale volume estimated by using gamma ray technique can be calibrated by shale volume obtained from experimental measurements on representative formation rock. Clay minerals present in shale can be determined by the X-ray Diffraction analysis of core samples. Cation exchange capacity of core sample is measured to determine actual amount of shale volume present in rock formation.

1.3 Lithology in Clay Model

Clay Model describes formation lithology in term of sand and clay. The clay comprises all the clay minerals, e.g. illite, montmorillonite, chlorite, kaolinite, which may present in the formation. Abundance of clay can be estimated by using Elemental Capture Spectroscopy log (7). Most of oil companies avoid (ECS) technique because it is very expensive. X-ray diffraction technique determines the types of clay minerals present in rock formation. Clay abundance obtained from experimental measurement on representative formation rock can be used to calibrate clay abundance estimated from clay indicator logging data. Above described techniques measure the clay abundance as

weight-percent of formation rock matrix, $W_{dry-clay}$, which is then latter transferred in to volume-percent of formation bulk volume using following Equation-3.

$$Vol_{dry-clay} = \frac{W_{dry-clay} \rho_{matrix} (1 - \phi_{total})}{\rho_{dry-clay}} \quad (3)$$

Here, ϕ_{total} is the formation total porosity. $\rho_{dry-clay}$ is the dry clay density, which can be determined by XRD analysis of core samples. ρ_{matrix} is the shaly sand matrix porosity and can be obtained from representative core analysis measurements. $Vol_{dry-clay}$ is clay abundance as volume percentage of shaly sand bulk volume. Also there are some other techniques developed for the estimation of clay volume but those are not accurate (8). In clay model to calculate sand volume in shaly sands both pore volume and shale are excluded.

Clay minerals have the property to bind the formation water. The water bound to clay minerals is known as clay-bound water. The volume of clay bound water can be estimated form following Equation-4 & Equation-5 (9,10,11).

$$Vol_{clay-bound-water} = V_Q Q_v \phi_{total} \quad (4)$$

$$Vol_{clay-bound-water} = V_Q * CEC * \rho_{dry-clay} * Vol_{dry-clay} \quad (5)$$

Here, ϕ_{total} is the formation total porosity. Q_v in Equation -4 is the clay cation-exchange-capacity in milliequivalent per unit volume of pore fluids. Q_v can be determined by experimental measurement on representative core samples and brine sloution. V_Q is the amount clay-bound water bind with one milliequivalent of clay counter ions. $Vol_{dry-clay}$ is the volume of dry clay. $\rho_{dry-clay}$ is the dry-clay density. In Equation-5, CEC is the clay Cation Exchange-Capacity in milli equivalents per unit mass of dry clay. There are different methods for the determination of CEC of core samples (12, 13). CEC can also be determined, if we know about dominant clay mineral abundance in typical formation (2). $Vol_{clay-bound-water}$ is the volume of clay bound water per unit bulk volume of formation.

The clay bound water saturation in the pores S_{cbw} can be obtained using the Equation-6.

$$S_{cbw} = Vol_{clay-bound-water} / \phi_{total} \quad (6)$$

Clay- bound-water affects the porosity and resistivity reading of logging tools. It is necessary to estimate all these effect in order to improve accuracy of calculated effective-porosity and water-saturation in shaly sands evaluation. For this, it is necessary to have knowledge of clay minerals abundance in formation for the estimation of clay bound water on logging tools. Therefore, estimating dry-clay volume is essential to measure the accurate effective porosity and water saturation in shaly sands.

1.4 Porosity in Shaly Sands

Density tools, neutron porosity and sonic log tools (14, 15) can be used to measure the total porosity in shaly sands. The density tools respond to electron density of formations which is then correlated to bulk density, ρ_b : as given in Equation-7

$$\rho_e = \rho_b \left(\frac{2Z}{A} \right) \quad (7)$$

Here, ρ_e is the electron density, ρ_b is the bulk density, Z is the atomic number and A is the atomic weight. Equation-8 is used to calculate the porosity from bulk density ρ_b .

$$\rho_b = \phi \rho_f + (1 - \phi) \rho_{ma} \quad (8)$$

Here, ρ_f is density of mud filtrate and ρ_{ma} is matrix density of clean sand.

Neutron porosity tools respond primarily to the amount of hydrogen present in formation. Since the oil and water contain practically the same amount of hydrogen per unit volume, the responses reflect the liquid filled porosity in clean formations. The sonic log simply records time, ζ , required for a sound wave to travel 1 ft of formation, known as interval transit time, Δt or slowness, ζ , is the reciprocal of sound wave speed. The interval transient time is characteristics of formation and depends upon its lithology and porosity. Following equation-9 can be used to obtain the porosity from sonic log.

$$\Delta t_{\log} = \phi \Delta t_f + (1 - \phi) \Delta t_{ma} \quad (9)$$

Here, Δt_{\log} is the reading on sonic log in μ , Δt_{ma} is transient time of matrix material and Δt_f is transient time of saturating fluid. Shale model, clay model can be used to obtain effective porosity.

1.5 Effective- Porosity from the Shale Model.

Effective porosity, $\phi_{effective}$, is the pore-space in the formation that is neither in the shale nor in the clay. The effective pore spaces contain hydrocarbon and non-clay water. Non-clay water is the formation-water that is neither bound to clay nor to shale. In the absence of light hydrocarbons effects on tool, porosity can be approximated as given in equation-10;

$$\phi_{total} = \phi_{effective} + \phi_{sh} V_{sh} \quad (10)$$

Here, ϕ_{sh} is the shale porosity, relative to shale volume. V_{sh} is the shale volume relative to formation bulk volume. Estimation of ϕ_{sh} is very difficult, therefore it is usually approximated by ϕ_{total} and above eq-10 acquire the following form

$$\phi_{total} = \phi_{effective} + \phi_{total} V_{sh} \quad (10-a)$$

Shale porosity is estimated from 100 % shale section but it can not be correct due to following reasons. First, the selection of a 100 % shale section can be wrong. Second, measurement of porosity tools can be wrong due to presence of hydrocarbon in that

section. Third, 100 % shale may not exist in the whole shaly sand interval to be evaluated. Fourth, the selection of 100 % shaly sand interval may vary from one log analyst to another. Due to above mentioned reasons effective porosity obtained from the above equation is not accurate.

Similarly effective porosity obtained from the equation-10-a is also inaccurate, since the approximation of shale-porosity by total porosity is inaccurate most of time.

1.6 Effective-Porosity from Clay Model

The term $\phi_{sh} V_{sh}$ in equation-10-a is equivalent to the volume of clay-bound water (8). Therefore total porosity can be described as in term of effective porosity and clay bound water.

$$\phi_{total} = \phi_{effective} + Vol_{clay-bound-water} \quad (10-b)$$

$\phi_{effective}$ is the formation effective porosity, which represents the pore-space that contain the formation fluid that are not bound to clay or shale.

1.7 Resistivity logging

The electrical resistivity of formation rock can be described as its ability to impede the flow of electrical current through the formation. Evaluating a reservoir for its water and hydrocarbon saturation involves the saturation formation water resistivity, R_w ; the formation factor F , or porosity, Φ ; and true formation resistivity R_t . To determine the R_t different induction log or Dual lateral logs are run (16, 17).

1.8 Water Resistivity

Formation water resistivity, R_w , can be found from SP (Spontaneous Potential) curve, water catalogs, produced water samples or water saturation curves from 100 % water bearing formations(18,19,20,21). In clean formation, from SP curve response, R_w can be calculated by using Equation-11

$$SP = -K \text{Log} \frac{R_{mf}}{R_w} \quad (11)$$

Where K is temperature dependent coefficient and its is

$$K = 65 + 0.24 T_{0C} \text{ dependent coefficient}$$

R_w can also be derived from Resistivity-Porosity Logs

$$R_{wa} = \frac{R_t}{F} \quad (12)$$

Here, R_{wa} is apparent water resistivity.

For clean water bearing zones, $R_t = R_0$. Here, $R_0 = F R_w$ and R_{wa} value derived from Equation-12 is equal to R_w in 100 water bearing section.

This technique work best over intervals in which the formation remains constant or changes only gradually.

1.9 Formation Factor and Porosity

Experimentally it is proved that the resistivity of clean, water bearing formation (i.e., one containing no appreciable amount of clay and no hydrocarbons) is proportional to the resistivity of brine with which it is fully saturated. The constant of proportionality is called formation factor, F (36). Thus if R_0 is resistivity of non shaly formation rock 100 % saturated with brine of resistivity R_w , then formation factor F can be calculated by Equation-13.

$$F = R_0 / R_w \quad (13)$$

For given saturating brine water, the greater the porosity of formation, the lower the resistivity R_0 of the formation, and the lower the formation factor F . Therefore, formation factor is inversely related to porosity. F is also function of pore structure and pore size distribution.

Archie proposed (22), based on observations, a formula relating porosity, ϕ , and formation factor, F ; the relation ship is

$$F = a / \phi^m \quad (14)$$

Here, m is the cementation factor or exponent. The cementation exponent and constant a can be determined empirically. The value of a depends upon porosity and for sand stone is 0.62.

1.10 Water Saturation

In formation containing hydrocarbon, the resistivity is a function not of only F and R_w but also S_w . Here, S_w is the fraction of pore volume occupied by formation water and $(1-S_w)$ is the fraction of pore volume occupied by hydrocarbon.

Archie determined (23) experimentally (that water saturation of clean formation can be expressed in term of true resistivity as

$$S_w^n = FR_w / R_t \quad (15)$$

Here, n is saturation exponent.

Archie water saturation equation was developed for clean, non shaly rocks. Archie's Equation can be expressed in term of conductivity, which is the reciprocal of resistivity.

$$C_t = \phi_{total}^m \cdot S_w^n \{C_w\} \quad (15-a)$$

Here, C_t is the formation conductivity which can be obtained from deep resistivity log. C_w is the formation water conductivity. ϕ_{total} is the formation total porosity. The cementation exponent m and saturation exponent n can be determined by experimental measurements on representative formation rock and fluid.

The Electrical Parameters m and n in Archie's Model.

m and n parameters of representative formation rock (core plug) and fluid for Archie's equation are measured experimentally. For this purposes the representative formation rock (core plug) and fluid brine is needed. First total porosity of each core plug is measured. Second, the plugs are saturated to 100 % with formation-brine ($S_{wt}=1.0$) having high resistivity (R_w). The reciprocal of R_w is C_w , which is the conductivity of formation. Third, the true R_t resistivity, of each fully-saturated plug is measured. The true resistivity of 100 % brine saturation is known as R_0 . The reciprocal of R_0 is C_0 , which is true conductivity of a core plug at 100 % brine saturation. For fully-saturated rock ($S_{wt}=1.00$), Archie equation reduces to Equation-15-b

$$C_w / C_0 = R_0 / R_w = \phi_{total}^{-m} \quad (15-b)$$

The formation resistivity factor (R_t / R_0) of each plug is cross-plotted, on logarithmic scale, against total porosity (ϕ_{total}) of same plug. According to Equation (15-b), the negative of slope of cross plot is m . To obtain the value of n each fully saturated core plug is de-and at each step S_w and R_t are measured at each step. According to Equation-15-a the de-saturation plug satisfy the following equation

$$C_0 / C_t = R_t / R_0 = S_w^{-n} \quad (15-c)$$

Formation resistivity Index (R_t / R_0) of each plug at every de-saturation step is cross plotted on logarithmic scale, against the water saturation of same plug at the same de-saturated step. According to equation 12 negative of slope is the vale of n .

Archie's developed the saturation for clean sands, therefore it does not account the excessive conductivity caused by presence of clay in shaly sands. Hence, water saturation obtained using Archie's equation for shaly sand is over estimated than actual water saturation of formation.

There are several water saturation equations have been developed to account the extra conductivity due to presence of clay in shaly sand formations (10,12,24,31,33,35,37, 40) In such equations to account the effect of extra conductivity, caused by clay, in shaly sand C_w in Archie's equation is replaced by C_{we} . Those equations express effective conductivity C_{we} in term of C_w and function of shale or function of clay. They modify Archie equation to one of following forms;

$$C_t = \phi_{total}^{m^v} S_{wt}^{n^v} \{C_{we}\} \quad 16$$

$$C_t = \phi_{total}^{m^v} S_{wt}^{n^v} \{C_w + X\} \quad 16-a$$

Here, X is function that is needed to account for the conductivity caused by shale or clay present in shaly sands. The parameters m^v and n^v are general forms of electrical

properties and they reduces to Archie's m and n when function X becomes zero in equation 16-a.

1.11 Water-Saturation Using Shale Model.

In shale model, the function X in Equation-16-a is expressed in term of shale attributes, e.g. shale-volume (V_{sh}) and shale conductivity (C_{sh}). In shaly sand method using this technique (12, 25) develop Equation-16-a with the function, $X = f(V_{sh}, C_{sh})$. Water saturation, S_{wt} , obtained using Equation-16a is accurate if input quantities $C_t, C_w, \phi_{total}, m^v, n^v$ and $f(V_{sh}, C_{sh}, \dots)$ are accurately measured. Laminar Sand-shale simplified model and Dispersed Shale simplified Models were developed on sand shale model concepts.

1.11.1 Laminated Sand-shale simplified Models

In, this model, a saturation equation was suggested for laminated shaly sand with ϕ and S_w for clean-sand streaks: In laminar shale model, R_t , the resistivity in the direction of bedding plane, is related to R_{sh} (the resistivity of shale laminae) and to R_{sd} (the resistivity of clean sand laminae) by parallel resistivity relationship,

$$1/R_t = \frac{1 - V_{lam}}{R_{sd}} + \frac{V_{lam}}{R_{sh}} \quad (17)$$

Here, V_{lam} is the bulk volume fraction of shale, distributed in laminae, each of more or less uniform thickness.

For clean-sand laminae, $R_{sd} = F_{sd} R_w / S^2$, where F_{sd} is the formation resistivity factor of clean sand. Since $F_{sd} = a / \Phi^2_{sd}$ (where ϕ_{sd} is the sand-streak porosity) and $\phi = (1 - V_{lam}) \phi_{sd}$ (where ϕ is bulk formation porosity), then

$$1/R_t = \frac{\phi^2 S_w^2}{(1 - V_{lam}) a R_w} + \frac{V_{lam}}{R_{sh}} \quad (18)$$

Water saturation, S_w , can be obtained by the accurate determination of input $R_t, R_w, \phi, V_{lam}, R_{sh}$. R_t is obtained from deep resistivity log data of rock formation. Methods for determination of R_w, ϕ and V_{lam} have already been discussed.

1.11.2 Dispersed Shale Simplified Model

This model was developed to account the extra conductivity causes by shale when shale is distributed in shaly sand in dispersed manner. In this model L.De Witte suggested that

formation conducts electrical current through network composed of pore water and dispersed clay. He developed water saturation Equation-19 on the basis of his assumption.

$$1/R_t = \frac{\phi_{im}^2 S_{im}}{a} \left(\frac{q}{R_{sh}} + \frac{S_{im} - q}{R_w} \right) \quad (19)$$

Here, ϕ_{im} is inter matrix porosity, which includes all the spaces occupied by fluids and dispersed shale

S_{im} is the fraction of inter matrix porosity occupied by the formation water, dispersed shale mixture,

q is the fraction of inter matrix porosity occupied by dispersed shale,

And

R_{shd} is the resistivity of dispersed shale.

Also, it can be shown that

$$S_w = S_{im} - q / (1 - q) \quad (20)$$

Here, S_w is the water saturation in the fraction of true effective formation porosity.

Combining equation-19 & 20 and solving for S_w yields equation-21

$$S_w = \frac{\sqrt{\frac{aR_w}{\phi_{im}^2}} + \sqrt{\left[\frac{q(R_{shd} - R_w)}{2R_{shd}} \right]^2} - \frac{q(R_{shd} + R_w)}{2R_{shd}}}{1 - q} \quad (21)$$

ϕ_{im} can be obtained directly from sonic log since dispersed clay in the rock pores is seen as water by sonic measurement. The value of q can be obtained from a comparison of sonic and density log. Indeed, if $\rho_{shd} = \rho_{ma}$, then $q_{sv} = (\phi_{sv} - \phi_d) / \phi_{sv}$, where ϕ_{sv} and ϕ_d are the sonic and density derived porosities, respectively. The value of R_{shd} is more difficult to evaluate and it is taken as equal to R_{sh} from nearby shale beds. When R_w is small compared to R_{shd} and sand is not too shaly, Equation reduces to simplified form 21-a.

$$S_w = \frac{\sqrt{\frac{aR_w}{\phi_{im}^2 R_t}} + \sqrt{\frac{q}{4}} - \frac{q_w}{2}}{1 - q} \quad (21-a)$$

1.11.3 Total Shale Relationship

On the basis of shale model concept, Lab investigation and field experience, a more practicable Equation-28 for water saturation determination was developed, which is independent shale distribution in shaly sand

$$1/R_t = \frac{\phi^2 S_w^2}{(1-V_{sh})aR_w} + \frac{V_{sh}S_w}{R_{sh}} \quad (22)$$

Here, R_{sh} is taken equal to resistivity of adjacent shale beds and V_{sh} is shale fraction as obtained from total shale indicator.

1.12 Water-Saturation Using the Clay Model.

When the clay model is used, the function X in Equation-16-a is expressed in terms of clay parameters, e.g. clay-bound water (V_{cbw}), clay-volume (V_{cl}) and clay-conductivity (C_{sh}). Accurate S_{wt} can be obtained by making use of Clay Model if input quantities, $C_t, C_w, \phi_{total}, m^v, n^v$ and $\xi(V_{cl}, V_{cbw}, C_{cbw} \dots)$ are accurate. Methods for determining the accurate value for $C_t, C_w, \phi_{total}, m^v, n^v$ have already been discussed. Accuracy of functional expression $\xi(V_{cl}, V_{cbw}, C_{cbw} \dots)$ depends how much accurately extra conductivity caused by clay is fit in the model and accuracy of input quantities in this function, e.g. V_{cl}, V_{cbw} and C_{cbw} .

1.12.1 Waxman-Smits Model. Clay-Model concept was used by Waxman-Smits to account the extra conductivity caused by presence of clay in sand. In Waxman-Smits water saturation determination equation-22, the extra conductivity, $\xi(V_{cl}, V_{cbw}, C_{cbw} \dots)$, is expressed as BQ_v / S_{wt} .

$$C_t = \phi_{total}^{m^0} S_{wt}^{n^0} \left\{ C_w + \frac{BQ_v}{S_{wt}} \right\} \quad (22)$$

Here, Q_v is the clay cation-exchange-capacity in milli equivalent per unit pore volume, meq/cc . B is the specific conductivity of exchangeable cations, which is measured in mohm/m per meq/cc. m^0 and n^0 are electrical parameters for Waxman-Smits equation. The clay- cation-exchange capacity, Q_v , can be obtained by experimental measurements on representative core samples and fluids. Q_v can be determined from the following equation-30 if CEC measurements are available (13).

$$Q_v = \rho_{dry-clay} Vol_{dry-clay} CEC / \phi_{total} \quad (23)$$

CEC method is used for measuring Q_v from core. In this method, CEC is determined by grinding the representative rock formation core samples in to fine powder. To determine the Potassium, Calcium and Magnesium ions present on core surface sample are saturated with sodium chloride solution, Na^+ ions displaces exchangeable cations K^+ , Ca^{2+} and Mg^{2+} from clay surface sites. Exchangeable Na^+ cations are measure by saturating the sample with ammonium chloride solution. Afterwards, amount of cation-exchange ions concentration is measure using Atomic Absorption Spectrometer. In this way CEC is calculated and hence, Q_v is obtained. Titration method can also be used to measure amount of exchangeable cations.

Q_v can also be determined by using the membrane potential method. In this method potential is created across liquids, having two sodium-chloride brine of different morality, with core sample acting as a membrane (26). Then generated potential difference is related to Q_v .

Q_v from representative core plugs can also be determined by Multiple- salinity method (27,28, 38). In this method core plug is fully saturated with brine (Sw= 1.0) and the Waxman-Smith equation-22 reduces to following equation

$$C_0 / C_w = \phi m_{total} [1 + BQ_v / C_w] \quad (22-a)$$

The basic salinity is changed stepwise. At each step both C_0 and C_w are measured. C_0 is cross plotted against C_w , the intercept of slope with the axis is the negative of BQ_v . Dividing BQ_v with B gives the Q_v can be obtained.

Counter ion Equivalent Conductance, B , depends on salinity and temperature (27) as shown in Equation-24.

$$(24) \quad B = B_{max} \left[1 + ae^{\left(\frac{C_w}{\gamma} \right)} \right] \quad (24)$$

Where, B_{max} , a , and γ are temperature dependent constant. This expression is only valid for sodium ion and can not be used for the formation water containing the significant quantity of divalent cation, i.e. calcium. In case of calcium abundance, B , can be obtained by dividing BQ_v with Q_v .

The electrical parameters m^* and n^* in the Waxman-Smiths model can be obtained for a core by saturating the core with 100% brine (equal to the formation water salinity) and measuring C_0, C_w, ϕ_{total} and BQ_v . After this, Brine salinity (C_w), is changed in incremental steps at which C_w and C_0 are measured. Then C_0 and C_w are cross plotted. According to equation-18 the slope of the straight line section is equal to $((\phi_{total})^{m^*})$. Cementation exponent, m^* , can be obtained by using measured core porosity values (ϕ_{total}) value. To measure n^* C_w is kept at constant value equal to original formation

conductivity and S_{wt} is changed from 100 % to lower values in incremental steps at which S_{wt} and C_t are obtained for the same core.

Now, all the core quantities required for Waxman-Smiths equations are known except n^* Equation-22b- can be used to determine n^* value

$$\frac{C_0}{C_t} \left[1 + \frac{BQ_v}{C_w S_{wt}} \right] = S_{wt}^{-n} \left[1 + \frac{BQ_v}{C_w} \right] \quad (22-b)$$

Second method to obtain m^* and n^* values is to make the use of experimentally measured Archie's m and n . Comparison of two Archie's and Waxman-Smiths model leads to Equation-25 which relates m^* to m and other factors of formation obtained formation evaluation analysis.

$$\phi_{total} \left[1 + \frac{BQ_v}{C_w} \right] = \phi_{total}^{-m} \quad (25)$$

Similarly, value of n^* can be obtained by comparing Archie and Waxman-Smiths model in another way.

$$S_{wt}^{-n} \left[1 + \frac{BQ_v}{C_w S_{wt}} \right] = S_{wt}^{-n} \left[1 + \frac{BQ_v}{C_w} \right] \quad (25-a)$$

In Waxman-Smiths equation it is assumed that conductivity of formation water and conductivity of clay cations, BQ_v / S_{wt} work independently in pore spaces of reservoir rock. The Waxman-Smiths equation takes in to account formation water conductivity and clay conductivity separately. The Waxman-Smiths equation models the formation, C_{we} , conductivity by $\{C_w + BQ_v / S_{wt}\}$. This means that conductivity of formation remains constant, and true conductivity increases with formation shaliness, BQ_v / S_{wt} (2). In those days it was difficult to measure the CEC at situ, therefore, Dual-Water model was developed (9, 10).

1.11.2 Dual Water Model

The dual water models were developed as practical solution of Waxman-Smiths saturation relationship. The dual water is based on three premises. (i) The conductivity of clay is due to its CEC. (ii) The CEC of pure clay is proportional to the specific surface area of clay. (iii) In saline solutions, the anions are excluded from a layer of water around the surface of grain.

In Dual Water Model, clay is model as consisting of two components bound water and clay minerals. The clay minerals are models as being as electrical inert; the clay electrical conductivity is modelled as being derived form, C_{wb} , the conductivity of bound water,.

The amount of bound water varies according to clay type, being higher for finer clays (with higher specific surface area), such as montmorillonite, and lower coarse clays, such as kaolinite.

The dual water model express the effective conductivity, C_{ew} , as a

$$[C_{wf}(S_{wf}/S_{wt}) + C_{cbw}(S_{cbw}/S_{wt})]$$

Dual water model equation can be written in one of two forms as expressed in Equation-26-a & 26-b

$$C_t = \phi_{total}^{m^0} S_{wt}^{n^0} \left\{ C_{wf} \frac{S_{wf}}{S_{wt}} + C_{cbw} \frac{S_{cbw}}{S_{wt}} \right\} \quad (26-a)$$

$$C_t = \phi_{total}^{m^0} S_{wt}^{n^0} \left\{ C_{wf} + S_{cbw} \frac{(C_{cbw} - C_{wf})}{S_{wt}} \right\} \quad (26-b)$$

Here, S_{wf} is the formation water saturation (not clay bound water). S_{cbw} is the clay bound water saturation. S_{wt} is total water saturation, i.e. $S_{wt} = S_{wf} + S_{cbw}$. The conductivity of free water is C_{wf} . The conductivity of clay bound water is C_{cbw} and it is obtained according to dual water model theory (9,10).

To obtain accurate water saturation using dual water models require accurate in put quantities $C_t, C_{wf}, C_{cbw}, S_{cbw}, \phi_{total}, m^0$ and n^0 . Accurate value of C_t can be directly taken from deep resistivity log. C_{wf} can be obtained experimentally from representative formation water samples. The clay bound conductivity, C_{cbw} , can be obtained according to Dual Water Model theory from clay portion of deep resistivity log (9,10). The S_{cbw} can be obtained from following equation $S_{cbw} = Vol_{clay-bound-water} / \phi_{total}$. The method for obtaining accurate value of ϕ_{total} is already described.

The Electrical Parameters in Dual-Water Model can be obtained for a core by experimentally measuring $C_t, C_{wf}, C_{cbw}, S_{cbw}, \phi_{total}$ of core. The value of m^0 can be obtained by keeping the constant water saturation $S_{wt} = 1.0$ and the water salinity, hence C_{wf} , equal to salinity of formation water. C_t at $S_{wt} = 1.0$ is measured which is also called C_0 (the conductivity of rock saturated with 100 % water). Afterwards, C_{wf} is changed in increments at which C_{wf} and C_t are measured. After getting suitable data set of C_{wf} and C_t by this way, the following dual water equation-26c can be used to obtain m^0 .

$$\frac{C_0}{C_{fw}} = \phi_{total}^{m^0} \left[1 + S_{cw} \left(\frac{C_{cbw}}{C_{wf}} - 1 \right) \right] \quad (26-c)$$

In case of n^0 determination C_{wf} is kept constant at value equal original formation water conductivity and S_{wt} is changed from 100 % to lower values step wise and at each step

C_t is measured. Following form of Dual water model Equation 36-d can be used to determine the value of n^o .

$$\frac{C_0 \left[C_{wf} + \frac{S_{cbw}}{S_{wt}} (C_{cbw} - C_{fw}) \right]}{C_t (C_{fw} + S_{cbw} (C_{cbw} - C_{fw}))} = S_{wt}^{-n} \quad (26-d)$$

Experimental measured Archie's m and n value can also be used by establishing relation between Archie and Dual water model. Following relation-26e works well to obtain value m^o .

$$\phi_{total}^{-m} \left[1 + S_{cbw} \left(\frac{C_{cbw}}{C_{fw}} - 1 \right) \right] = \phi_{total}^{-m^o} \quad (36e)$$

Another relation between two modes can be used to obtain the value of n^o

$$S_{wt} \frac{\left[C_{fw} + \frac{S_{cbw}}{S_{wt}} (C_{cbw} - C_{fw}) \right]}{\left[C_{fw} + S_{cbw} (C_{cbw} - C_{fw}) \right]} = S_{wt}^{-n^o} \quad (26 f)$$

Another method is to value of m^o and n^o make the approximation of dual water model m^o with experimentally measure Archie's m and Dual-Water n^o by Archie's n . After solving the Dual –Water equation for S_{wt} , non clay water saturation can be found by following Equation-27.

$$S_{wf} = S_{wt} - S_{cbw} \quad (27)$$

The non clay water saturation, S_{wf} , is the volume of non-clay water relative to total pore volume. Effective water saturation can be obtained by using the following equation-28.

$$S_{w_{effective}} = S_{wf} \left(\frac{\phi_{total}}{\phi_{effective}} \right) \quad (28)$$

After simplification of Equation-28 we get the following equation 28-a for effective water saturation determination.

$$S_{w_{effective}} = \frac{S_{wf}}{(1 - S_{cbw})} \quad (28-a)$$

There are different computer based programs (8,29,30,35) available for computation of water saturation by making the use of traditional model. The optimum in put values is used obtained from logging tools.

Volan model (8) is computer based application of dual water Model to determine the accurate water saturation of S_{wt} in shaly sand formations. The Volan Model makes the use of following dual water model equation.

$$C_{wa} = C_t F$$

$$C_{wa} = S_w^2 \left[C_w + \left(\frac{S_{wb}}{S_{wt}} \right) (C_{wb} - C_w) \right] \quad (26g)$$

Here, C_{wa} is the apparent conductivity of formation. C_t is measure conductivity of non invaded formation. F is formation factor corresponding to ϕ_{total} .

The Cyber look program(28) is computer-assisted well site interpretation method and use the dual water model to account for the effects of clay fraction, lithology, and hydrocarbon for the determination of reservoir parameters. The following form of Dual-water-model equation-26h is used in cyber Look program.

$$C_0 = \phi_t^2 [S_{wb} C_{wb} + (1 - S_{wb}) C_w] \quad (26h)$$

Juhasz (29) suggested Normalized Waxman-Smits equation in absence of core data measurement..

$$C_t = C_w \phi^m S_w^n + (C_{sh} \phi_m^{sh} - C_w) (V_{sh} \phi_{sh} S_w / \phi) \quad (27)$$

Aim of study

- 1) To measure water saturation, using Waxman and Smits equation by performing CEC measurements on core samples.
- 2) Comparison of Waxman and Smits water saturation results with water saturation results obtained by using different water saturation models i.e., Archie's Model, Laminated Sand and Shale Model, Total Shale Relation, Dispersed Shale Simplified Model, Volan Model, Cyber Look Program, and Normalized Waxman and Smits water saturation equation to know how much difference is in water saturation results between Waxman and Smits water saturation and each above mentioned model water saturation.
- 3) To identify the causes of water saturation differences between “Waxman and Smits saturation resistivity relationship” and other used models for water saturation determination.
- 4) Inter comparison of water saturation results between deviated drilled well # 03 A (Valdimar field) and vertical drilled well # 03 P (Valdimar field) obtained by each method by relating their formation bedding plains through comparing their R_t values.

- 5) Comparison of Waxman and Smits water saturation results obtained by using our lab CEC results and Core Lab (UK) CEC results.

For this work a through characterization of samples was necessary. Characterization include the determination of specific surface area, cations exchange capacity, X ray diffraction, conductivity, grain density and porosity.

2 MATERIAL AND METHODS

Ten core samples were collected at following depths 9238fts, 9242fs, 9251fts, 9252fts, 9254fts, to 9329fts, 9351fts, 9356fts, 9368fts, 9370 fts of well # 03A from, Danish Vladimir field located in North Sea, were provided by MASEK OIL COMPANY. Company also provided log data of wells #3A and #3 P and chemical data of well #3A

2.1 SAMPLES PREPARATION

The objective of cleaning the samples is to remove chloride and oil for sample matrix. Samples were cleaned in multiple extraction assembly apparatus similar to Soxhlet extractor, which works on batch extraction principal. In batch extraction all of the extracting solvent is added to sample at the beginning of extraction and it is used in case where mass transport through matrix is rate-limiting step. In extractors, the samples were placed in extraction thimble made of glass. 300 to 400 ml methanol solvent is placed in round bottom flasks and heating the solvent in round bottom flasks start extraction. Hot methanol vapors are condensed in condenser and fall down in thimble where they remain in contact with sample and dissolved the fraction of chloride in it from sample matrix. With the passage of time the more and more solvent is added, and the level of solvent rises in the thimble, as it reaches to top, organic solvent is fall down in to bottom flak. Equilibrium is established between the evaporation and condensation processes. Occasionally, presence of chloride in methanol of thimble is checked with silver nitrate the extraction is carried out (3 to 4 week) until it is make sure that there no more chloride left on the sample matrix. To remove the oil from samples same procedure is repeated with toluene. The presences of emulsion in toluene solvent in thimble show presence of oil in sample. The extraction is carried out (1-2) week until there is no sing of emulsion left. Compact samples take more time for cleaning.

Following methods were used in connection with the characterization of chalk samples

2.2 CONDUCTIVITY

Conductivity of Core samples was measure at Core lab (UK).

2.3 GRAIN DENSITY AND POROSITY

Grain density and Porosity of core samples were also measured at Core lab (UK).

2.4 SPECIFIC SURFACE AREA

Micrometric Gemini III 2375 apparatus was used to measure the specific area of core samples and IR (insoluble residues), using nitrogen as an adsorbate. The samples were out gassed for 4 hours at 50 °C to preserve the chalk structure by removing the clay-bound water. Specific surface area was found using the five pints (0, 05 to 0, 3) BET method, (the test work was carried out in duplicate).

2.5 X- RAY DIFFRACTION

In order to detect as many plains as possible oriented glass slide method was used to obtain X-ray diffractogram. 0.03 g weighed of IR (powder insoluble residue) of each sample was mixed in 1.5 ml water to make slurry. Four types of diffractograms were obtained by giving four different treatments to IR of each sample pasted on glass slides drying, glycolation, and heating at 350 °C and 550 °C respectively. The diffractogram of each original dry powder samples were also obtained. The following parameters were used in the Philips Diffractometer: CuK α radiation, receiving angle: 0, 20, automatic divergence slit angle, and angle step: 0,1^o/2sec. The detection range was 3^o-65^o 2 θ for water treated samples and 3^o-40^o 2 θ for glycol, and heated at 350 °C and 550 °C samples.

2.6 CATION EXCHANGE CAPACITY

Clay's ability to release the cations was determined by cation exchange capacity test. Cation exchange tests were carried out by the exchange of Na¹⁺ by 1M NH₄Cl and exchange of Ca²⁺, Mg¹⁺ and K¹⁺ by 1 M NaCl Solution. 30 ml exchange solution was added to 3 gm sample and shaken for 30 minutes, followed by centrifugation for 10 minutes at 3000 rpm. The supernatant was withdrawn and the procedure was repeated until it was assured that there is no considerable amount of releasable ions left on the clay sites. The collected supernatants were filtered through 0, 2 μ m filter. The desired elements were determined by using Atomic Absorption Spectrometer. Standards solutions were run before running the supernatants to determine the desired element.

3 CHARACTERISATION OF CHALK

3.1 X-RAY DIFFRACTION

To explain the X-ray diffraction study of samples, the sample collected at depth 9242 fts was selected. All major chalk peaks with their plains detected in diffractogram of dry powder chalk samples are given in table (4.1). Three diagnostic peaks for limestone were detected at $23.1\ 2\theta$ (3.84721\AA), $29.5\ 2\theta$ ($3.0255\ \text{\AA}$), and $57.5\ 2\theta$ ($1.60149\ \text{\AA}$) with intensity 11, 100 and 7 respectively in each sample as shown in fig (3.1). All chalk relating peaks appearing in the diffractogram of dry powder samples diminished in the diffractogram of insoluble residues (obtained after removing limestone by HCl from samples) saturated with water. Diffractograms of all dry powder chalk samples and IR (insoluble residue) are given in Appendix (A).

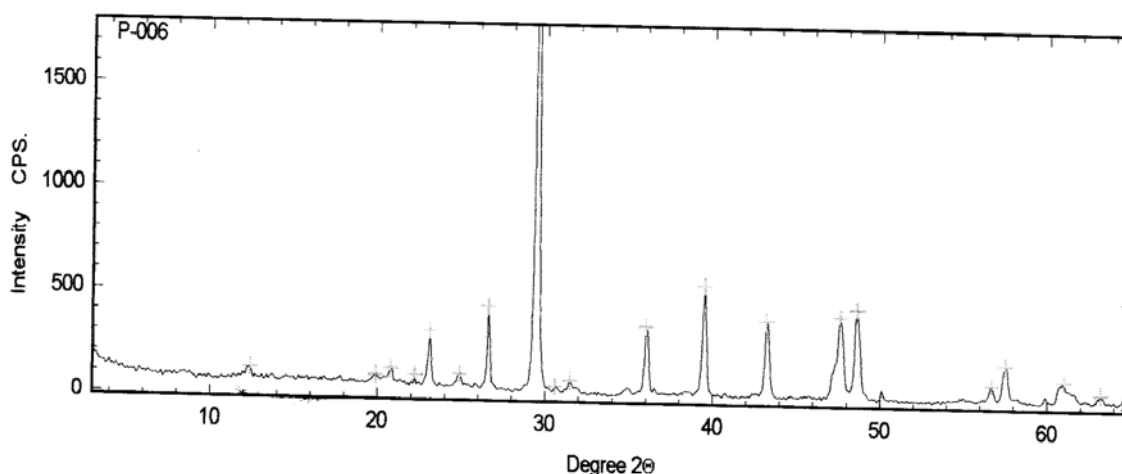


Fig 3.1: Identified Peaks at oriented mounts X-ray Diffractogram of dry powder chalk sample collected at depth 9242fts.

3.1.1 IMPURITIES IN CHALK SAMPLES

In order to determine impurities in chalk samples, X-ray diffraction study of insoluble residues (obtained after removing limestone by HCl) was conducted. Diffractogram of water saturated IR (insoluble residue) shows that it contains clay and silica. Peaks detected at distance $20.8\ 2\theta$ (4.26713\AA), $26.6\ 2\theta$ (3.3484\AA), $36.5\ 2\theta$ (2.4597\AA), $37.6\ 2\theta$ ($2.39026\ \text{\AA}$), $42.4\ 2\theta$ ($2.13011\ \text{\AA}$), $50.1\ 2\theta$ ($1.81928\ \text{\AA}$), $54.8\ 2\theta$ ($1.67384\ \text{\AA}$), and $59.9\ 2\theta$ (1.54293\AA) correspond to silica peaks in sample as shown in fig (3.2). The three peaks detected at distance $8.5\ 2\theta$ ($10.39421\ \text{\AA}$), $17.7\ 2\theta$ ($5.00688\ \text{\AA}$) and $26.6\ 2\theta$ ($3.3484\ \text{\AA}$) with intensity 25, 12 and 94 respectively as shown in figure (3.2) are diagnostic peak for illite clay. Those peaks did not shift at all in diffractogram of glycol treated IR (insoluble residue) and also did not disappeared on heating IR at $550\ ^\circ\text{C}$ as shown in fig (3.3) that confirm Illite clay is present in samples. Other peaks at $19.9\ 2\theta$ ($4.45804\ \text{\AA}$), $32.9\ 2\theta$ ($2.7209\ \text{\AA}$), $40.2\ 2\theta$ ($2.24146\ \text{\AA}$) and $45.4\ 2\theta$ ($1.99608\ \text{\AA}$) in diffractogram of water saturated IR also corresponds to Illite clay. Not any other type of clay was found in samples.

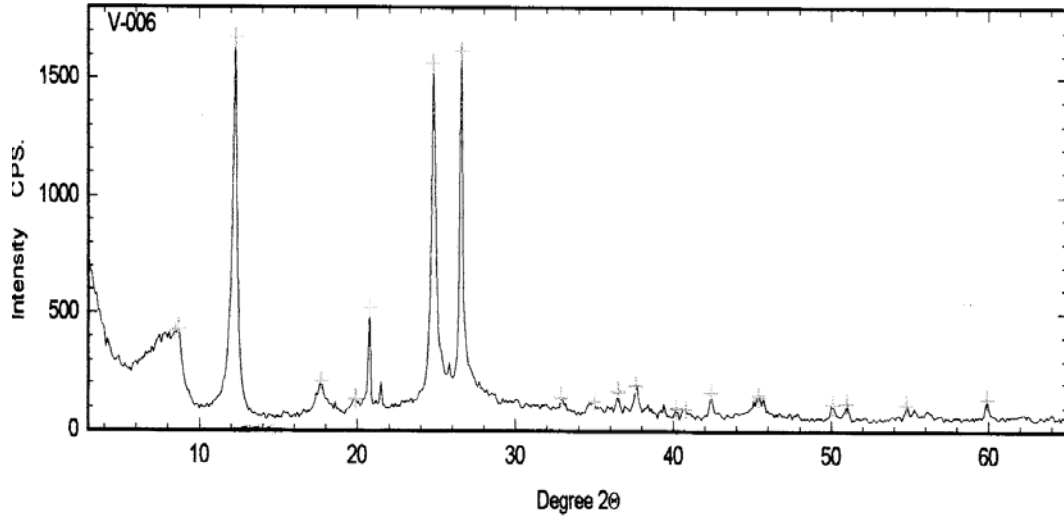


Fig 3.2: Identified Peaks at oriented mounts X-ray Diffractogram of IR of chalk sample saturated with water collected at depth 9242fts.

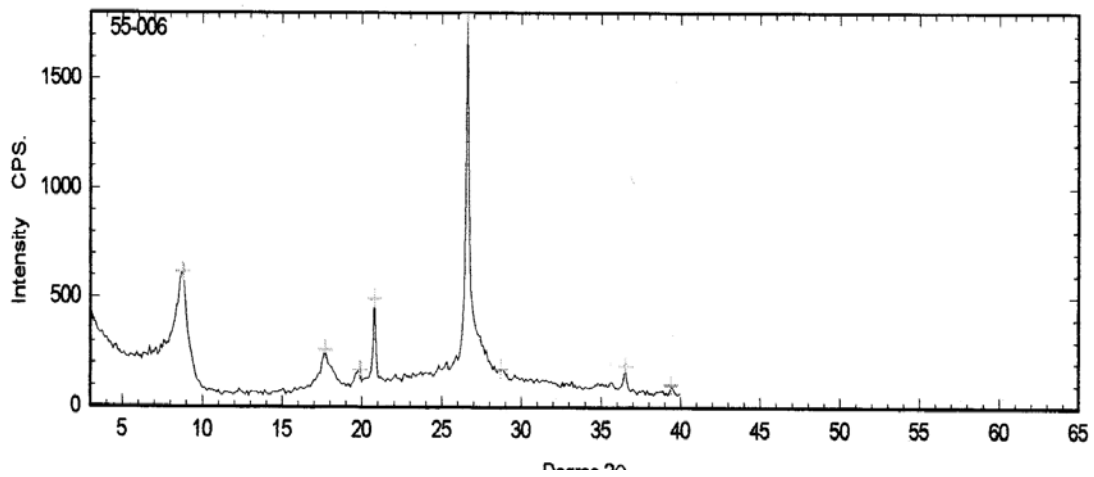


Fig 3.3: Identified Peaks at oriented mounts X-ray Diffractogram of IR of chalk sample heated at 550 °C collected at depth 9242fts.

Table 3.1: Shows Identified peaks with their reflection plains for limestone at oriented mounts ray Diffractrogram of dry powder chalk sample collected at depth 9241fts.

h k l	2 θ	\AA
0 1 2	23.1	3.8472
1 0 4	29.5	30255
0 0 6	31.5	2.83782
1 1 0	36	2.49274
1 1 3	39.5	2.27955
2 0 2	43.2	2.0925
0 1 8	47.6	1.90883
1 1 6	48.6	1.87186
2 1 1	56.7	1.62217
1 2 2	57.5	1.60149
2 0 8	61	1.51772
1 2 5	63.2	1.47008

Table 3.2: Shows Identified peaks with their reflection plains for silica at oriented mounts X-ray Diffractrogram of IR chalk sample saturated with watert collected at depth 92422fts.

h k l	2 θ	d (\AA)
100	20.8	4.26713
110	36.5	2.45973
111	37.6	2.39026
200	42.4	2.13011
112	50.1	1.81928
202	54.8	1.67384
211	59.9	1.54293

Table 3.3: Shows Identified peaks with their reflection plains for Illite clay at oriented mounts X-ray Diffractrogram of IR chalk sample saturated with water collected at depth 9242fts.

h k l	2 θ	d (\AA)
002	8.5	10.39421
004	17.7	5.00688
110	19.9	4.45804
006	26.6	3.3484
-116	32.9	2.7209
220	40.2	2.24146
136	45.4	1.99608

3.2 SPECIFIC SURFACE AREA

BET measurement of chalk samples and IR (insoluble residues) are given in table (3.4). Specific surface area values of chalk samples were found from 5.53 to 11.7433 m²/g, are larger than chalk specific surface area, reveal that samples are not pure chalk. Limestone occurs in large aggregate particles, resulting in very small specific surface area. Samples may contain impurities like clay, quartz and coarse particles. Particles in clay and silica occur in small size, causing an increase in total specific surface area of samples. Specific surface area values of insoluble residues (obtained after removing limestone by HCl from samples) found between 18.344 and 37.3916 m²/g. Since, IR (insoluble residues) may contain coarse particles, silica and clay; obviously IR specific area would be higher than samples specific surface area as earlier explained. X-ray diffraction study identified the illite clay in chalk samples. Illite clay usually has specific surface area between 97 and 113 m²/g. Specific surface area values of IR are less than illite clay, reveal that insoluble residues are not only clay but also contain other matter which is not as much finely divided as illite particles. Presence of silica peaks in the X-ray diffractogram of IR confirm above argument.

Table 3.4: Results of SSA of chalk sample and IR. Literature Values are from Nybak, E (2000).

Result	BET	
	Core sample SSA m ² /g	IRSSA m ² /g
9238-9	8.6 097	32.03
9242-8	11.7433	37.3916
9251-2	8.5688	30.6189
9254-6	8.6772	34.0361
9256-1	9.4904	33.4579
9351-1	7.7070	30.3447
9352-1	5.5286	18.329
9329-2	11.5740	34.0953
9368-9	5.7361	24.2282
9370-2	6.1001	22.5782
Literature values	Mineral Name	SSA m ² /g
	Smectites	82-767
	Kaolinite	15-23
	Montmorillonite	700-800
	Fled spar	1
	Sandstone	1

3.3 CATION EXCHANGE CAPACITY

Cation exchange capacity results of core sample are given in table (3.5). CEC is determined as sum of exchanged cations by concentrated solution of 1M NH_4Cl and 1M NaCl and expressed in mille equivalent per 100 g.

Results from AAS measurements and processing of data for CEC are given in [Appendix\(D\)](#).

CEC of sample depends upon the volume and type of shale. Finer clays like smectites (due to large specific surface) have higher CEC and coarse clays like kaolinite (due to small specific surface) have lower CEC values. Cation exchange capacity of samples was found between 14.87566 and 31.68 meq/100g as shown in fig (3.4). Figure (3.5) and fig (3.6) show that there is some linear relationship between Q_v (cation exchange capacity per unit pore volume) and specific surface area of chalk samples and specific surface area of IR (insoluble residues) respectively. Also, CEC is proportional to volume clay. Figures (3.7) and fig (3.8) show some linear relationship between Q_v and IR, and volume of shale respectively. CEC of samples is comparable to illite CEC i.e., 10-40 mg/l as shown in table (3.5). X-ray diffraction study of IR of chalk sample also identified illite clay in chalk samples. CEC values obtained by Core lab (UK) are very low as compared to our CEC measurements. Only reason which can be given is cleaning of samples. We cleaned our samples in six weeks to ensure that there is no more oil left bound to samples matrix. Presence of oil hinders the contact between exchange solution and sample matrix, causing decrease in cations exchanging capacity of samples.

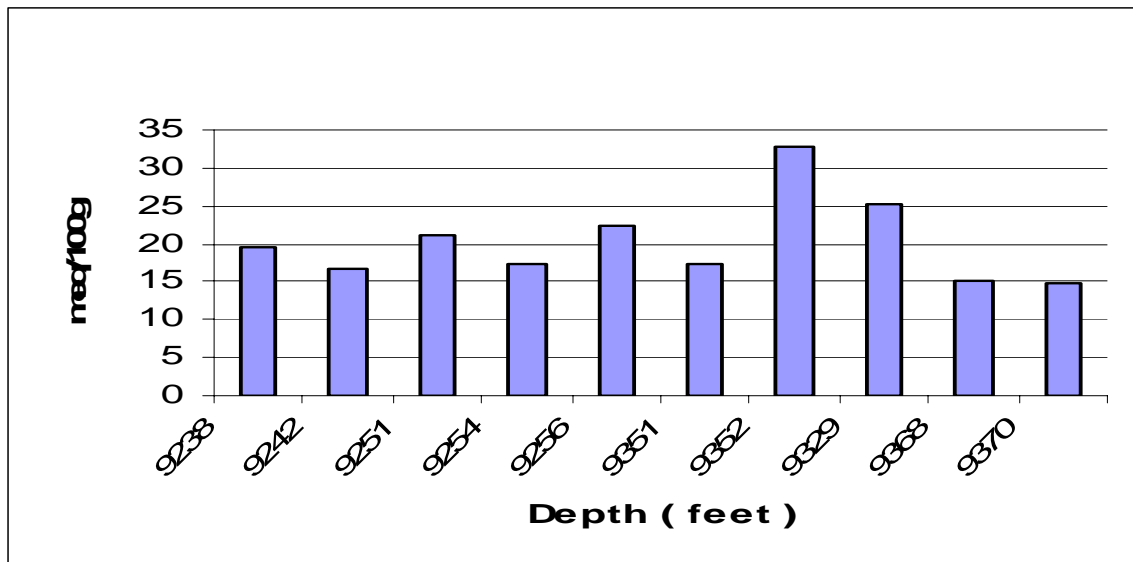


Fig 3.4: Cation exchange capacity of core samples collected at different depths.

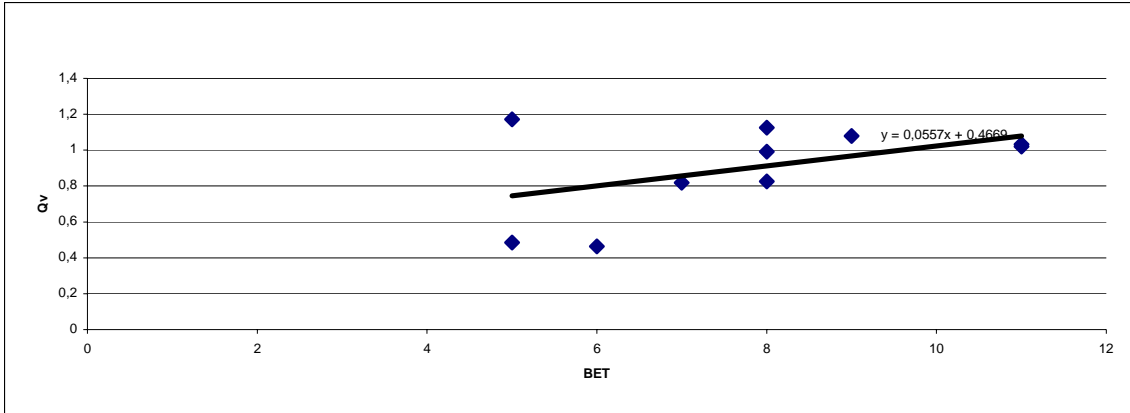


Fig 3.5: Relationship between Q_v and BET of chalk samples

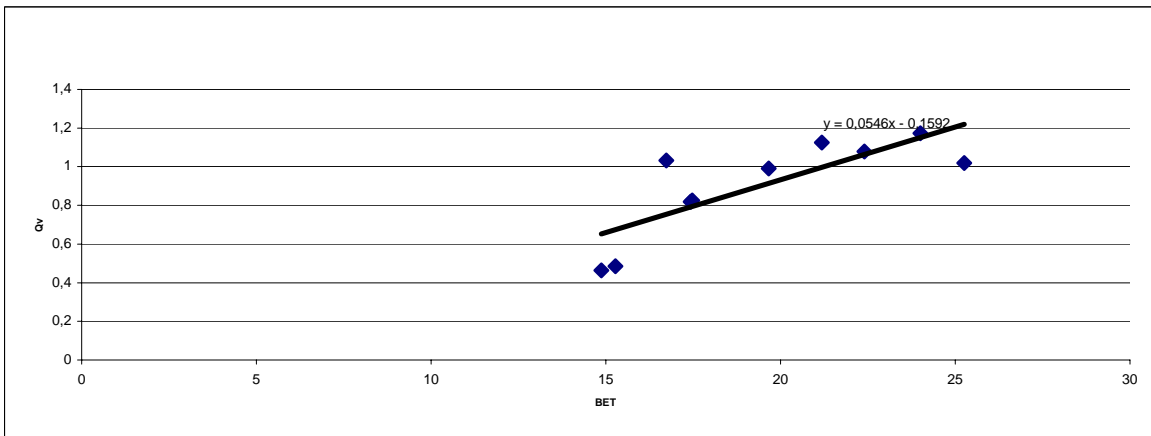


Fig 3.6: Relationship between Q_v and BET of IR of chalk samples

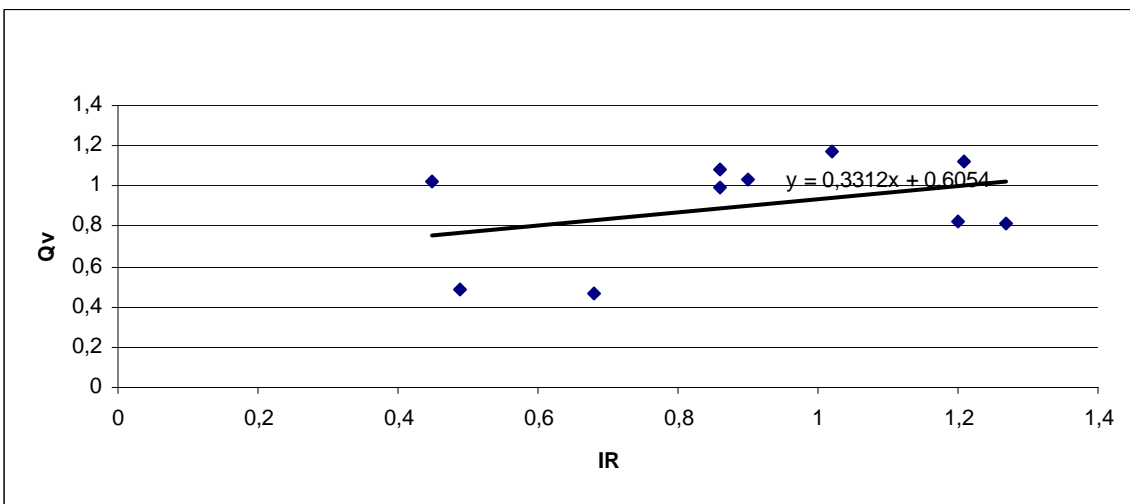


Fig 3.7: Relationship between Q_v and IR of shale of chalk samples

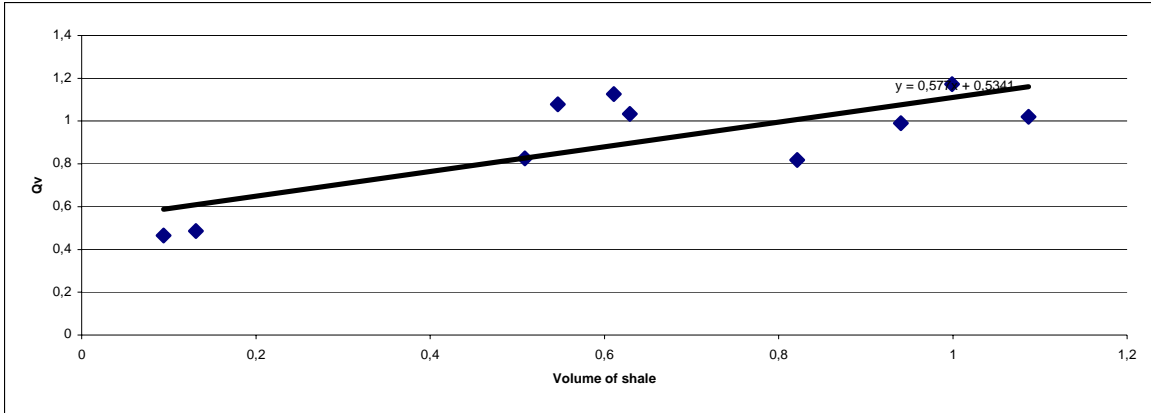


Fig 3.8: Relationship between Q_v and shale volume of chalk samples.

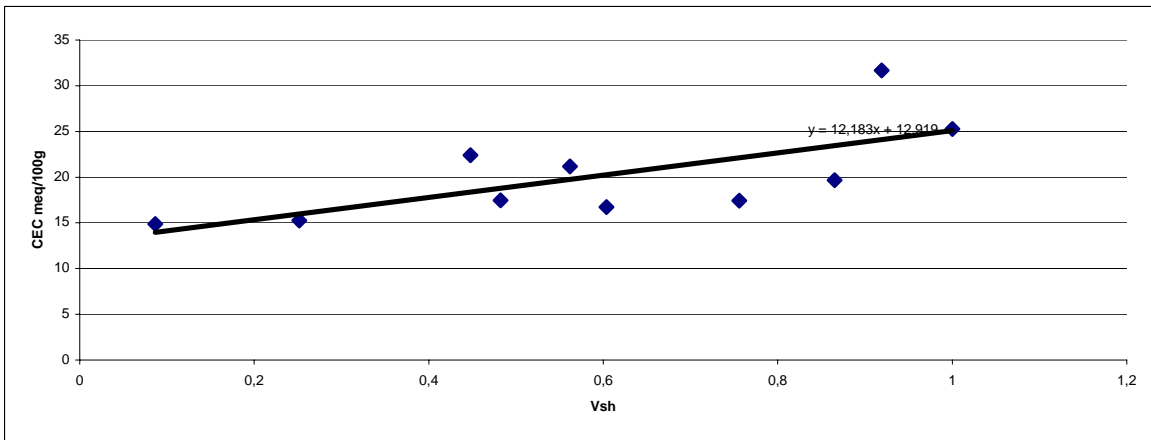


Fig 3.9: Relationship between cation exchange capacity and shale volume of chalk samples.

Table 3.5: Cation exchange capacities of samples collected at different depths. Literature Values are from Nybak, E (2000).

Results	Depth	Mg ²⁺ meq/100g	Ca ²⁺ meq/100g	K ¹⁺ meq/100g	Na ¹⁺ meq/100g	CEC meq/100g
	9238-9	1.547893	15.75027	1.888265	0.472924	19.65935
	9242-8	1.407695	14.04122	0.956952	0.327047	16.73292
	9251-2	2.323769	15.34676	2.981582	0.531685	21.1838
	9254-6	1.04633	13.19977	2.697816	0.527023	17.47094
	9256-1	1.370833	17.47919	3.106038	0.446317	22.40238
	9351-1	0.897411	14.02212	2.204983	0.304412	17.42893
	9352-1	1.648537	29.7445	1.452255	0.490845	31.6876
	9329-2	2.189638	18.61112	3.274093	1.179946	25.2548
	9368-9	0.473661	13.10955	1.356673	0.36434	15.27632
	9370-2	0.440786	12.50888	1.67837	0.247625	14.87566
	Clay mineral					meq/100g
Literature values	Kaolinite					1-10
	Vermiculite					120-150
	Montmorillonite					80-120
	Smectites					70-150
	Illite					10-40

3.4 a, m, B VALUES

The values of “a” and “m” were derived by plotting graph between log of porosity values and log of formation factor. Slope of line gives m value 1.3367 and anti log of line intercept at y-axis gives a value 2.32. Where “a” is taken as 1 to determine “m” values, which was found 2.26 in UK lab results. B is the equivalent conductance of sodium clay-exchanged cations, 3.75 Keelan value of B was assumed in Core Lab results calculated from BQ_v . In our calculations B value was assumed 1.076 from BQ_v values using our Q_v values (CEC per unit pore volume). The calculations of B value are given in [Appendix \(D\)](#).

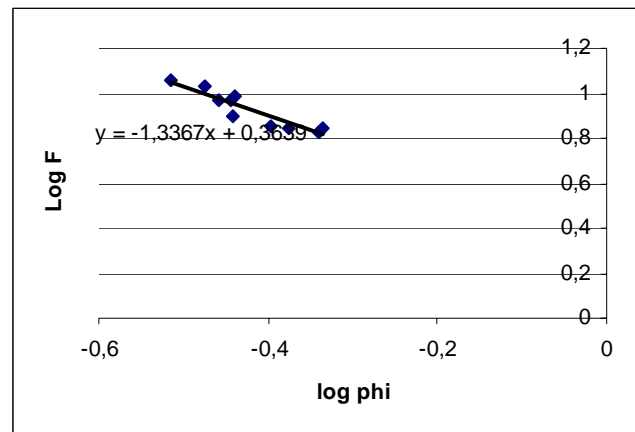


Figure 3.10: Graph between log of core sample porosity and Log of formation factor.

3.5 FORMATION WATER R_w and R_{wb}

Formation water resistivity was determined from NaCl concentration resistivity chart. The concentration of NaCl in formation water is 22000 ppm; the resistance of formation water was deduced as 0.127 ohm. R_{wb} was selected from R_{fa} curve in shale interval.

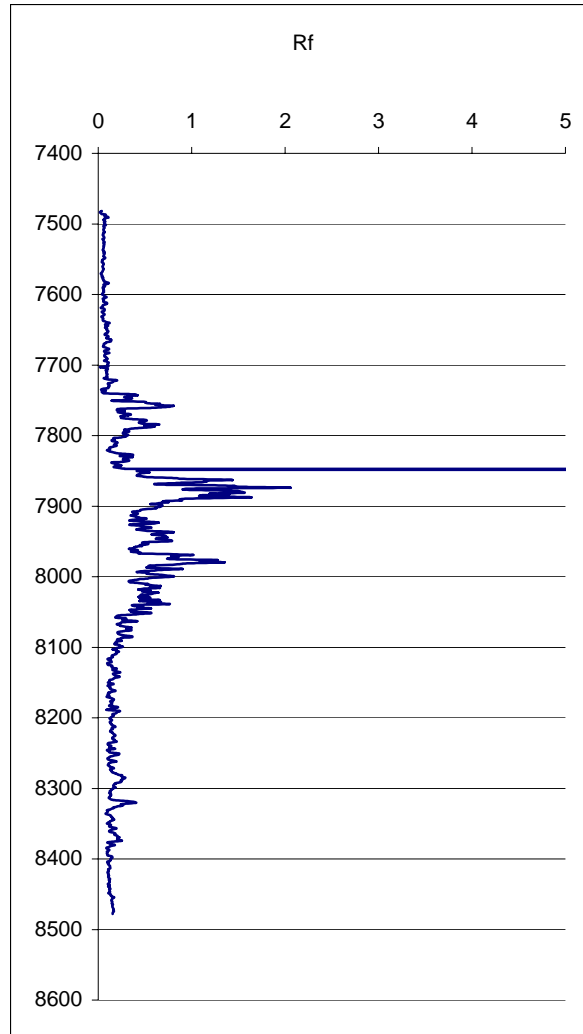


Fig. 3.11: R_{fa} of formation.

4 COMPARISON BETWEEN WAXMAN AND SMITS SATURAION RESISTIVITY RELATIONSHIP AND DIFFERENT WATER SATURAION MODELS.

4.1 COMPARISON BETWEEN WAXMAN AND SMITS SATURAION RESISTIVITY RELATIONSHIP AND ARCHIE WATER SATURATOIN EQUATION.

All water saturation determinations from resistively log in clean (non shaly) formations with homogeneous inter granular porosity are based on Archie's water saturation equation. Archie water saturation equation can be written as:

$$\frac{1}{R_t} = \frac{\phi^m S_w^n}{a R_w}$$

Waxman and Smits water Saturation equation can be written as:

$$\frac{1}{R_t} = \frac{S_w^2}{F^* R_w} + \frac{BQ_v S_w}{F^*}$$

Archie's water saturation model predicts 25 -35 % more water saturation than Waxman and Smits water saturation equation as shown in fig (4.1). Reason for higher S_w predicted by Archie's water saturation equation could be explained in following way. Water saturation depends upon the conductivity of formation and porosity. Higher the conductivity of formation higher will be the water saturation and **vice versa**. In Archie's water equation conductivity contributed by clay (in shaly formations) to the total formation conductivity is not taken in to account and formation water is only considered as conductive material in rock formation, while in reality clay contents in shaly formations also cause the current in formation, and make their conductivity contribution to total conductivity in addition to formation water conductivity. Archie's water equation use total conductivity i.e., formation water conductivity plus shale conductivity, that is always higher than the true conductivity of formation. Waxman and Smits have suggested that in order to determinate the true conductivity of formation (shaly formations), shale conductivity contribution ($BQ_v S_w / F^*$) should be excluded from apparent conductivity. In Waxman and Smits equation conductivity contribution of shale is related to CEC of clay.

Waxman and Smits water saturation use true conductivity of formation i.e., free from shale conductivity contribution, which is always lower than total conductivity of formation (in shaly formations), results in lowering of water saturation.

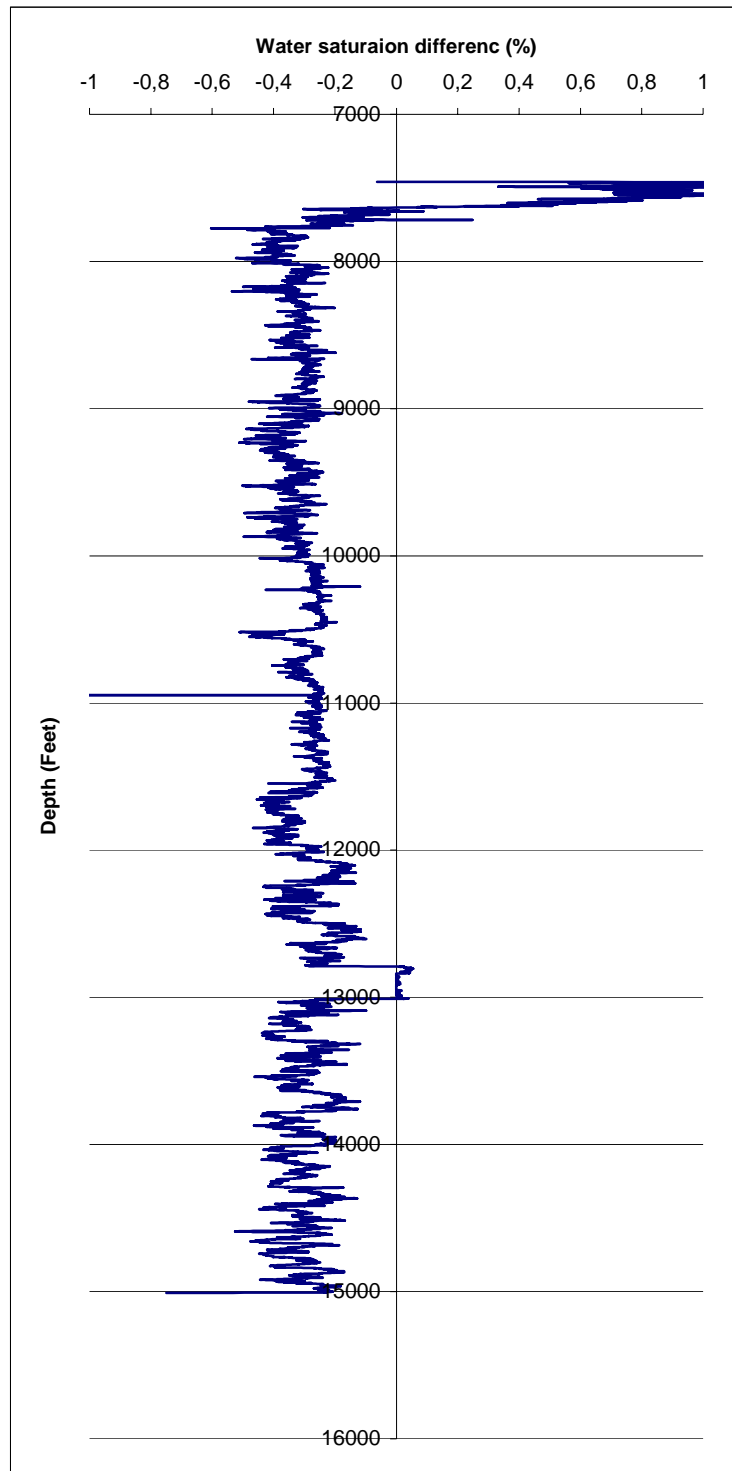


Fig 4.1: *Water saturation difference log between Waxman-Smits water saturation equation and Archie' water saturation equation.*

4.2 COMPARISON BETWEEN WAXMAN AND SMITS SATURATION RESISTIVITY RELATION AND LAMINATED SAND AND SHALE MODEL.

In laminar shale model, R_t the resistivity in the direction of bedding planes is related to R_{sh} (resistivity of the shale laminae) and to R_{sd} (the resistivity of the clean sand laminae) by a parallel resistivity relationship.

$$\frac{1}{R_t} = \frac{1 - V_{lam}}{R_{sd}} + \frac{V_{lam}}{R_{sh}}$$

For clean sand laminae, $R_{sd} = F_{sd} R_w / S_w^2$. $F_{sd} = a / \phi_{sd}$ (where ϕ_{sd} sand – streak porosity) and $\Phi = 1 - V_{lam}$ ϕ_{sd} (where ϕ_{sd} bulk formation porosity), then;

$$\frac{1}{R_t} = \frac{\phi^2 S_w^2}{(1 - V_{lam}) a R_w} + \frac{V_{lam}}{R_{sh}}$$

Laminated sand and shale model also considers conductivity contribution of shale in addition to formation water as like Waxman –Smits water saturation equation. V_{lam} / R_{sh} factor in Laminated Sand and Shale model equation represents the shale conductivity contribution to total conductivity of formation. Water saturation difference log shows that water saturation calculated by Waxman-Smits equation generally 0 to 16 % and 0 to 32 % at depths 7800 to 11000 fts and 11000 to 15000 fts respectively is higher than laminated shale model with exception at a few depths, where S_w predicated by Waxman-Smits is lower than laminated shale model as shown in fig (4.2). Reason for higher S_w predicted by Waxman-Smits water saturation equation can be explained in following way. Laminated sand and shale model consider volume of shale to account shale conductivity contribution made to total conductivity of formation. But, it is not necessary that whole shale is pure clay. Shale may consist of quarts, clay and coarse particles. Conductivity of clay is due to its CEC. The CEC of clay is proportional the specific surface area of clay. Clays like smectites occur in finely divided particle, have higher CEC values, because there is more surface area available for adsorption of cations on the negatively charged surface of clay. Higher the CEC; higher will be the conductivity of clay. Particles in coarse clays like kaolinite occur in aggregate result in small specific area. Smaller the specific surface area; the lower will be CEC. Shale conductivity term $BQ_v S_w / F^*$ calculates shale conductivity contribution more accurately rather than shale conductivity term V_{lam} / R_{sh} proposed by Laminated sand and shale model. Shale conductivity contribution predicted by V_{lam} / R_{sh} in Laminated sand and shale model is usually higher than the $BQ_v S_w / F^*$ shale conductivity term in Waxman-Smits equation as former accounts whole shale as pure clay. Higher shale conductivity contribution means that true conductivity of formation is lower. Lower the conductivity of formation, lower will be the water saturation and **vice versa**. At certain depths i.e., 10000-10700 fts and 10900-11700 fts water saturation determine by laminated shale model is higher that determined by Waxman-Smits water saturation equation, the only reason was that at these depths conductivity contribution of shale may be same or lower predicted by Laminated Sand

and Shale Model than actual conductivity contribution predicted by Waxman and Smits equation.

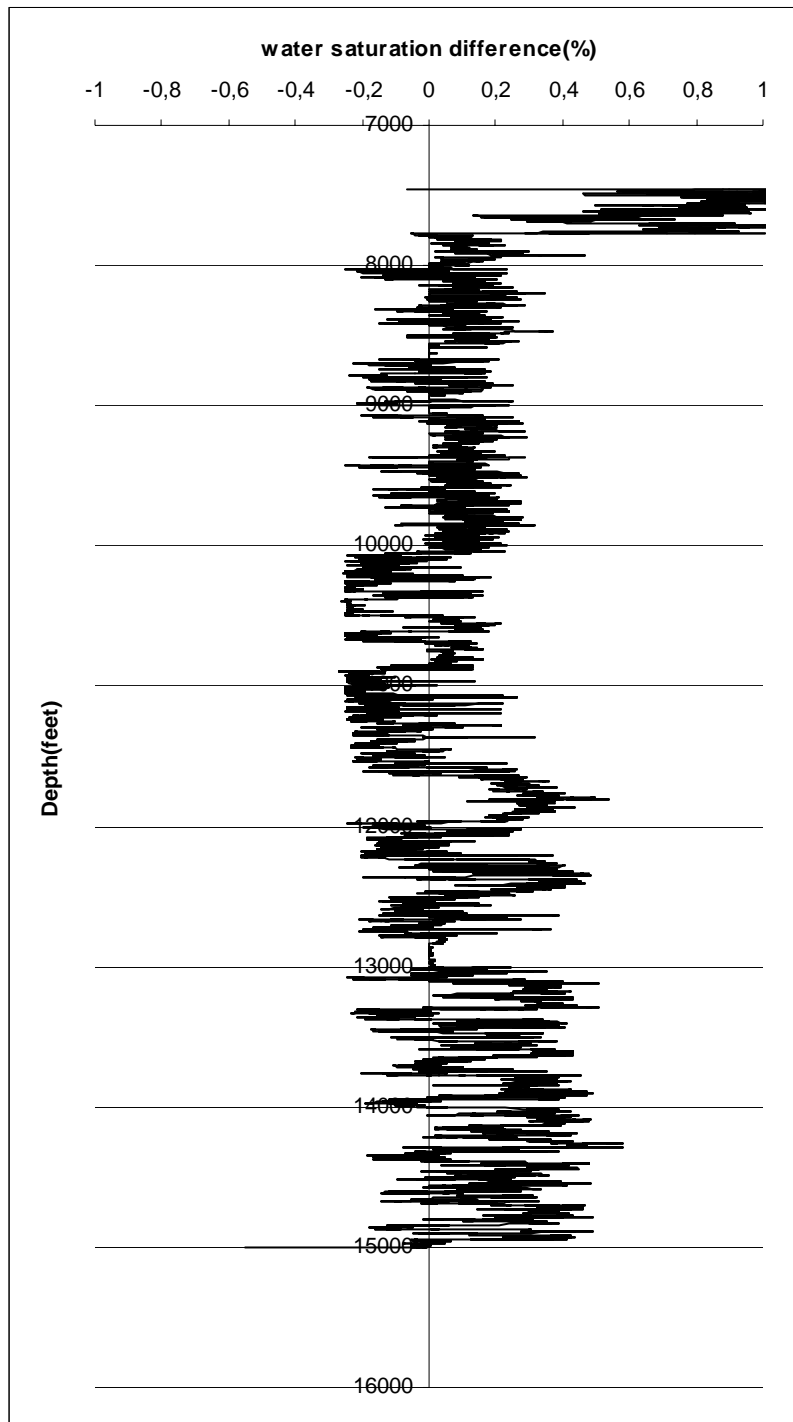


Fig4.2: *Water saturation difference log between Waxman-Smits water saturation equation and laminated Sand and Shale Model.*

4.3 COMPARISON BETWEEN WAXMAN AND SMITS SATURATION RESISTIVITY RELATION AND TOTAL SHALE RELATION.

Following relation ship is modified form of laminated shale model. Lab investigation and field experience showed that in order to get rid of mode of distribution of shale and to get more practicable water saturation values following relation works better.

$$\frac{1}{R_t} = \frac{\phi^2 S_w^2}{(1 - V_{sh}) a R_w} + \frac{V_{sh} S_w}{R_{sh}}$$

Water saturation difference log in fig (4.3) shows that Waxman-Smits resistivity relationship generally measures higher S_w from 0 to 20 % and from 0 to 38 % at depths 7800 to 11000 fts and at 11000 to 15000 fts respectively than Total Shale Relationship. In our study water saturation results obtained by Total shale relation are not working as S_w difference between Waxman and Smits equation and Total shale relation was higher than S_w difference between Waxman and Smits and Laminated sand and shale Model.

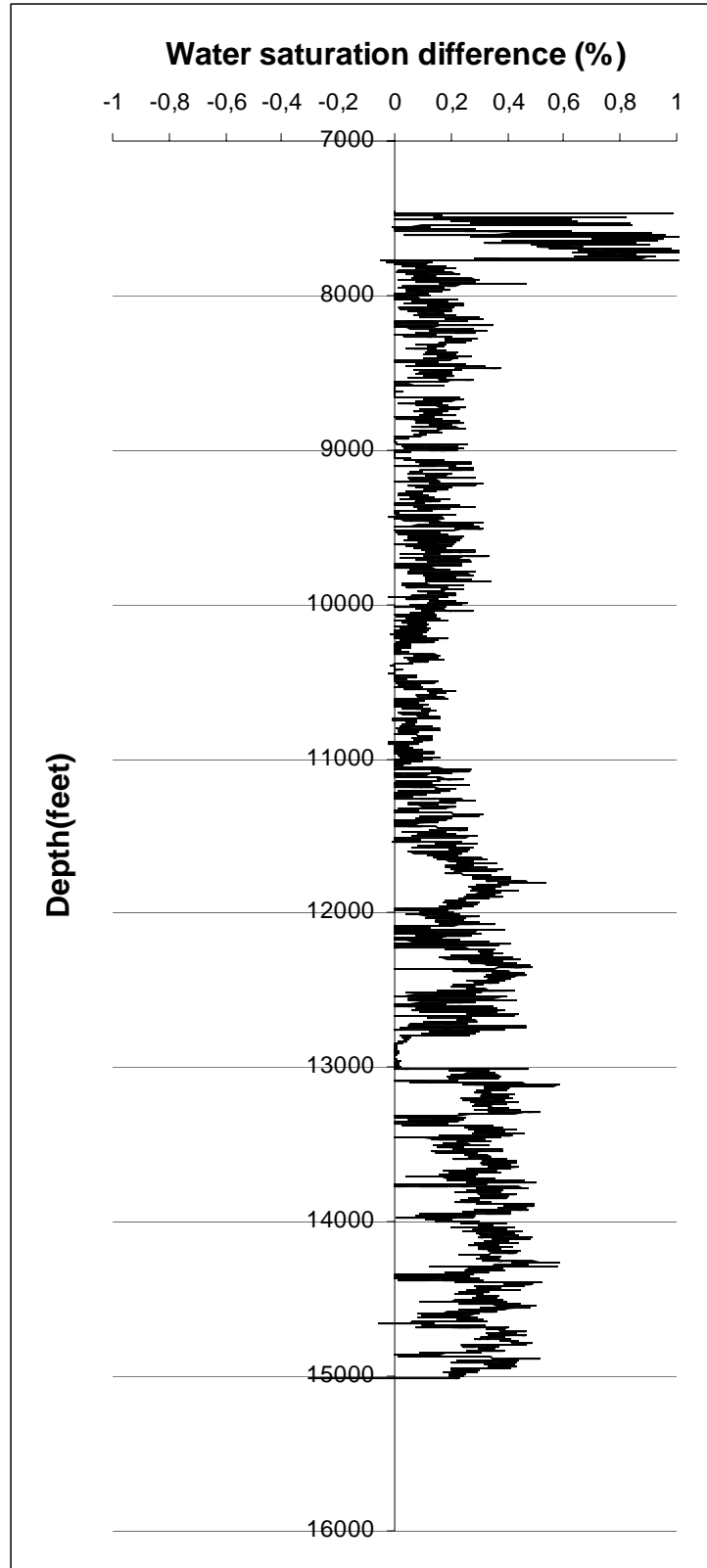


Fig 4.3: *Water saturation difference log between Waxman-Smits water saturation equation and laminated Sand and Shale Model.*

4.4 COMPARISON BETWEEN WAXMAN AND SMITS SATURATION RESISTIVITY RELATION AND VOLAN MODEL.

Volan Model uses the following equation to calculate actual water saturation.

$$C_{wa} = C_t F$$

$$C_{wa} = S_{wt}^2 \left[C_w + \left(\frac{S_{wb}}{S_{wt}} \right) (C_{wb} - C_w) \right]$$

Volan Model is based on dual water models. Waxman-Smits equation is source of dual water models. These were developed to make Waxman-Smits equation practicable in absence of core measurements. In dual water model, clay is modeled as consisting of two components, bound water and clay minerals. The clay minerals are modeled as electrically inert; the clay electrical conductivity is modeled as being derived from the conductivity of bound water, C_{wb} . C_{wb} is assumed to be independent of clay type. In Volan model $S_{wb} S_w (C_{wb} - C_w)$ factor represents conductivity contribution made by shale to total conductivity of formation. Water saturation difference log in fig (4.4) shows that water saturation calculated by Waxman-Smits resistivity relationship at depths 7800 to 11000 fts and 11000 to 15000 fts is 0 to 20 % and 0 to 35% higher than Volan model, which means that $S_{wb} S_w (C_{wb} - C_w)$ shale conductivity contribution factor accounts higher conductivity than actual conductivity contribution by shale as given by the $BQ_v S_w / F^*$ in Waxman-Smits equation. As result, the true conductivity used in Volan model would be lower due to higher conductivity contribution made by shale as predicted by $S_{wb} S_w (C_{wb} - C_w)$ factor. Lower the true conductivity; lower will be water saturation.

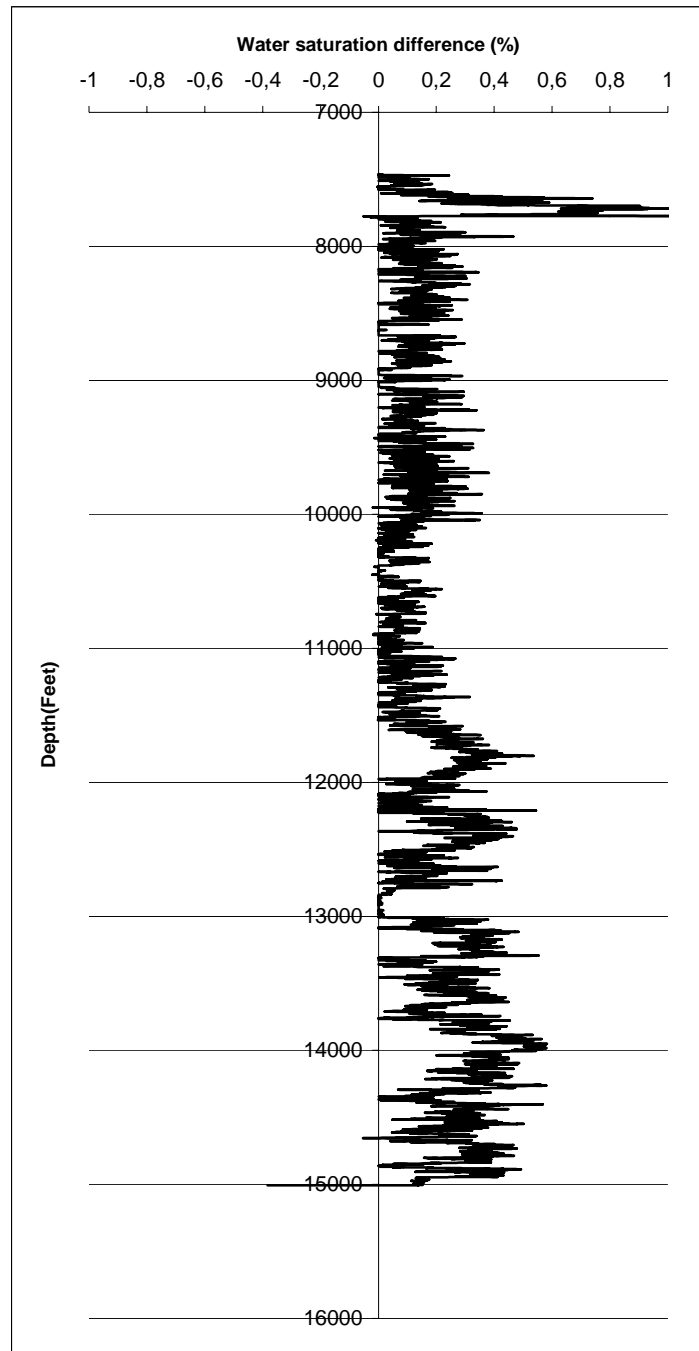


Fig 4.4: *Water saturation difference log between Waxman-Smits water saturation equation and Volan Model.*

4.5 COMPARISON BETWEEN WAXMAN AND SMITS SATURATION RESISTIVITY RELATION AND CYBER LOOK PROGRAM.

Cyber look program also uses the dual water model to account the effect of clay fraction i.e., conductivity of rock is function of formation water and clay bound water.

Cyber look program use the different approach than Volan model. In cyber look program, conductivity of 100% water bearing formation is used to calculate water saturation rather than apparent conductivity used in Volan model.

$$C_0 = \phi_t^2 [S_{wb} C_{wb} + (1 - S_{wb}) C_w]$$

Cyber look program calculate the S_w by sq root ration method that is almost identical to Archie water saturation equation. Water saturation log in fig (4.5) shows that Cyber Look Program predicted 20 to 30 % and 15 to 20 % higher water saturation than Waxman-Smits equation at depths 7800 to 11000 fts and at 11000 to 15000 fts respectively. Reason for predicting higher S_w saturation by Cyber Look program is that 100 % water bearing shaly formation conductivity equation accounts less shale conductivity contribution than the experiment determined by using Waxman-Smits equation. Lower the shale conductivity contribution to total conductivity, higher will be the water saturation.

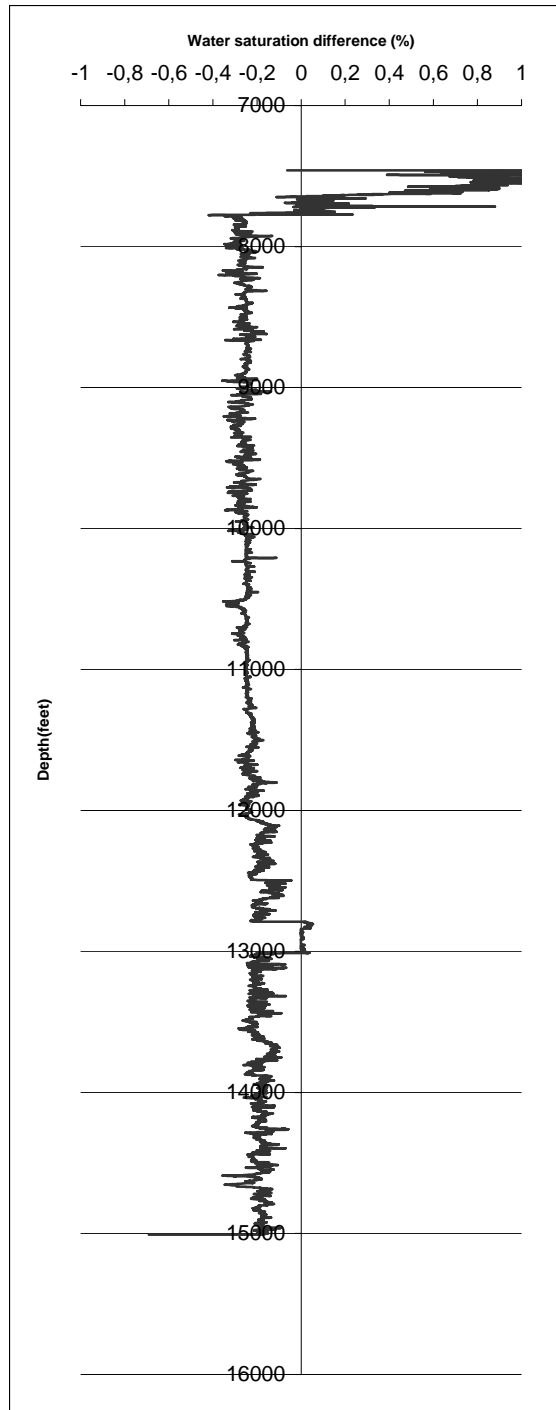


Fig 4.5: *Water saturation difference log between Waxman-Smiths water saturation equation and Cyber Look program.*

5.6 COMPARISON BETWEEN WAXMAN AND SMITS SATURATION RESISTIVITY RELATION AND NORMAIZED WAXMAN AND SMITS EQAUTION.

Normalized Waxman-Smits equation can be written as:

$$\frac{1}{R_t} = S_w^2 \phi_t^2 \left[\frac{1}{R_w} + \frac{Q_{vn}}{S_{wt}} \left(\frac{1}{R_{vsh}} - \frac{1}{R_w} \right) \right]$$

Waxman-Smits equation relates the rock resistivity to the resistivity of formation water and CEC of clay. Normalized Waxman-Smits equation is an alternate use of Waxman-Smits in absence of CEC measurements of core sample.

Where;

$$Q_{vn} = \frac{Q_v}{Q_{vsh}} = \frac{(V_{sh} \times \phi_{tsh})}{\phi_t}$$

Q_v is CEC of clay per unit pore volume.

When $BQ_v = Q_{vn} * BQ_{vsh} = Q_{vn} (C_{wash} - C_w) = (V_{sh} \Phi_{tsh}) / \Phi_t \cdot (\Phi_{tsh}^{-m} / R_{sh} - 1 / R_w)$ BQ_v in Waxman-Smits equation is replaced by log values i.e., $(V_{sh} \Phi_{tsh}) / \Phi_t \cdot (\Phi_{tsh}^{-m} / R_{sh} - 1 / R_w)$ the equation is called Normalized Waxman-Smits equation. Water saturation difference log in fig (4.6) shows that Waxman-Smits resistivity relationship equation measures higher water saturation by 0 to 15 % and 0 to 30 % at depths 7800 to 11000 fts and at depths 11000 to 15000 fts respectively than Normalized Waxman-Smits equation. Reason is same as earlier explained i.e., shale conductivity contribution was estimated higher by using log value than actual shale conductivity contribution measured by core measurements, resulting in lowering of true conductivity. Therefore, lower the true conductivity; lower would be water saturation.

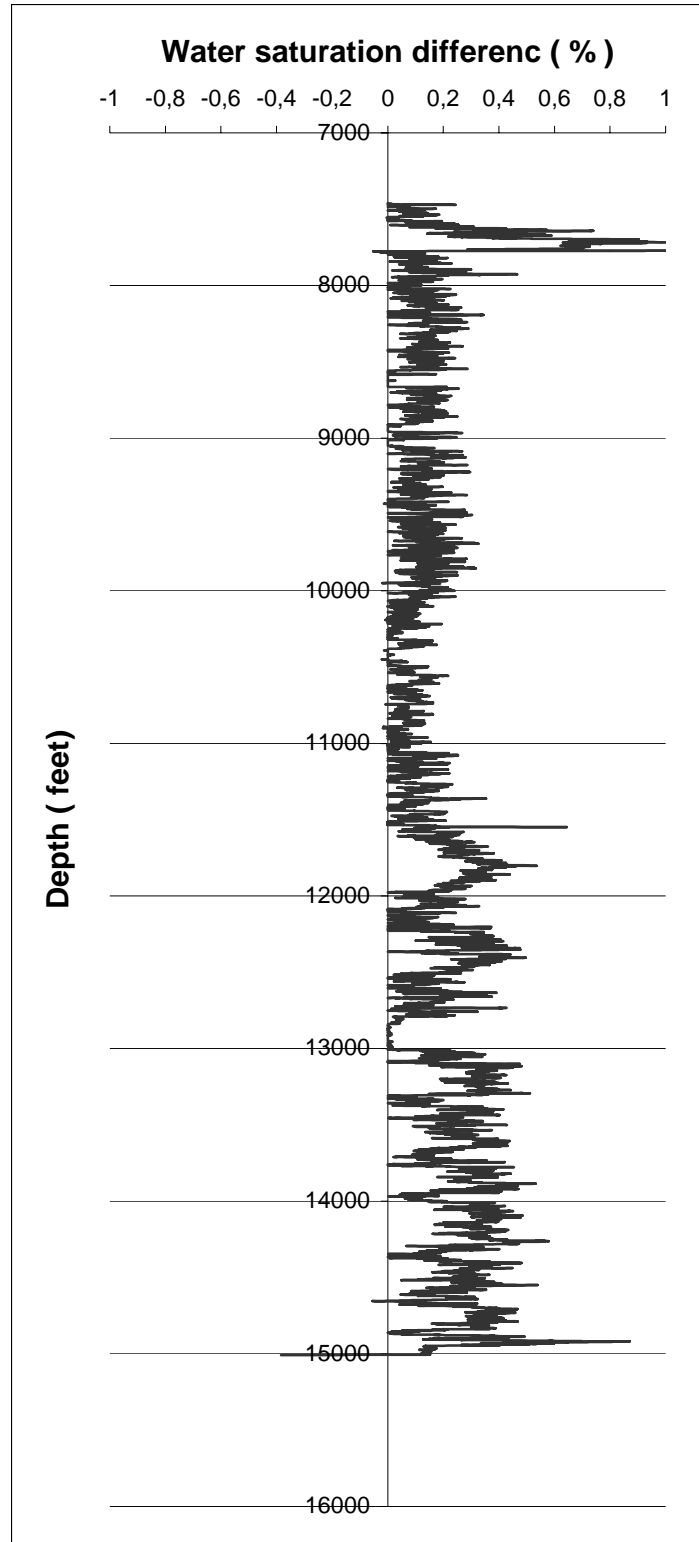


Fig 4.6: Water saturation difference log between Waxman-Smiths water saturation equation and Normalized Waxman- Smits water saturation equation.

4.7 COMPARISON BETWEEN WAXMAN AND SMITS SATURATION RESISTIVITY RELATION AND DISPERSED SHALE SIMPLIFIED MODEL.

In this model, resistivity of formation is related to pore water and dispersed clay.

$$\frac{1}{R_t} = \frac{Q_{im}^2 S_{im}}{a} \left(\frac{q}{R_{shd}} + \frac{S_{im} - q}{R_w} \right)$$

Formation conducts electrical current through a network composed of pore water and dispersed clay. Water saturation difference log in fig (4.7) shows that S_w calculated by Total dispersed shale Model at depth between 7750 to 8050 fts is almost similar to water saturation as calculated by Waxman and Smits, while at 8050 to 8400 fts water saturation calculated by Dispersed shale simplified model is higher than Waxman and Smits water saturation. In the first zone at 7750 to 8050 fts both methods almost measure the exact contribution of shale conductivity and hence the water saturation results are same. While in the second zone (8050 to 8400 fts) where the clay content was relatively higher, S_w is not same. Sonic, Density and Neutron tool response to clay minerals may vary in presence of high content of clay for porosity measurement, resulting variation in water saturation. Log data values of sonic porosity are very low in high shale content region of formation (8050-8400 fts), resulting in very high water saturation by model equation.

Note: - Well 3P Valdimar data has been used for comparison between Dispersed Shale Simplified Model and Waxman and Smits Water saturation.

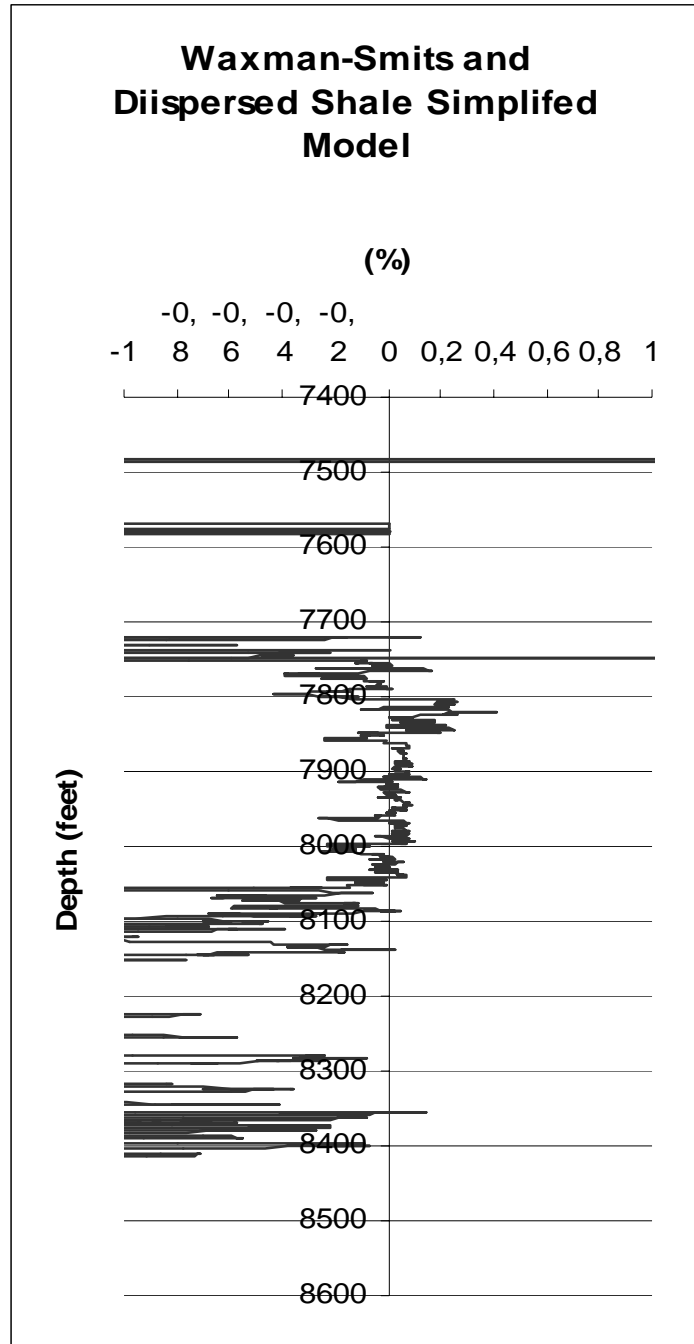


Fig4.7: *Water saturation difference log between Waxman-Smits water saturation equation and Dispersed Shale Simplified Model water saturation*

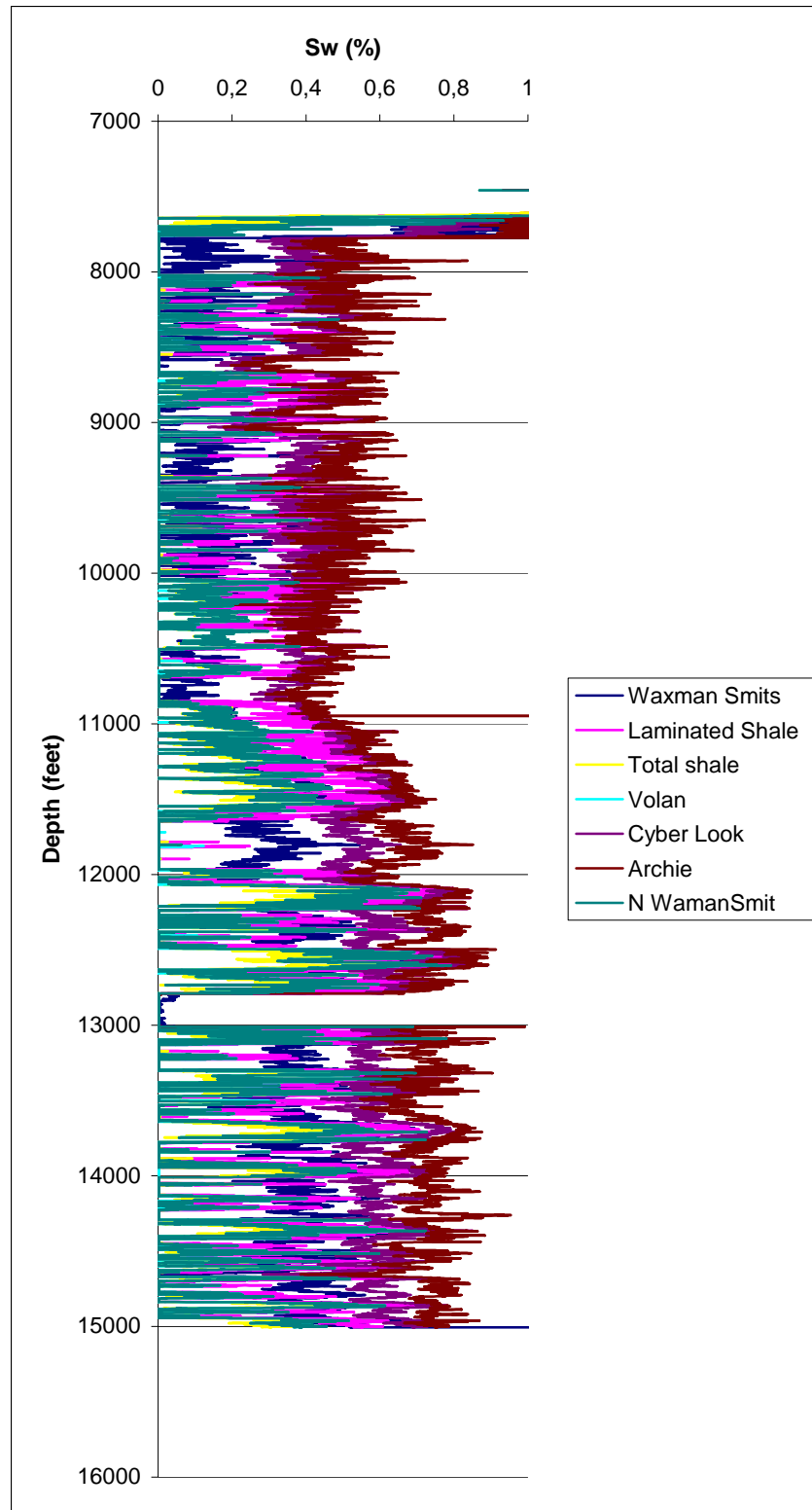


Fig. 4.8 Comparison water saturation obtained by different methods

Table: 4.1 Water saturation S_w results calculated by different water saturation methods

Name of water saturation methods	Sw at depth (7800-11000 ft)	Sw at depth (11000 to 15000 ft)
Waxman and Smits	0-25 %	30-60 %
Archie's	35 – 60 %	60 – 85 %
Laminated sand and shale Model	0-35 %	0-65 %
Total shale relationship	0-15 %	0 to 50 %
Volan Model	0-15 %	0 to 50 %
Cyber look Program	30 – 55 %	50 – 75 %
Normalized Waxman and Smits equation	0- 15 %	0-50 %
Dispersed shale simplified Model	5 to 35 %	50 to 100 %

Table 4.2 Difference in water saturation results calculated by Waxman-Smits and water saturation results calculated by other water saturation methods.

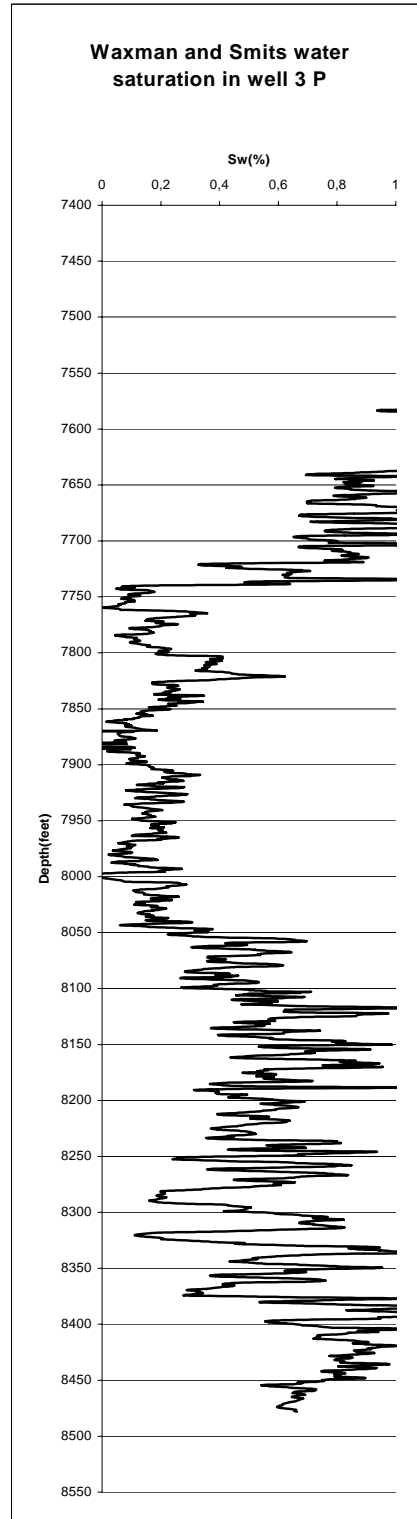
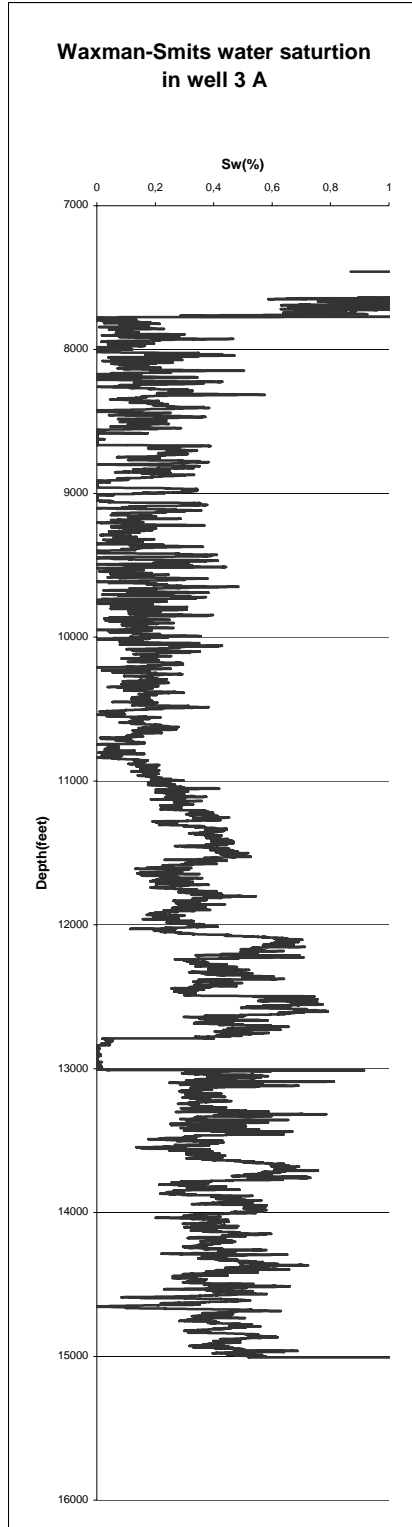
Name of Methods	Sw difference at depth (7800-11000 ft)	Sw difference at depth (11000 to 15000 ft)
Waxman-Smits and Laminated sand and shale Model	0 – 16 % (higher)	0 to 32 % (higher)
Total shale relation ship equation	0-20 % (higher)	0 to 38 % (higher)
Waxman and Smits and Volan Model	0 to 20 % (higher)	0 to 35 % (higher)
Waxman- Smits and Normalized Waxman-Smits	0 to 15 % (higher)	0 to 30 % (higher)
Waxman – Smits and Cyber Look Program	25 to 30 % (Lower)	15 to 20 % (Lower)
Waxman – Smits and Archie's Model	30 to 35 % (lower)	25 to 35 % (lower)

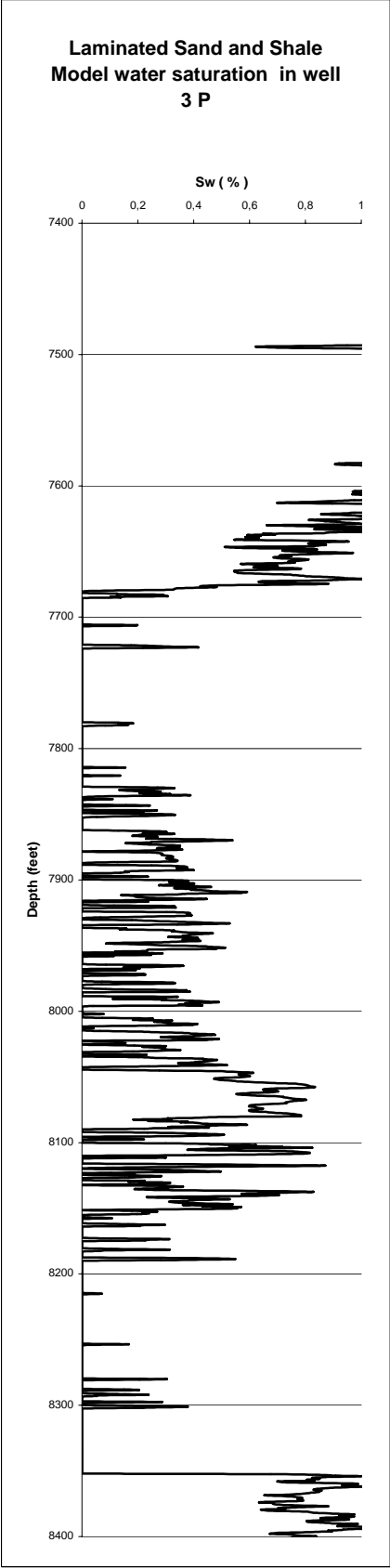
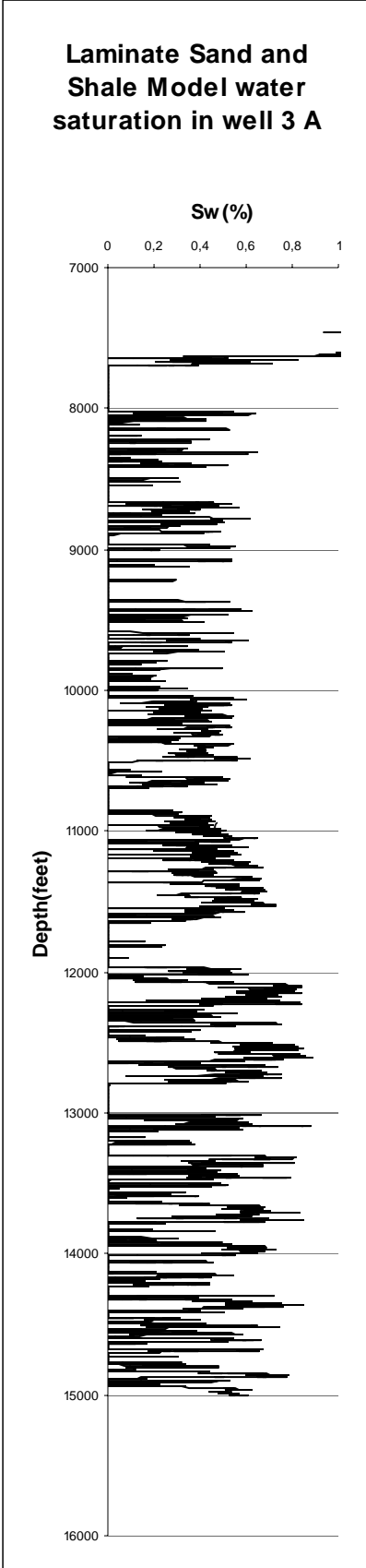
5 INTER COMPARISON OF WATER SATURATIONS RESULTS OBTAINED BY EACH METHOD IN WELLS NO 3 A AND 3 P

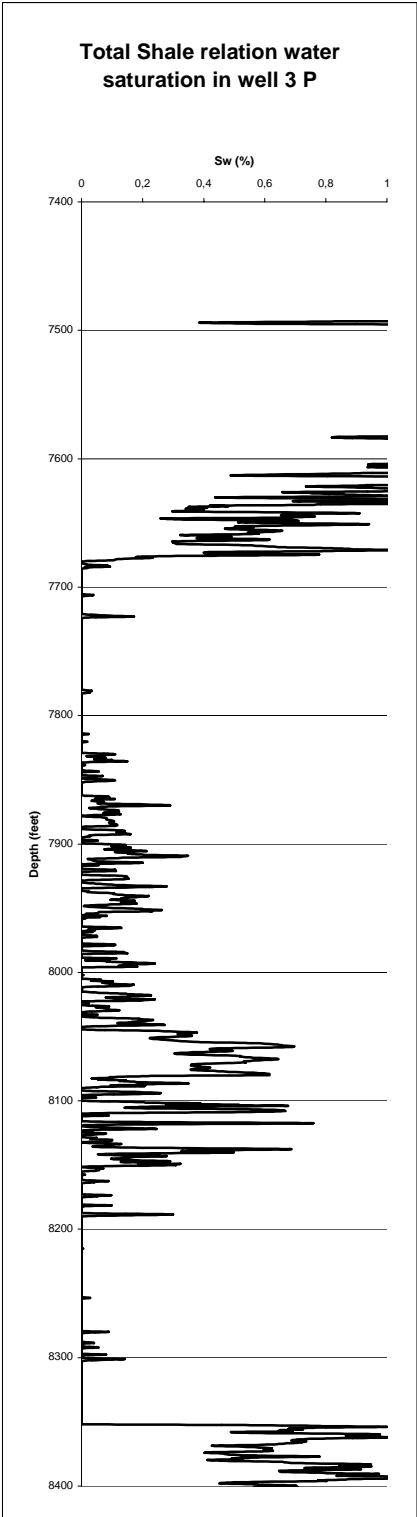
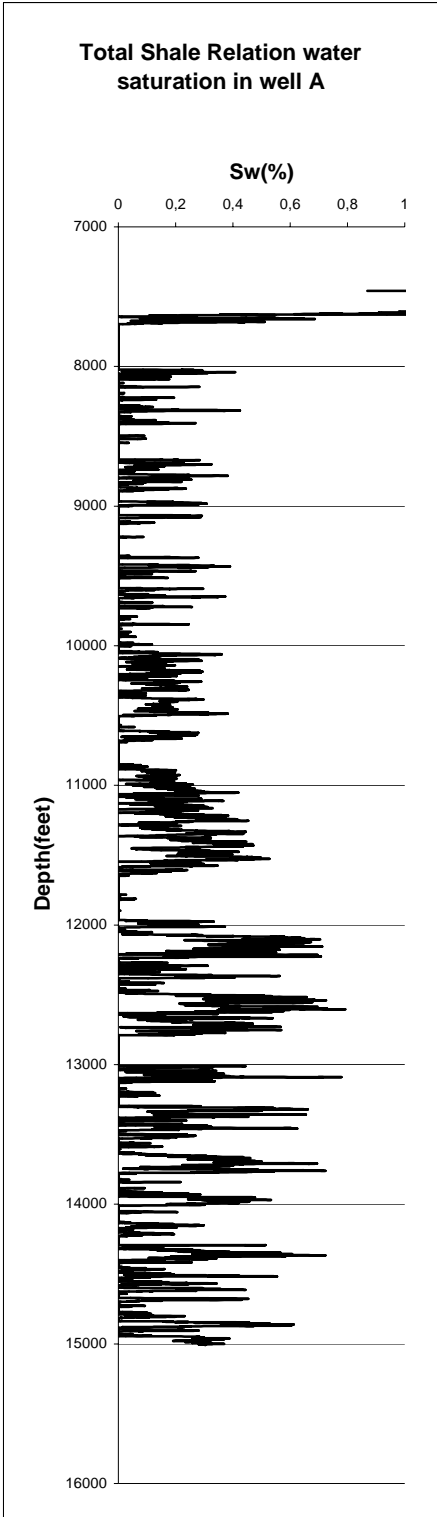
Well # 03 A is deviated vertically drilled well and well # 3 P is vertically drilled well. It was necessary to interrelate the layer of similar resistivity R_t to make water saturation comparison in both well, in absence of DVT log. Water saturation results calculated in both well by different model are given in table. In well # 3A depth at 7800- 11000fts and at depth 11000 to 150000 fts corresponds to depths at 7750 to 8050 fts and 8050 to 8300 fts respectively in well # 3 P. Water saturation is almost identical in upper zone of formation for each water saturation method. In lower zone in well 3 P water saturation calculated by Archie's method and Cyber look program is higher to some extent than well 3 A. Comparison of each method water saturation results in both wells in both well are given in table (5.1) and in water saturation logs in figures on proceeding pages.

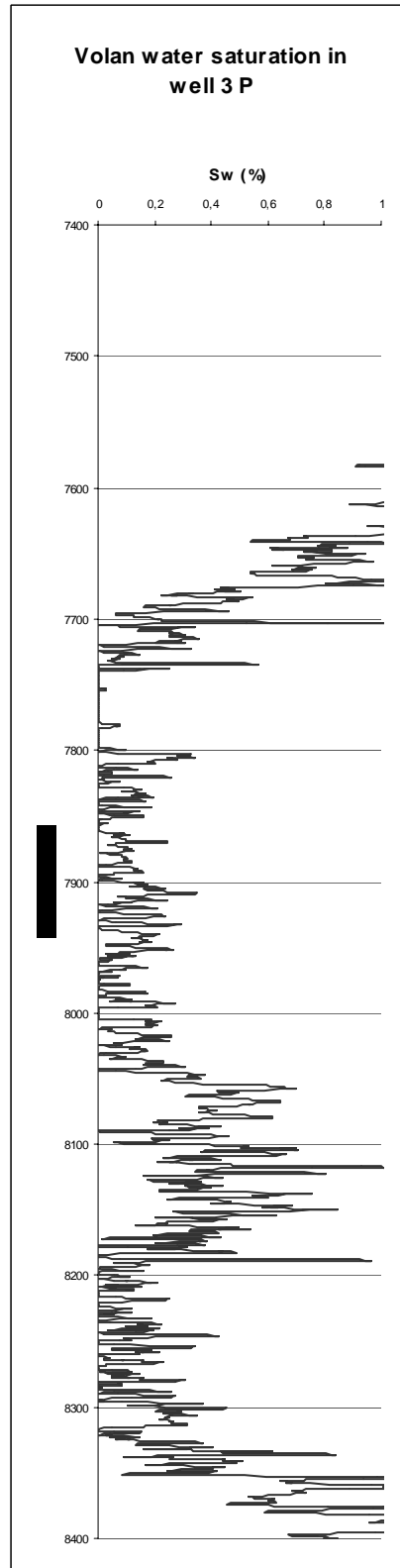
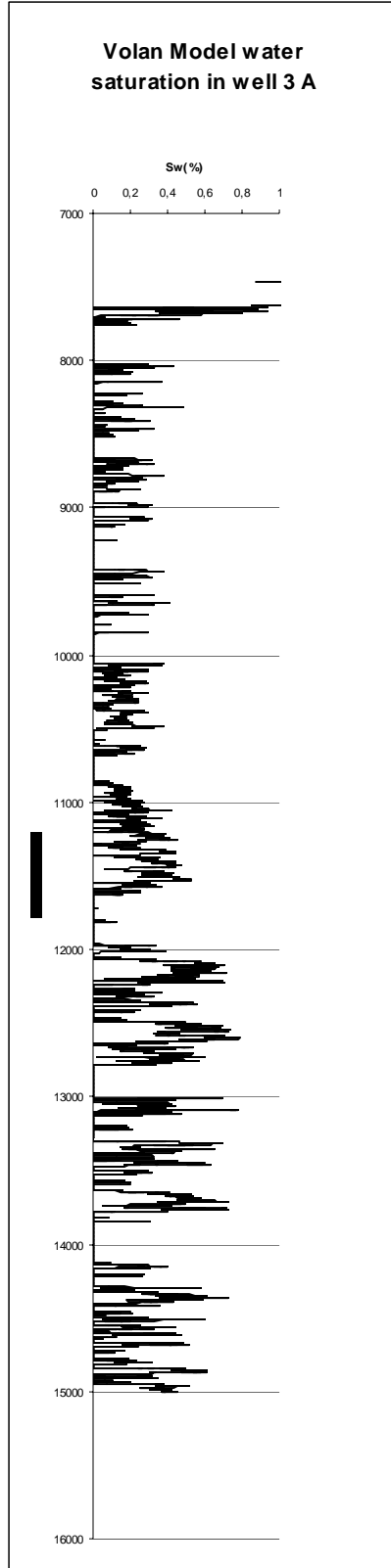
Table 5.1: Water saturation comparison between well 3 #A and well # 3 P obtained by different water saturation methods

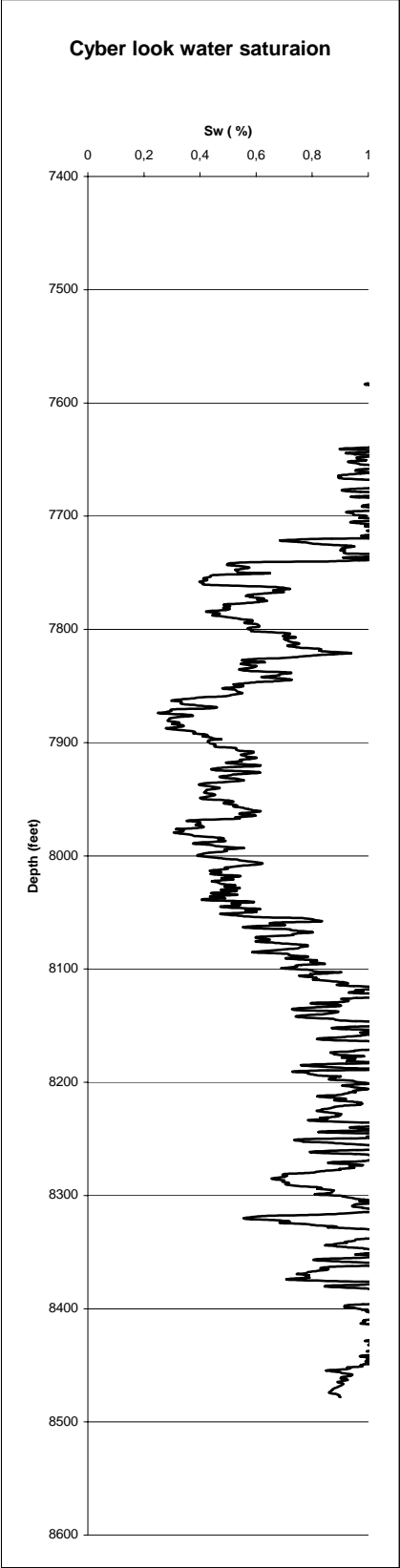
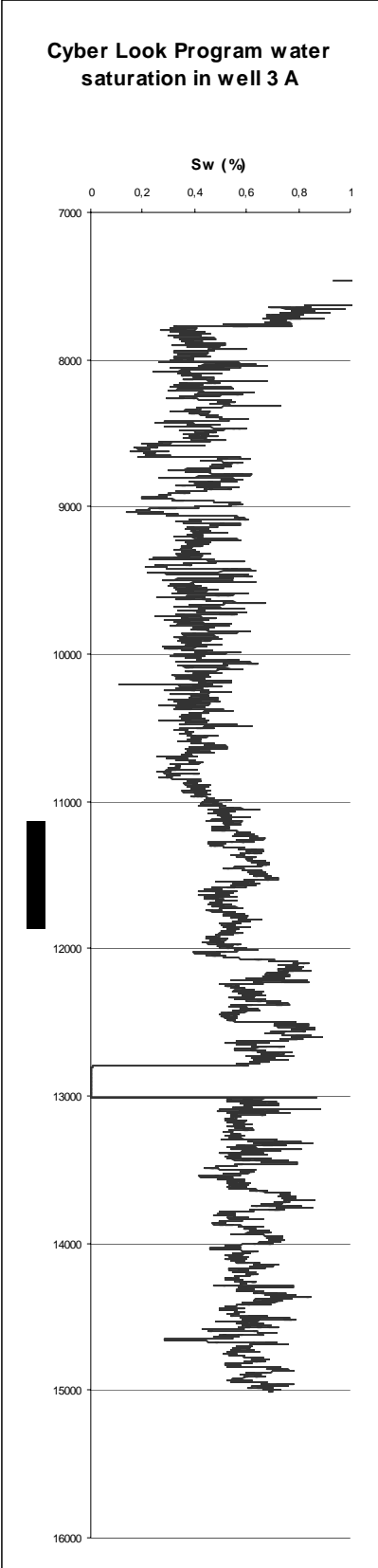
3 A well (deviated drilled well)			3 P (vertically drilled well)	
Name of method	S_w at depth 7800 to 11000 fts (upper zone)	S_w at depth 11000 to 15000 fts (lower zone)	S_w at depth 7750 to 8050 (upper zone)	S_w at depth 8050 to 8300 fts (lower zone)
Waxman and Smits equation	0 to 25 %	30 to 60 %	0 to 25 %	30 to 80 %
Laminated Sand and Shale Model	0 to 35 %	0 to 65 %	0 to 35 %	0 to 65 %
Total Shale Relation	0 to 15 %	0 to 50 %	0 to 15 %	0 to 50 %
Volan Model	0 to 15 %	0 to 50 %	0 to 15 %	0 to 50 %
Cyber Look Program	35 to 50 %	50- 70	35 to 55 %	75 to 100 %
Normalised Waxman and Smits equation	0 to 15 %	0 to 50 %	0 to 15 %	0 to 50 %
Archie's Model	35 to 60 %	60 to 85 %	35 to 65 %	75 to 100 %
Dispersed Shale Simplified model			5 to 35 %	50 to 100%

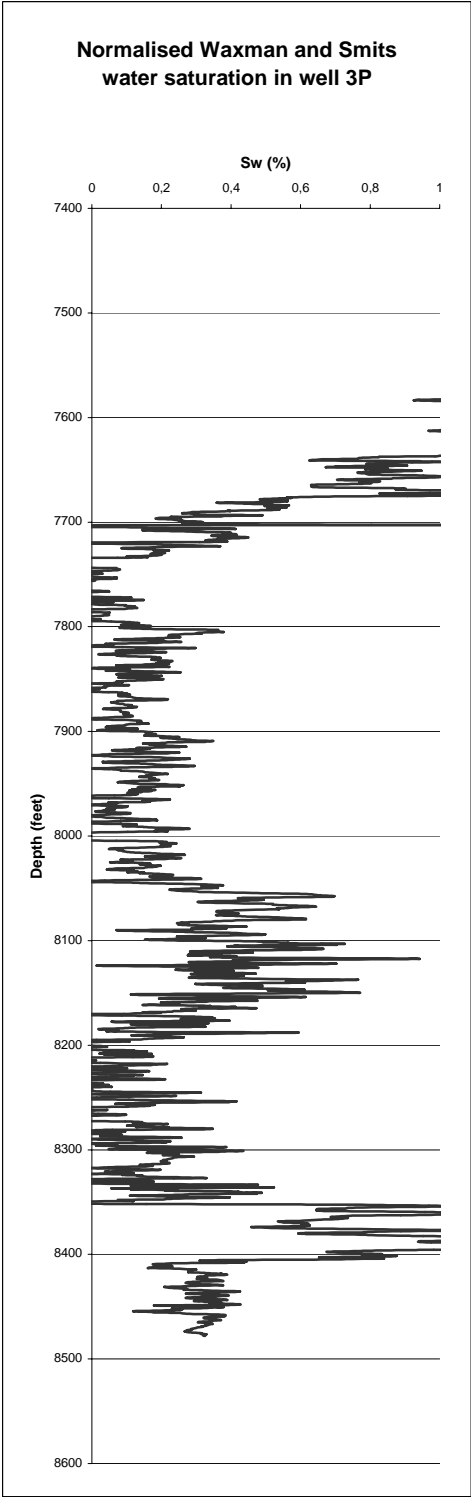
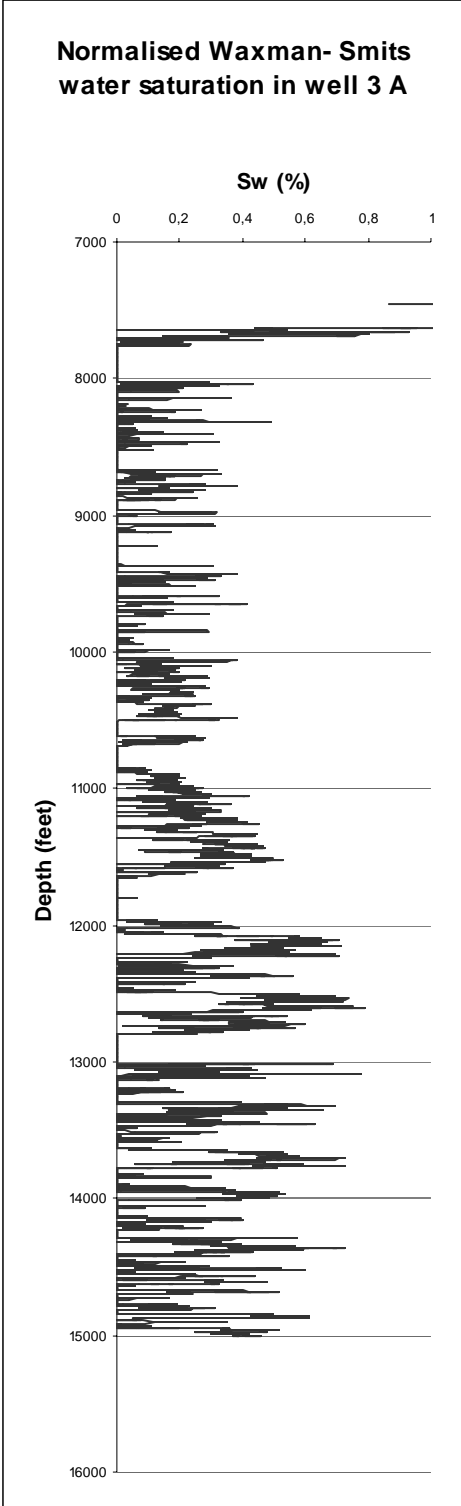


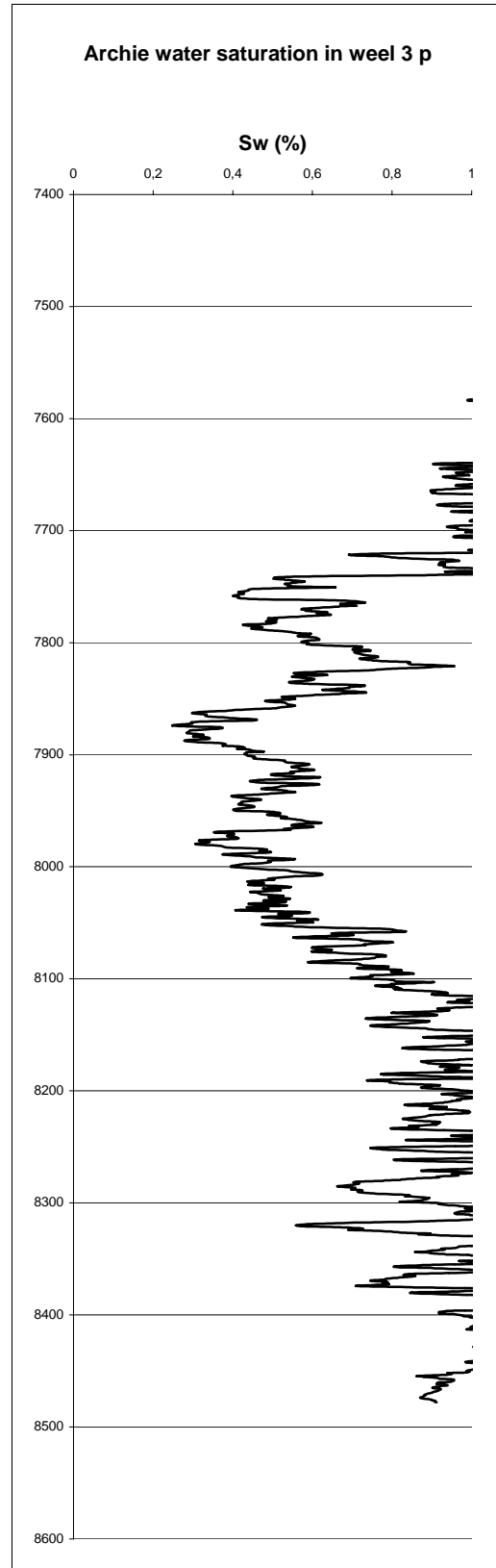
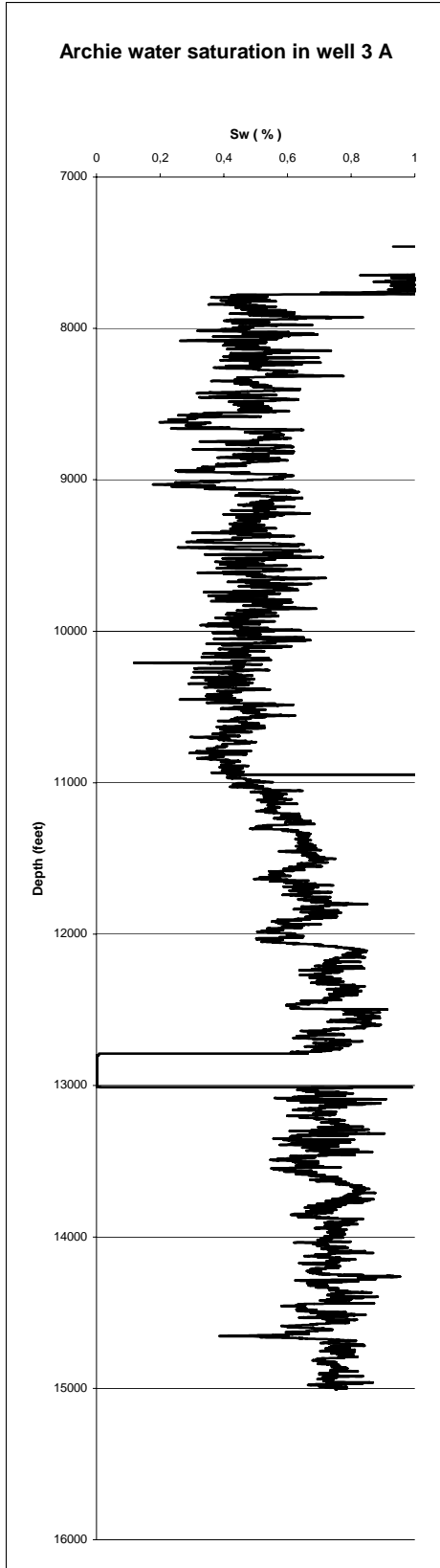


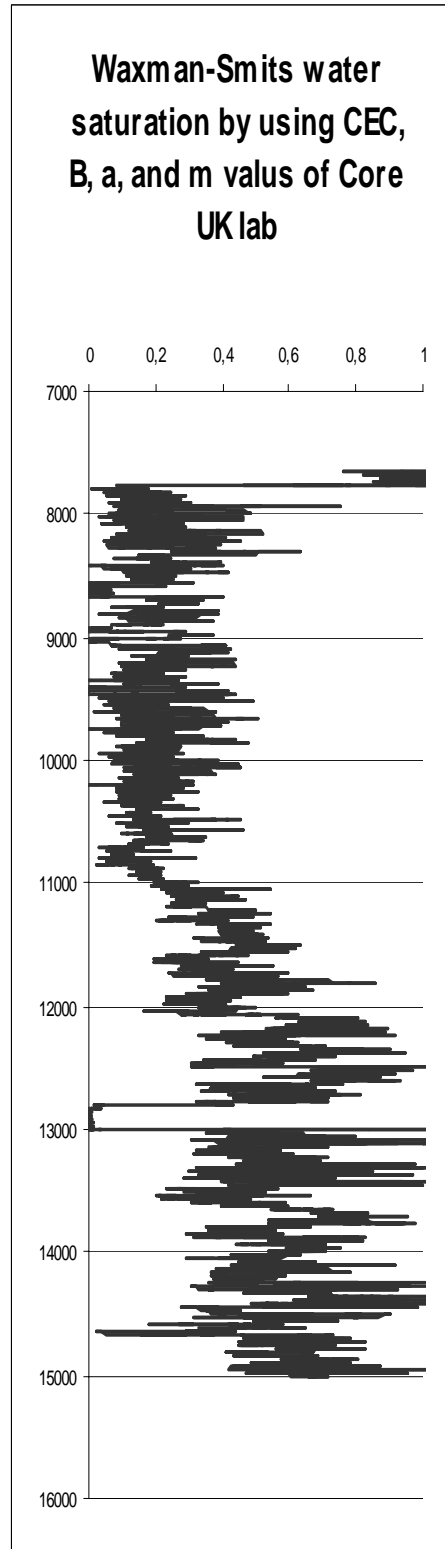
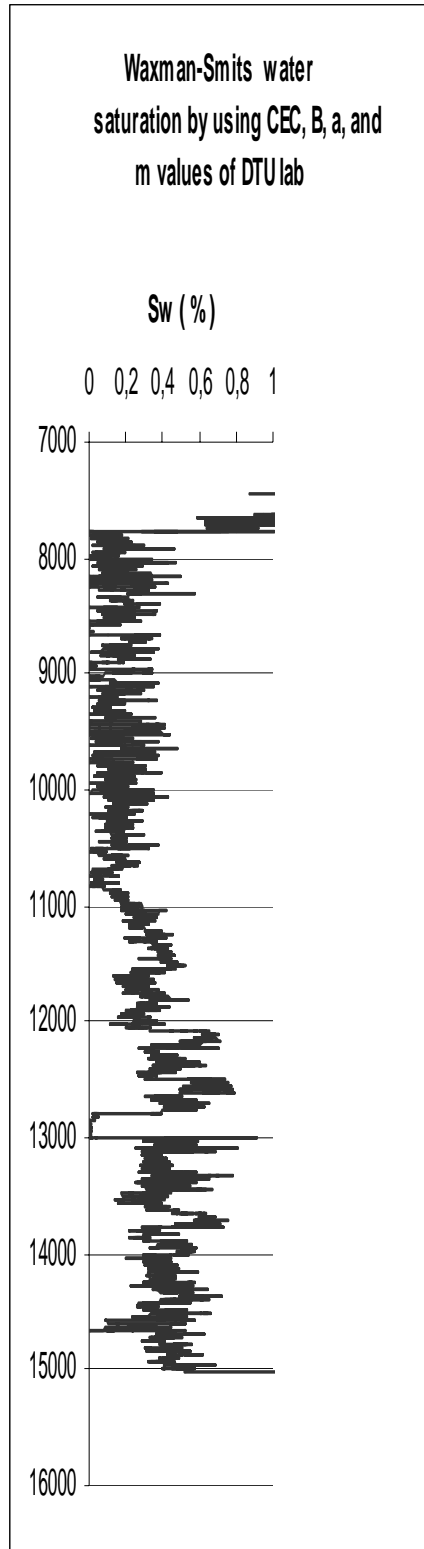


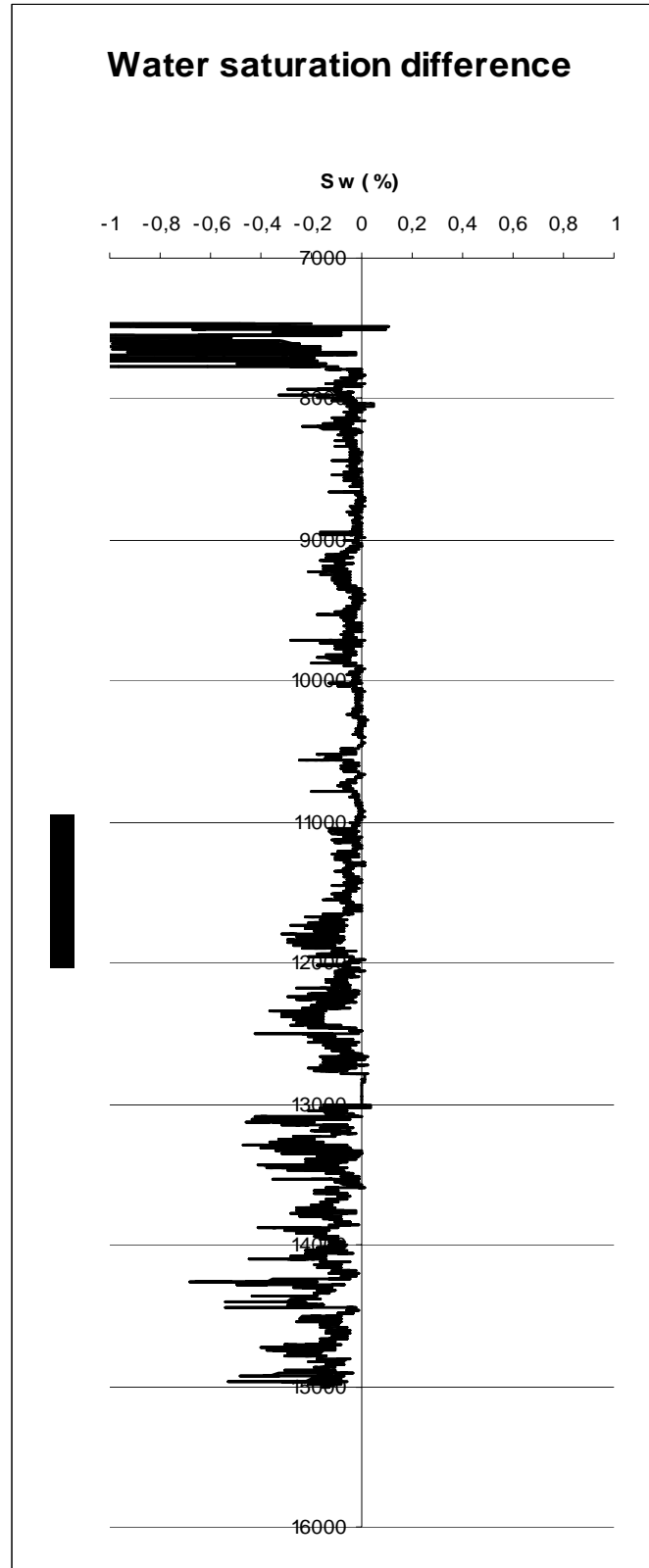












Waxman and Smits water saturation difference between DT Lab. results and Core Lab. (UK) results.

The water saturation obtained is lower by using DTU lab CEC results than water saturation obtained by Core Lab. (UK) CEC data.

6 Conclusion

X-ray study of core samples have characterized the reservoirs as limestone, containing with the impurities illite clay and silica.

Correct estimation of conductivity contribution of shale to total formation conductivity in addition to formation water conductivity is very important in determining water saturation in formation.

From the comparison of water saturation results between Waxman and Smits saturation resistivity relationship and rest of the water saturation determination methods used in this study, the following results can be concluded.

Higher the true conductivity of formation; higher will be water saturation and vice versa. Laminated Sand and Shale only consider the volume of shale, and not the type of shale. This model can work better well, when fine and pure clay is present in formation. In that case shale conductivity predicted by V_{lam}/R_{sh} in Laminated Sand and Shale Model may be comparable to conductivity contribution estimated in Waxman and Smits equation by measuring the CEC of sample. But in case of shale containing coarse clay like, kaolinite and illite and silica and conductivity contribution predicted on the basis of volume and conductivity of shale would always be higher than the actual conductivity contribution made by the clay.

Dispersed shale simplified model water saturation results resemble to Waxman and Smits water saturation result at depth 7750 to 8050fts in well 3 P which means that this model is relatively close to Waxman and Smits equation.

Regarding, Volan model, which consider bound water conductivity instead of shale conductivity also overestimate shale conductivity contribution, and predict lower water saturation. Archie water saturation equation is generally applicable to determine S_w in clean formations.

Cyber look program use the 100 % water being shaly formation conductivities, which estimate conductivity contribution of shale very low, resulting higher water saturation.

Normalised Waxman and Smits equations, also does not take in to account the type of shale, so conductivity contribution by shale is not accurate, and giving not appreciable water saturation results.

Difference in water saturation result between Waxman and Smits and rest of model is relatively smaller at depth 7800 to 11000 fts in well as shown in table (4.2) that is identified as relatively less clay area as compared to lower zone at depth 11000 to 15000 fts which means that conductivity contribution of clay in high shaly formations predicted by other water saturation method is no more comparable to actual conductivity contribution given by Waxman and Smits equation.

Inter comparison of well 3A and 3 P shows that region at depths from 7800 to 11000fts and 11000 to 15000fts of 3A well correspond to depth 7750 to 8050fts and 8050 to 8300fts respectively.

Depth 8300fts in well 3P is deeper than deviated well 3A.

Water saturation results obtained by different methods in both well are almost similar in upper zone i.e., at depth 7800 to 11000 fts in well 3A and 7750 to 8050 fts in 3 P well almost identical but differ to some extent to in lower zone of both well. No model is substitutive of Waxman and Smits saturation equation in shaly formations containing high quantity of coarse clay.

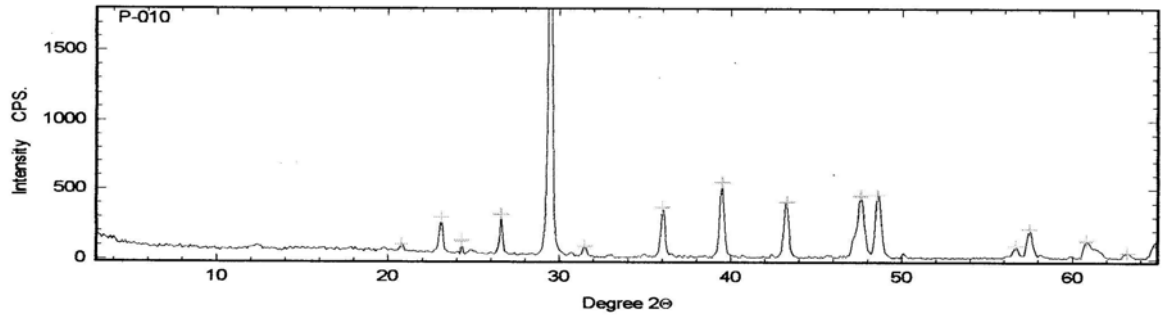
7 References

- 1 D. Bush and R. Jenkins: "Proper Hydration of Clays for Rock Property Determinations", J. of Pet. Technology, July 1970.
- 2 J.T Dewan: "Modern Open-Hole Log Interpretation" (Pen Well Publishing, 1983).
- 3 Worthington, A.E. and Meldau E.F: "Departure Curves For Self Potential Log", J. Pet. Tech, 1958.
- 4 Baldwin, J.L., Quirein, J.A., and Serra, O: "Theory and Practical Application of Natural Gamma Ray Spectroscopy", Trans., 1980 SPWLA Annual Logging Symposium.
- 5 A. Poupon, C. Clavier, J. Dumainor, R. Gaymard and A. Misk: "Log Analysis of Sand-Shale Sequences, A Systematic Approach", JPT, pp 867-881, July, 1970.
- 6 Poupon et al; Log Analysis in Formation with Complex Lithologies. J. Pet.Tech; Aug. 1971, pp995-1005.
7. Susan, L. Herron and M.H Micheal: "Quantitative Lithology: An Application for Open and Cased Hole Spectroscopy". SPWLA, 37th Ann. Sym.. June 16-19,1999.
8. Coates, Schulze and Throop: "VOLAN- AN Advanced Computational Log Analysis". 23rd SPWLA, Jul. 6-9, 1982.
- 9 Clavier, C. Coates, G. and Domanior: "The Theoretical and Experimental Bases of Dual Water Model for interpretation of Shaly Sands". SPE paper 6859,1977.
10. Clavier, C. Coates, G. and Domanior: "The Theoretical and Experimental Bases of Dual Water Model for interpretation of Shaly Sands". J.24, 1984.
- 11 Juhaz: "The Central role of Qv and Formation-Water Salinity in The Evaluation of Shaly formations", SPWLA, 20th Annual Logging Symposium, june 3-6, 1979.
- 12 P.F Worthington: "The Evaluation Shaly-Sand Concepts in Reservoir Evaluation", Log Analyst, 1985.
- 13 Mohammad A. Mian and Douglas W. Hilchie: "Comparison of Results from Three Cation Exchange Capacity (CEC) Analysis techniques" Log Analyst, 1982.
- 14 R.R Davis, J.E Hall., Flaum, C., L.Y Boutmey: "A Dual Porosity CNL Logging System", SPE Paper 10296, SPE Annual Technical Conference and Exhibition, 1981.
- 15 R Gaymard and A Poupon: "Response of Neutron and Formation Density Log in Hydrocarbon bearing Formations" The Log Analyst Sep-Oct 1968.
- 16 Barber T.D: "Introduction of Digital Dual Induction tool", Paper SPE 12049, Annual technical Conference, 1983
- 17 Moran, J.H. and Kunz: "Basic Theory of Induction Logging" Geophysics (1962).
- 18 Log Interpretation Charts, Schulmberger Well Service, Houston (1989).
- 19 Dunlap, H.F. and Hawthorn, R.R: "The Calculation of Water Resistivity From Chemical Analysis", Trans., AIME (1951)192.
- 20 Moore, E.J., Szasz, S.E., and Whitney, BF: "Determining Formation Water Resistivity From Chemical Analysis", J. Pet. Tech.(March 1966
- 21 Log Interpretation Charts, Schulmberger Well Service, Houston (1989).
- 22 G.E Archie: "The Electrical Resisitvity as an Aid in Determining Some Reservoir Characteristics", JPT, Jan; 1942.
- 23 G.E Archie: "Classification of Carbonate Reservoir Rocks and Petrophysical Considerations", Bull., AAPG, Feb, 1952, No.2.
- 2 4 Waxman M. H. and Smits, L. J.M. 1968. Electrical Conductivities in Oil-Bearing shaly Sand. Society of Petroleum Engineers, Journal 8, 107-122.

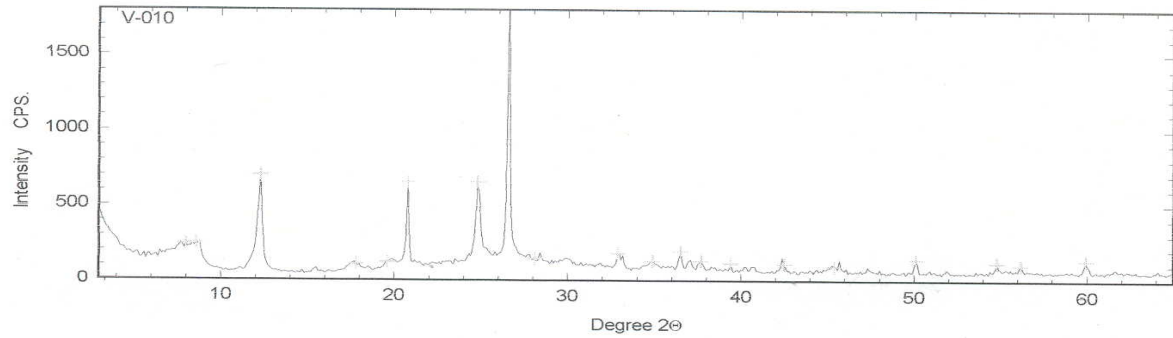
- 25 Poupon and Leveaux "Evaluation of Water Saturation in Shaly Formations", SPWLA 12th Ann. Sym; 1971.
- 26 Yuan and Diederix: "Role of Membrane Potential Measurements in Shaly Sand Evaluation", Log Analyst, Nov-Dec; 1989.
- 27 Waxman and Thomas: Electrical Cond. In Shaly Sands: "Relation between Hydrocarbon Saturation and Resistivity", JPT, Feb; 1974.
- 28 D. L Best and J.L Dumanior: "A COMPUTER-PROCESSED WELLSITE LOG COMPUTATION", SPE Paper 9039,1980.
- 29 Juhasz, Normalized Qv- The key to Shaly Sand Evaluation using Waxman- Smits Equation in the Absence of Core Data, SPWLA 22nd Annual Logging Symposium, 1981.

- 30 A Sibbit and C Mayer: "GLOBAL, A New Approach to Computer processed Log Interpretation" SPE Paper 9341, Annual Technical Conference and Exhibition, 1980.
- 30 G Tao and W Yue: "Electrical Transport properties of Fluid Saturated Porous Rocks by 2D Lattices Gas Automota" SPE Paper 88535, SPE Asia Pacific Oil and Gas Conference and Exhibtion, Pert Austeralia, October, 2004.
- 31 Z.A Bassiouni and M.N Lau: "Development and Field Application of Shaly Sand Petrophysical Model Part III- Field Applications" , SPE Paper 20388, 1990.
- 32 Wharton,P Russel, Hazen, A Gray, Rau and N Rama: "Advancement In Electromagnetic propagation logging" SPE Paper 9041, 1980.
- 33 T Pritchard, N Colley and J Bedford, "The Quantification of Hydrocarbon Reservoir in Thinly laminated Shaly-Sandstone Formations" SPE Paper 81077, 2003.
- 34 H.H Yuan "Salinity Dependence of Shaly Sand Formation Resistivity Factor, F*" SPE Paper 22665, Annual Technical Conference and Exhibtion, October 1991, Dallas, Texas.
- 35 Z Bruce, H Jeffry and H Donald: "Water Saturation Estimation Using Equivalent Rock Model",SPE Paep 90143, SPE Annual Technical Conference and Exhibition, September 2004, Houston, Texas.
- 36 Deakin and JW Mark: " Wettability , Formation Resistivity Factor and Excess Conductivity" SPE Paper 16518, 1987.
- 37 Jin, Minquan, Sharma and M Mukul: "A Method for Shaly Formation Evaluation using a Single Membrane Potential Measurement" SPE Paper 23590, 1991.
- 38 A, hardwick: "X is: A New Shaly Parameter For Resistivity Log Evaluation" SPE Paper 19576, 1989.
- 39 P.F Worthington, Gaffaney and Cline "Improved Quantification of Fit –for-Purpose Saturation Exponents" SPE Paper 88950, 2204.
- 40 T.S Ara, S Talbani, Vaziri and M .R Islam "In Depth Investigation of Validity of the Archie Equation in Carbonate Rocks" SPE Paper 67204, 2001.

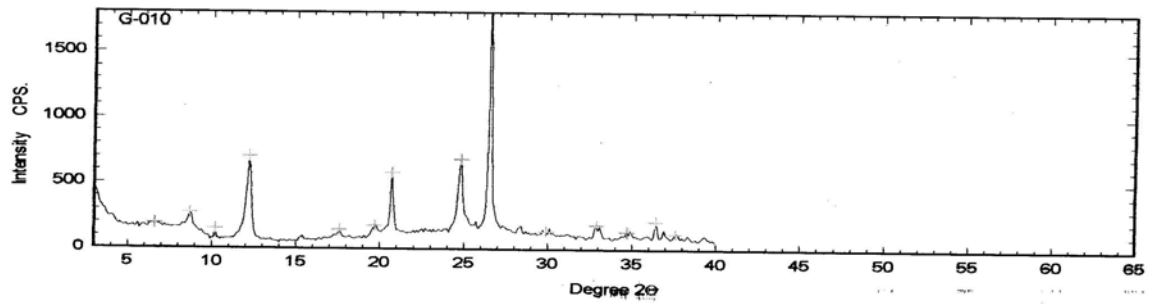
APPENDIX A
X Ray Diffractograms



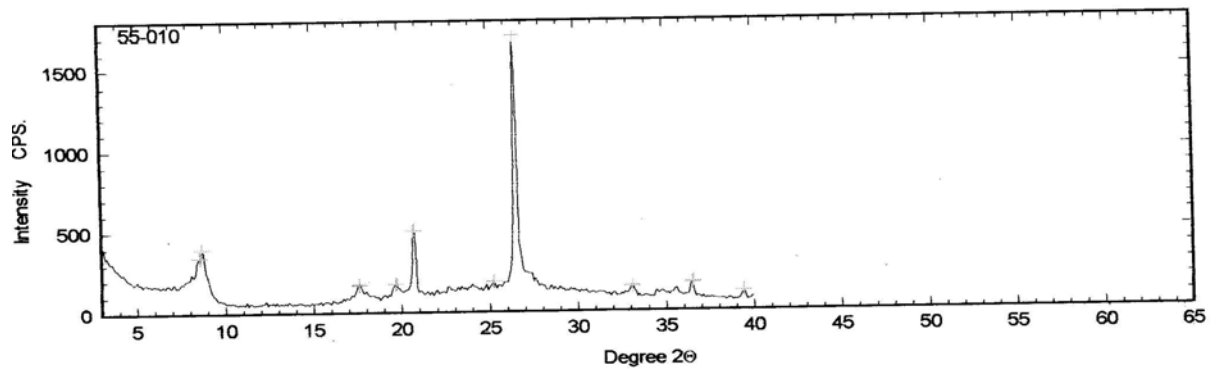
Diffractogram of dry powder chalk sample collected at depth 9351fts.



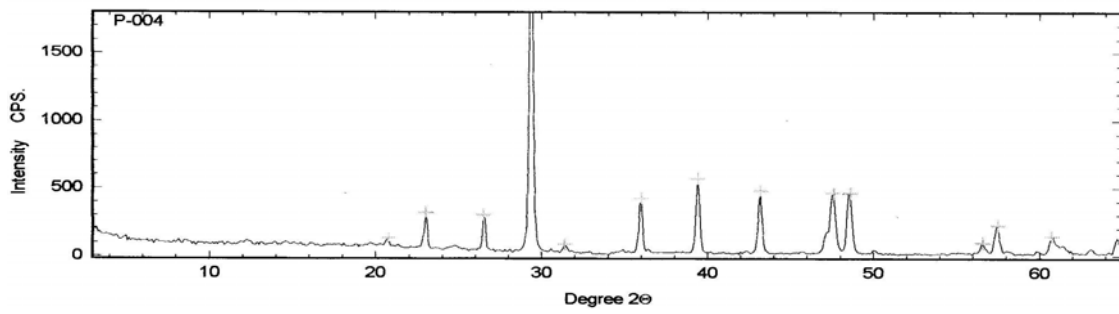
Diffractogram of IR of chalk sample collected at depth 9351fts saturated with water.



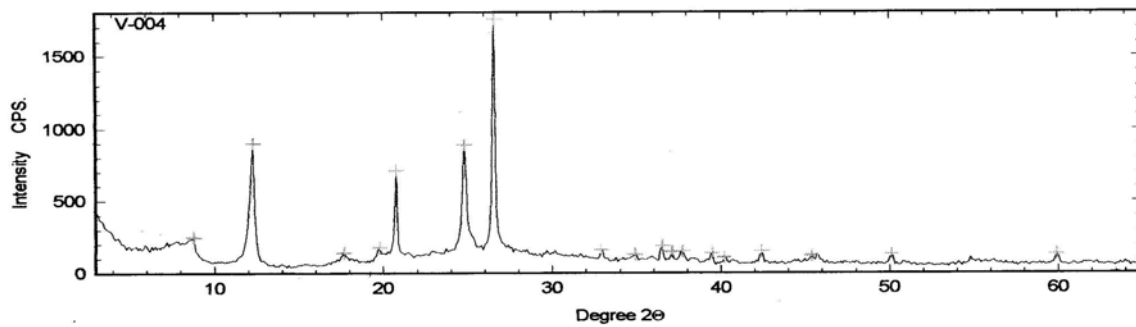
Diffractogram of IR of chalk sample collected at depth 9351fts treated with glycol.



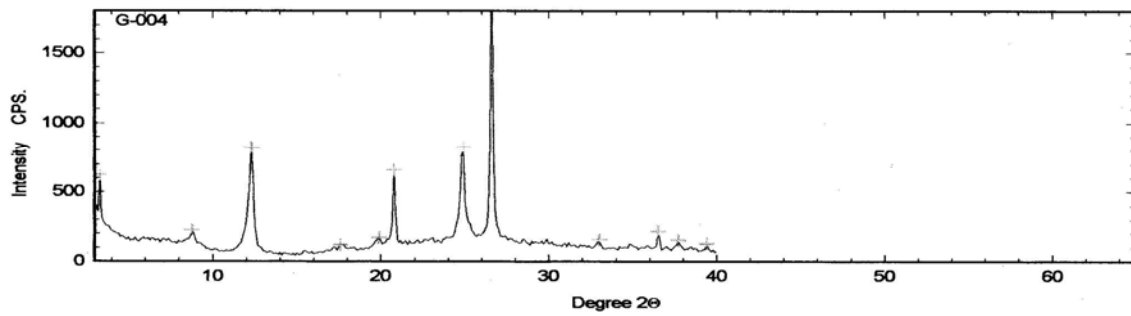
Diffractogram of IR of chalk sample collected at depth 9351fts heated at 550°C.



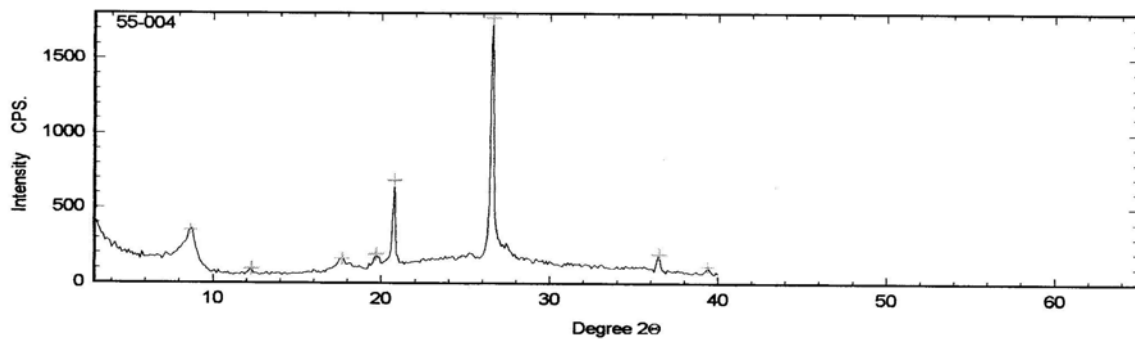
Diffraction pattern of dry powder chalk sample collected at depth 9251fts.



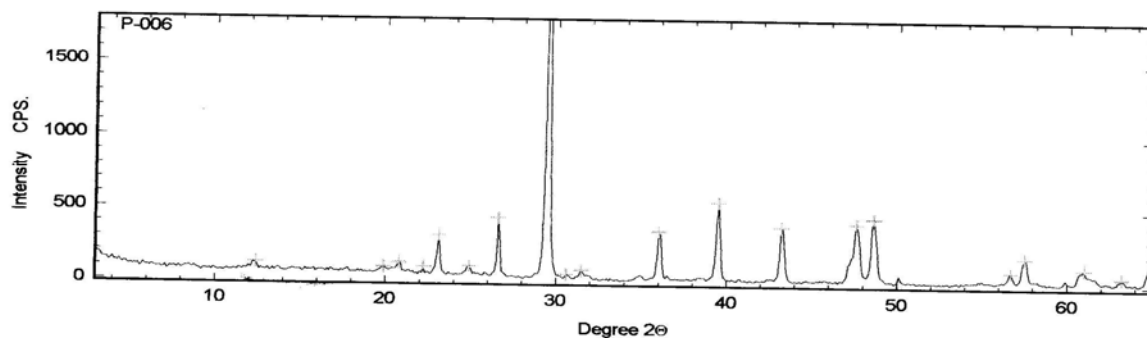
Diffraction pattern of IR of chalk sample collected at depth 9251fts saturated with water.



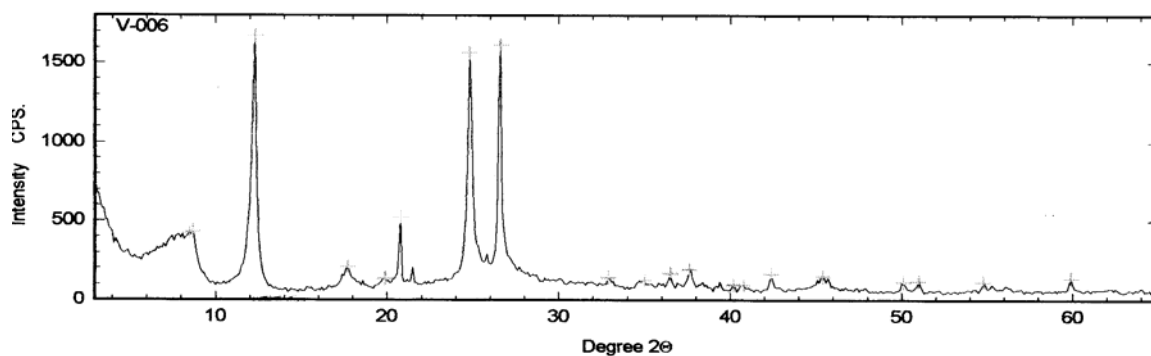
Diffraction pattern of IR of chalk sample collected at depth 9251fts treated with glycol.



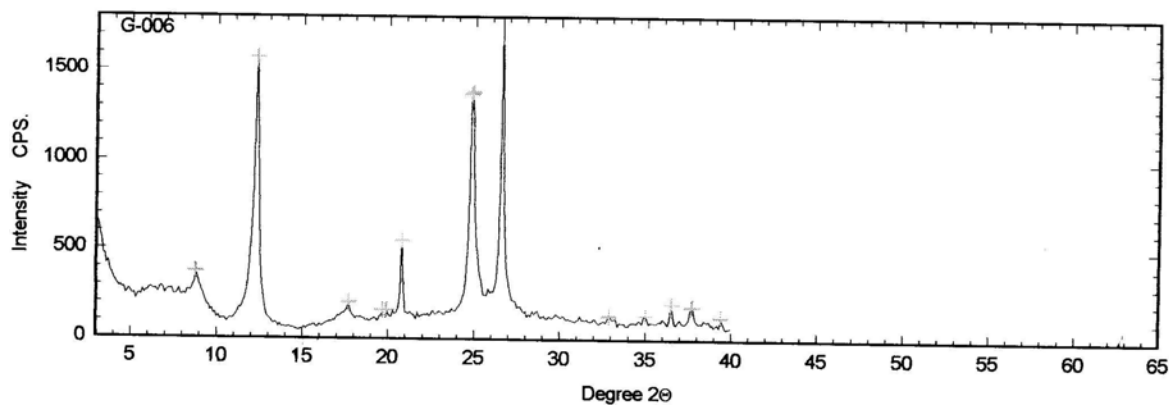
Diffraction pattern of IR of chalk sample collected at depth 9251fts heated at 550 °C.



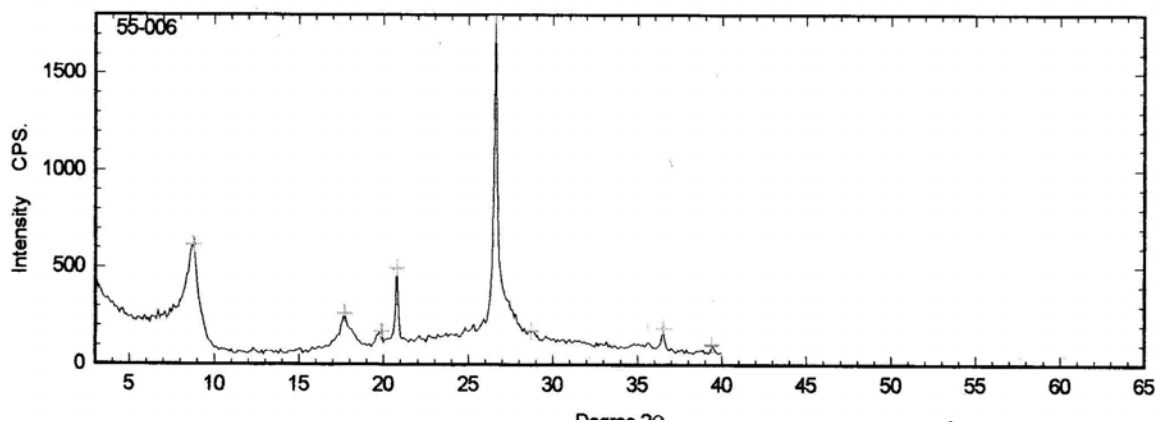
Diffractogram of dry powder chalk sample collected at depth 9242fts.



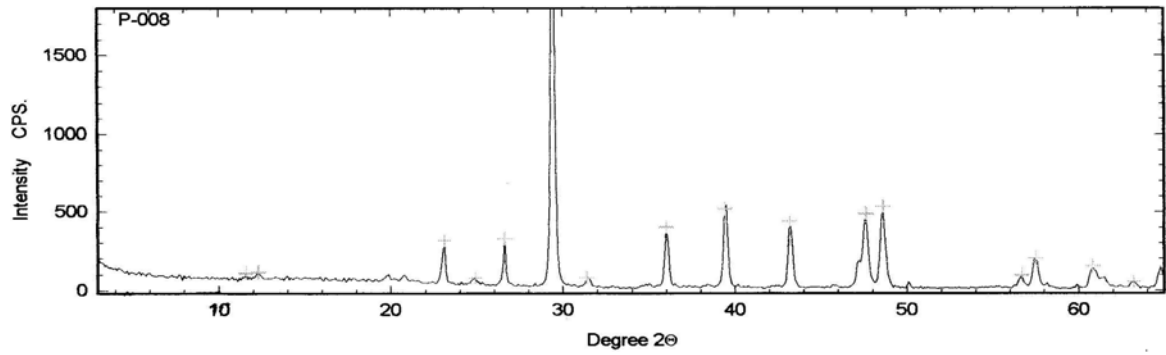
Diffractogram of IR of chalk sample collected at depth 9242fts saturated with water.



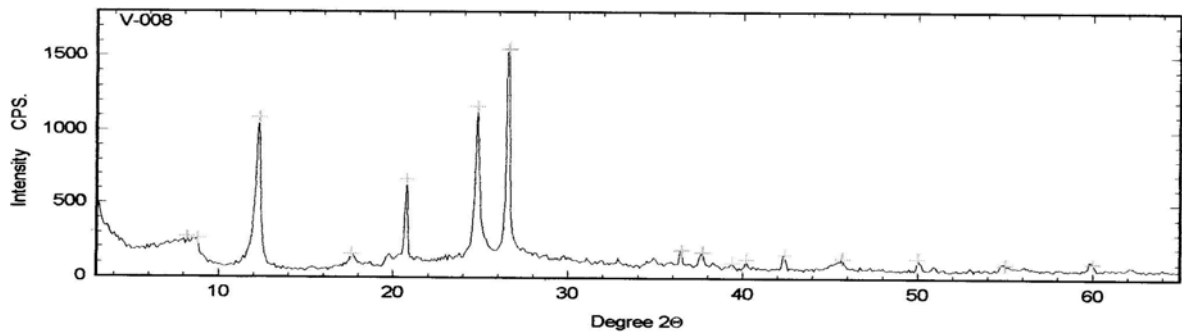
Diffractogram of IR of chalk sample collected at depth 9242fts treated with glycol.



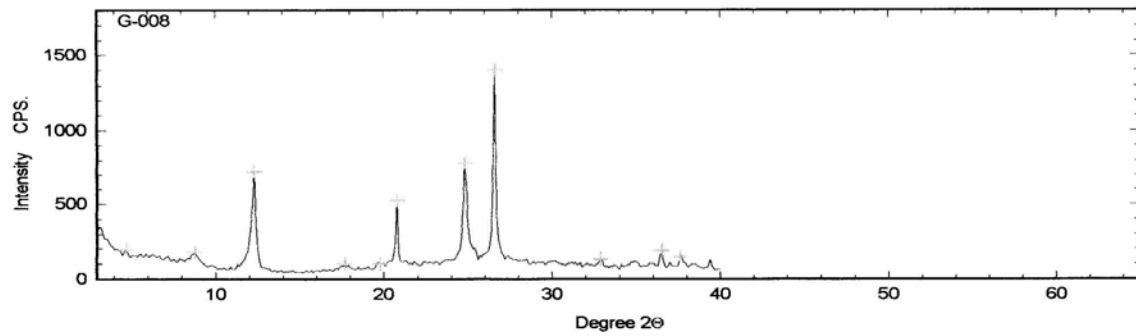
Diffractogram of IR of chalk sample collected at depth 9242fts heated at 550 °C.



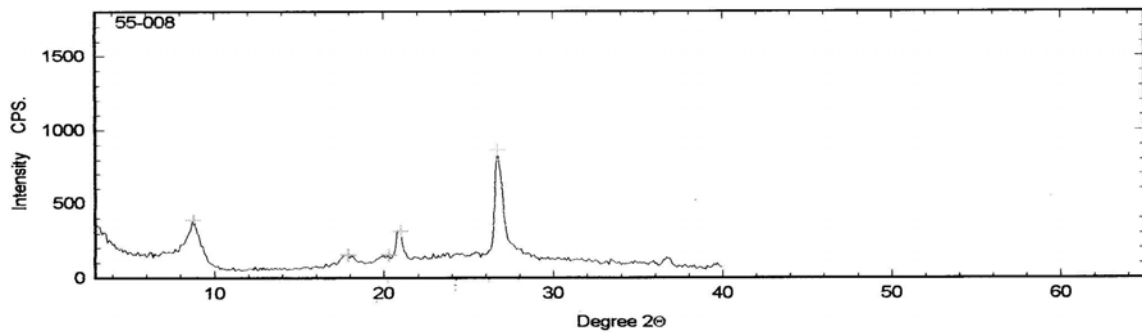
Diffractogram of dry powder chalk sample collected at depth 9254fts.



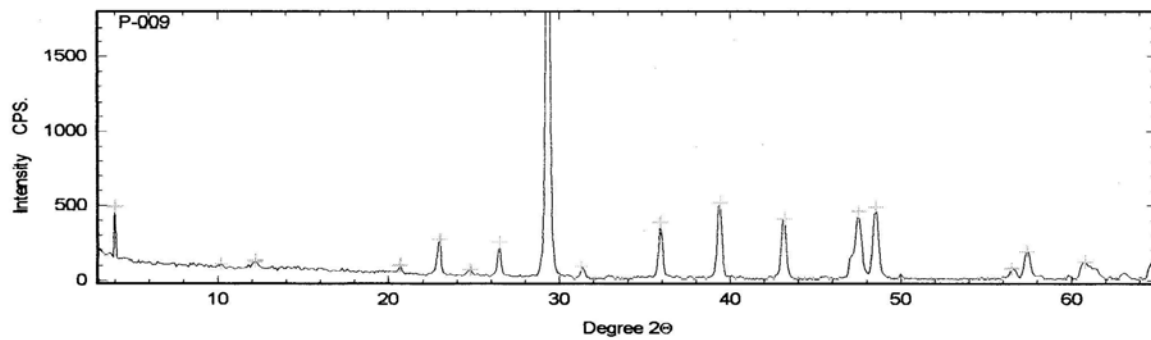
Diffractogram of IR of chalk sample collected at depth 9254fts saturated with water.



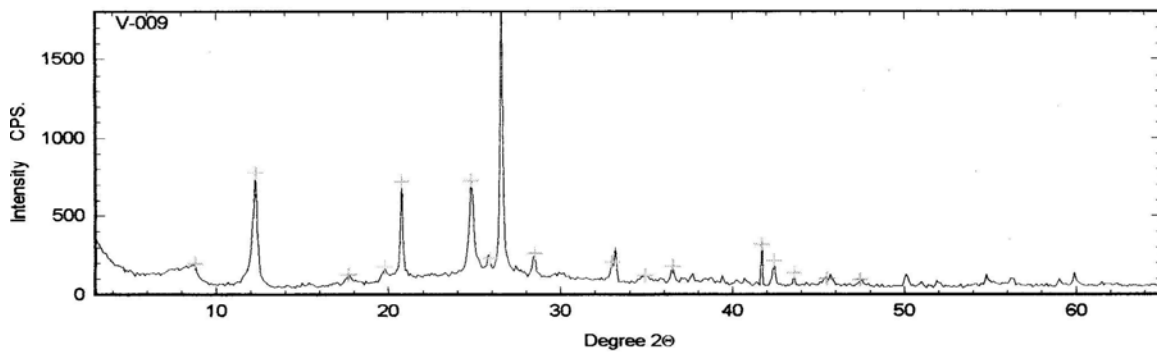
Diffractogram of IR of chalk sample collected at depth 9254fts treated with glycol.



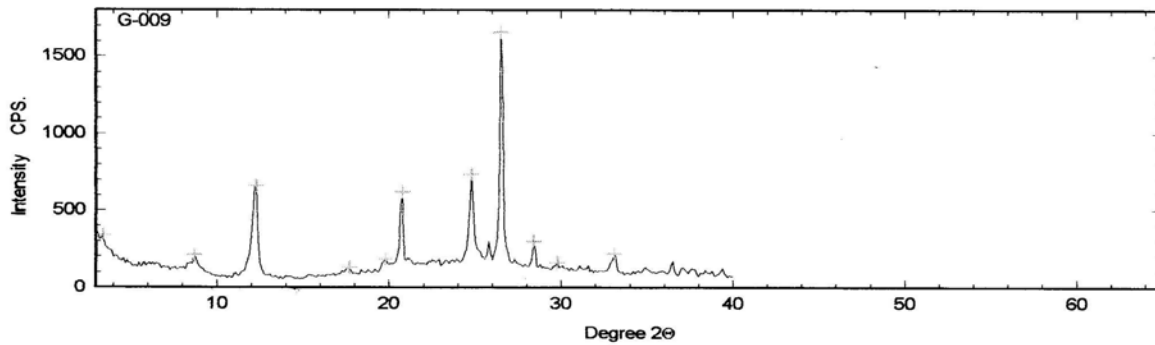
Diffractogram of IR of chalk sample collected at depth 9254fts heated at 550 °C.



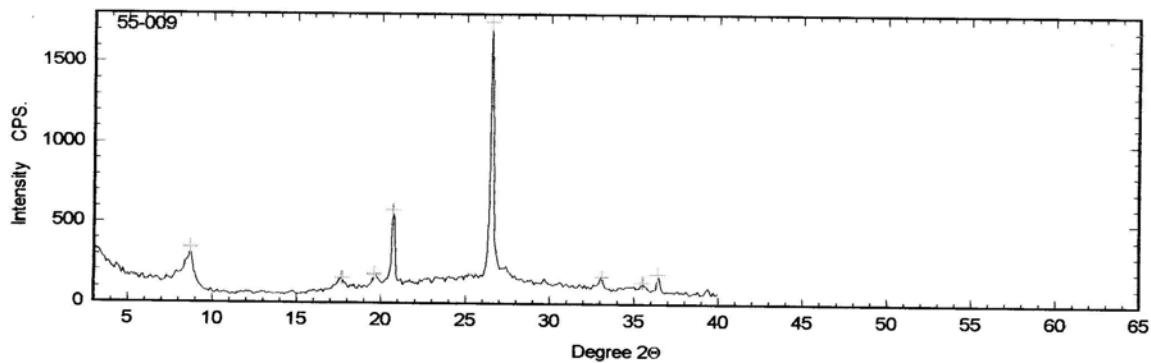
Diffractogram of dry powder chalk sample collected at depth 9352fts.



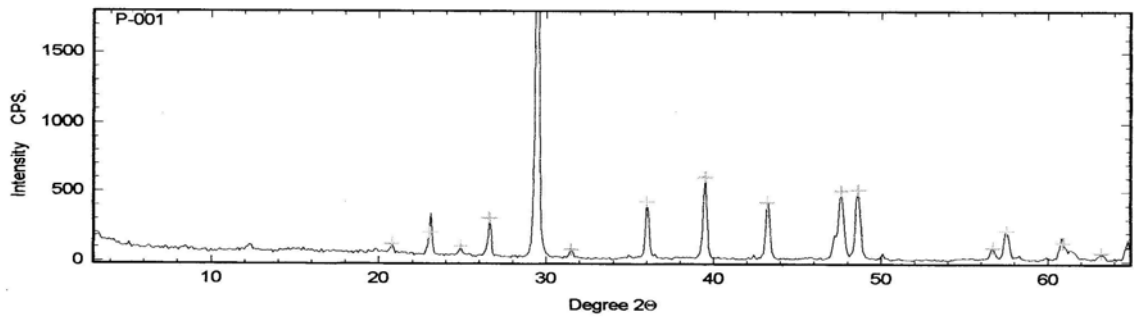
Diffractogram of IR of chalk sample collected at depth 9352fts saturated with water.



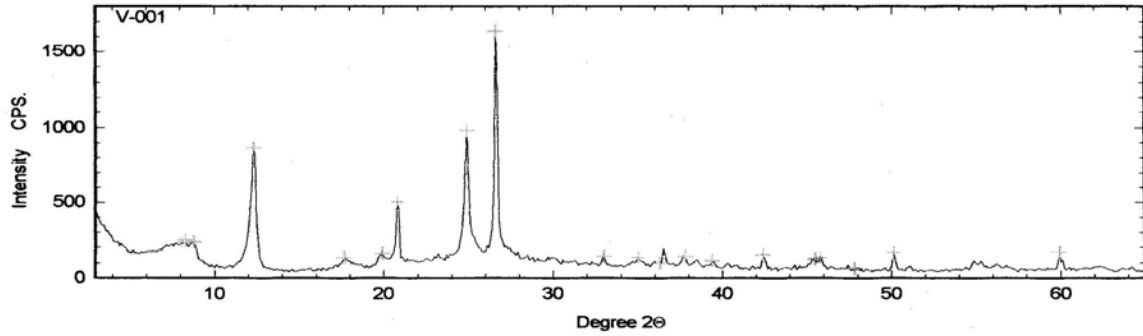
Diffractogram of IR of chalk sample collected at depth 9352fts treated with glycol.



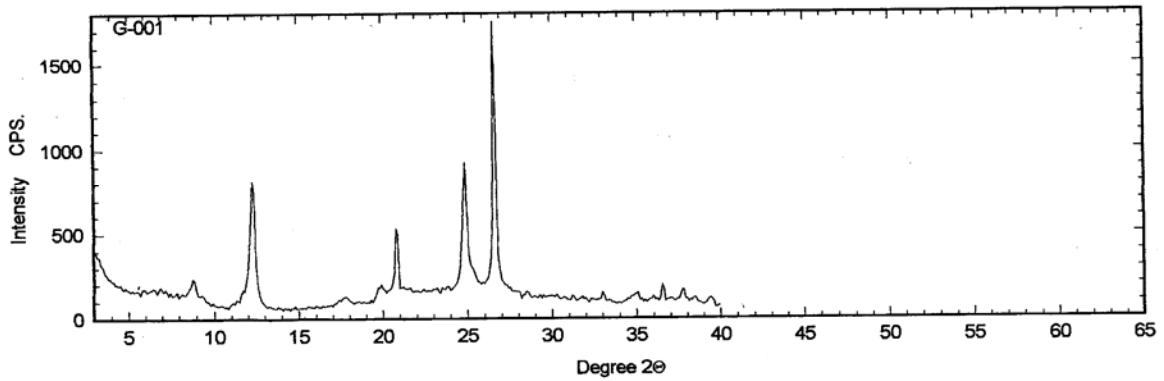
Diffractogram of IR of chalk sample collected at depth 9352fts heated at 550 °C.



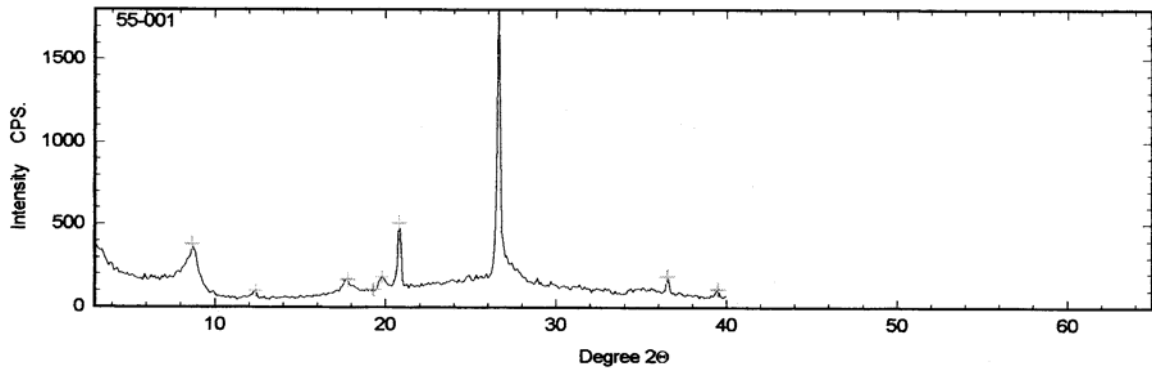
Diffractogram of dry powder chalk sample collected at depth 9238fts.



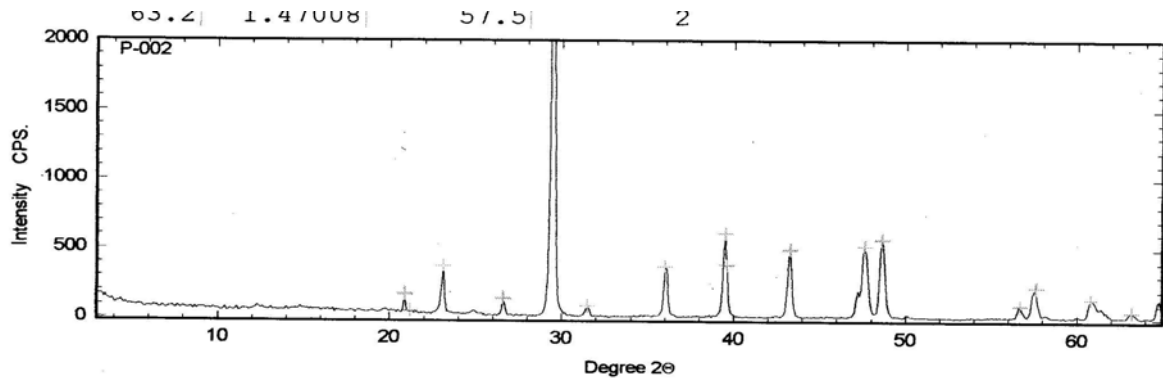
Diffractogram of IR of chalk sample collected at depth 9238fts saturated with water



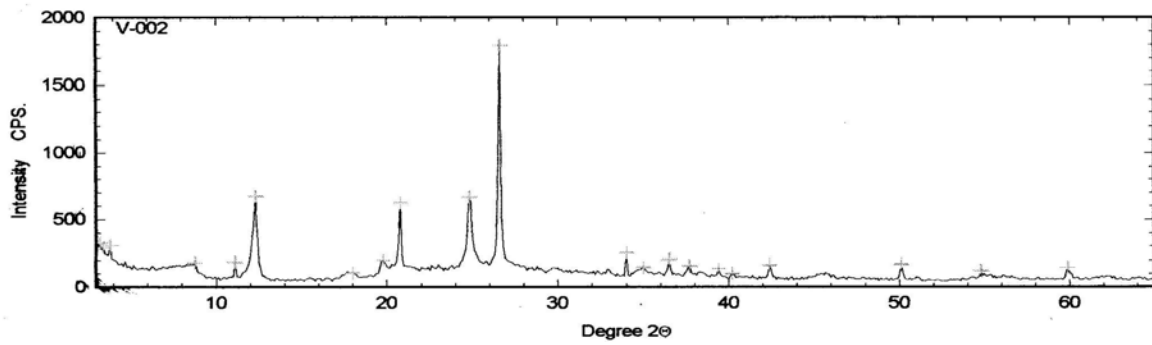
Diffractogram of IR of chalk sample collected at depth 9238fts treated with glycol.



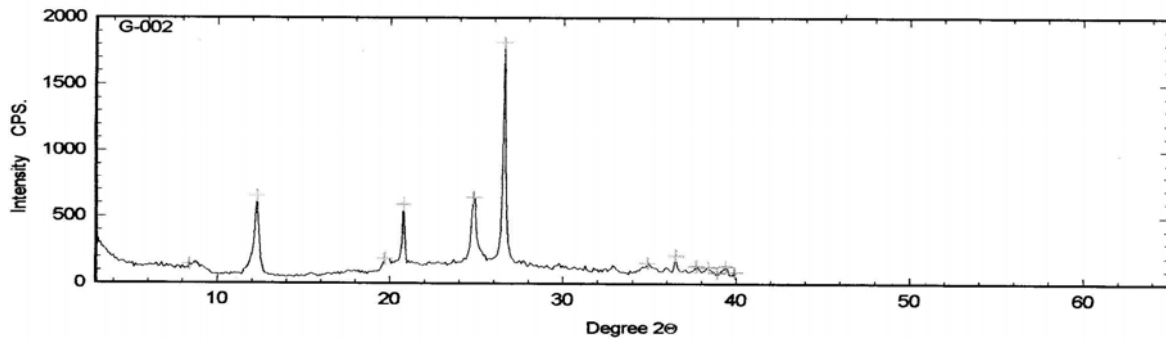
Diffractogram of IR of chalk sample collected at depth 9238fts heated at 550 °C.



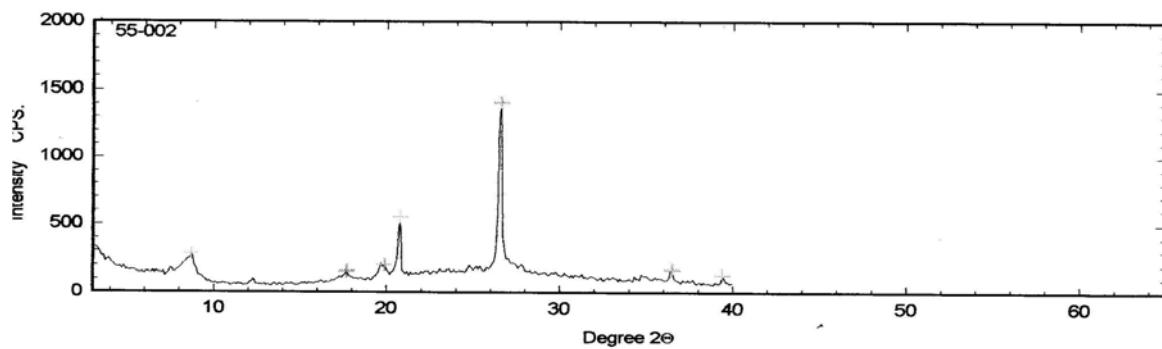
Diffractogram of dry powder chalk sample collected at depth 9368fts.



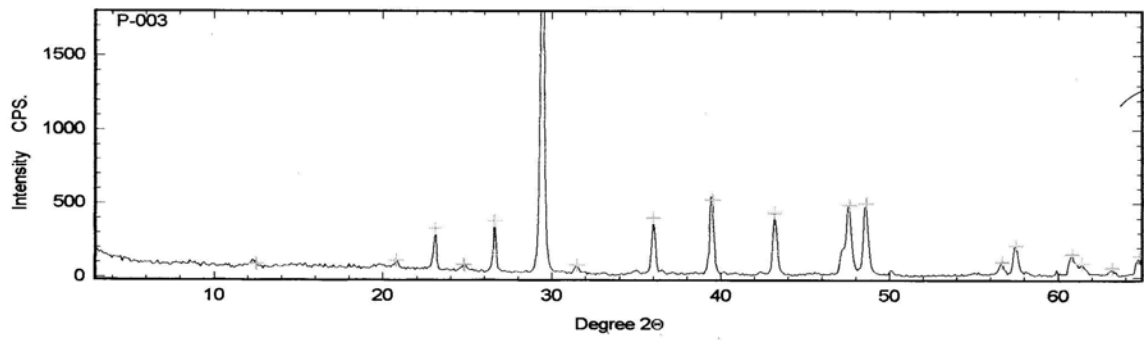
Diffractogram of IR of chalk sample saturated collected at depth 9368fts with water.



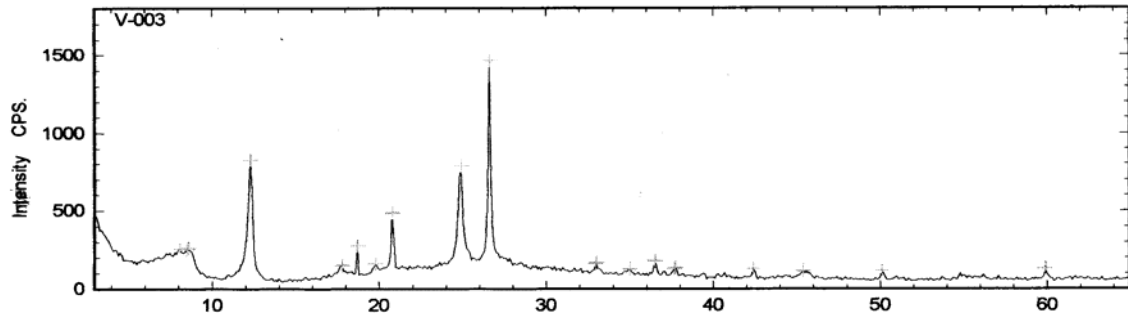
Diffractogram of IR of chalk sample with collected at depth 9368fts treated with glycol.



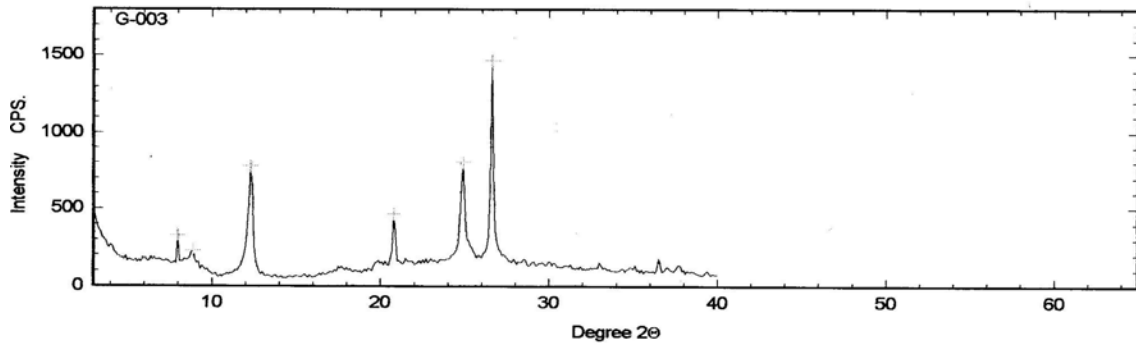
Diffractogram of IR of chalk sample collected at depth 9368fts heated at 550 °C.



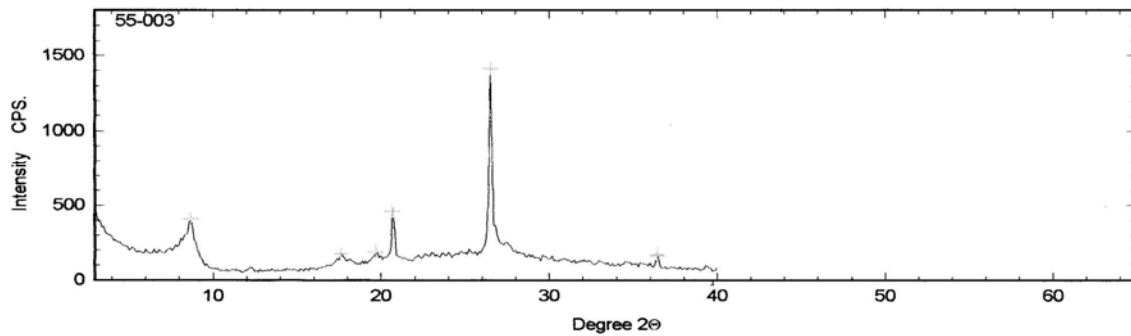
Diffractogram of dry powder chalk sample collected at depth 9256fts.



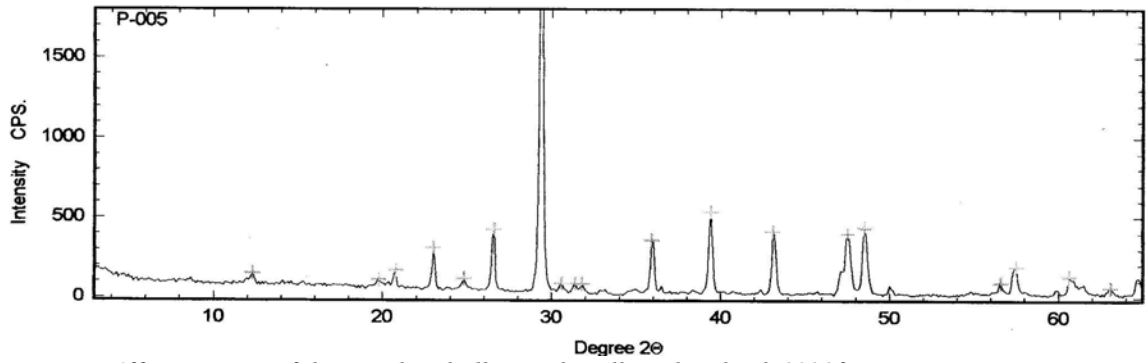
Diffractogram of IR of chalk sample collected at depth 9256fts saturated with water.



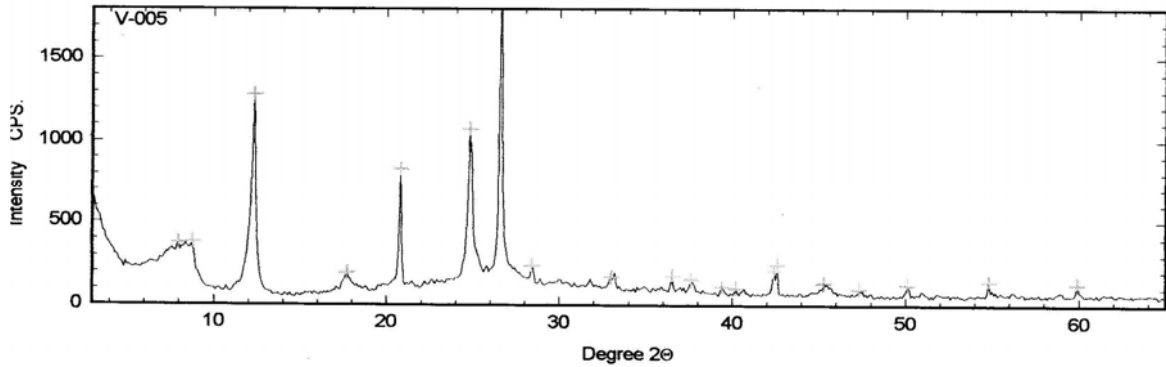
Diffractogram of IR of chalk sample with collected at depth 9256fts treated with glycol.



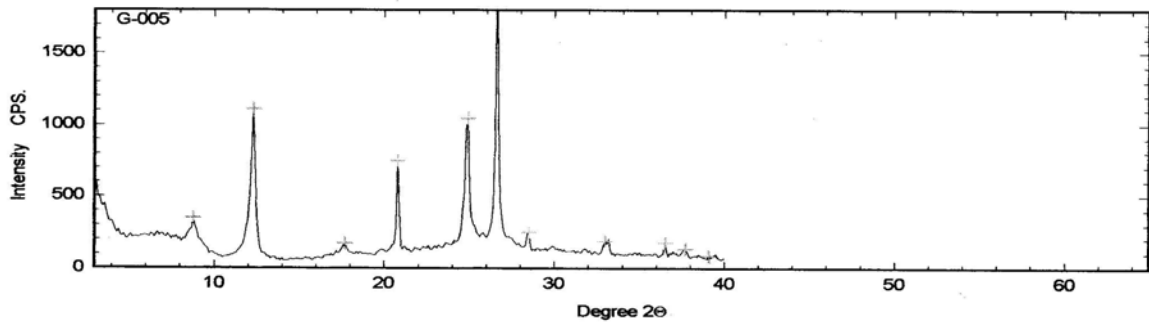
Diffractogram of IR of chalk sample heated collected at depth 9256fts at 550⁰C.



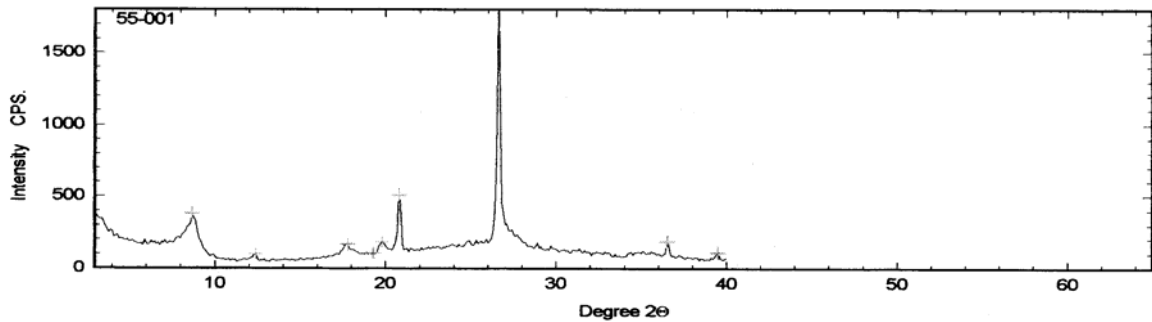
Diffractogram of dry powder chalk sample collected at depth 9329fts



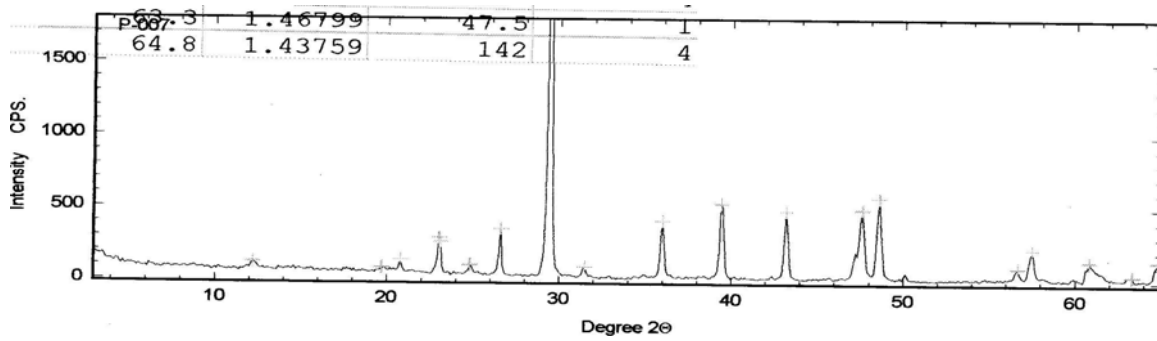
Diffractogram of IR of chalk sample collected at depth 9329fts saturated with water.



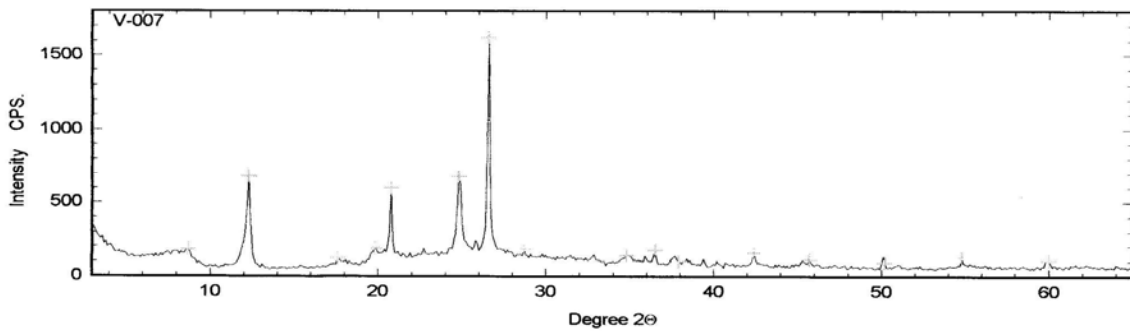
Diffractogram of IR of chalk sample collected at depth 9329fts treated with glycol.



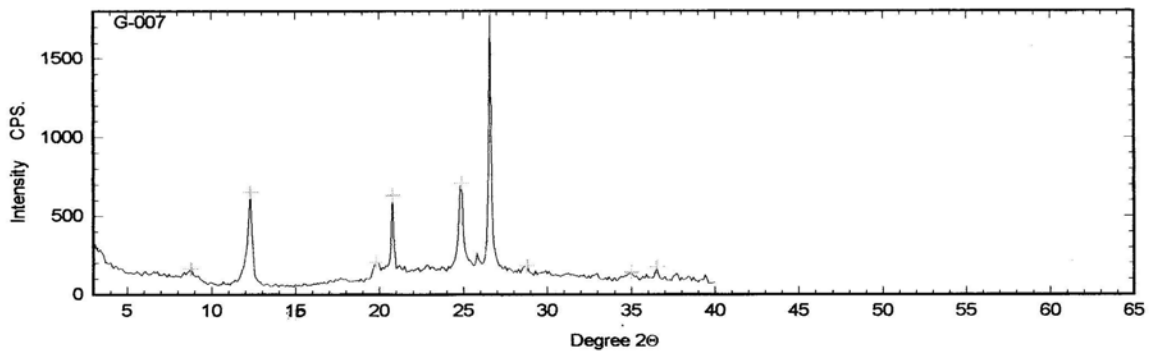
Diffractogram of IR of chalk sample collected at depth 9329fts heated at 550°C .



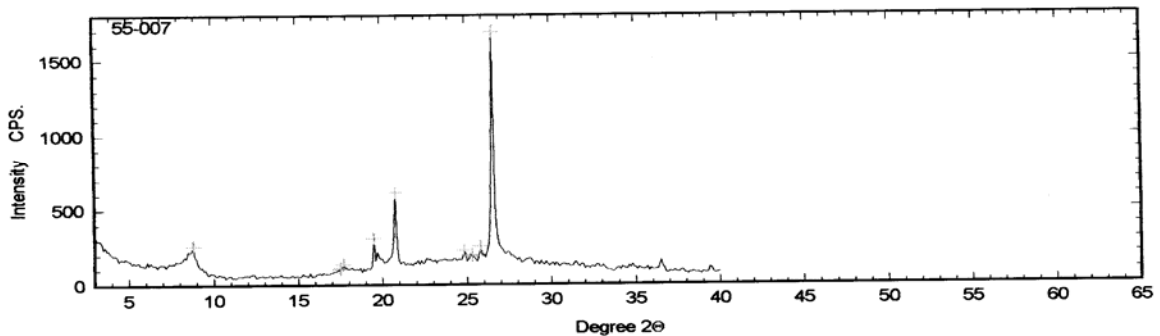
Diffractogram of dry powder chalk sample collected at depth 9370ftsp.



Diffractogram of IR of chalk sample collected at depth 9370fts saturated with water.



Diffractogram of IR of chalk sample collected at depth 9370fts treated with glycol.



Diffractogram of IR of chalk sample collected at depth 9370fts heated at 550 °C.

APPENDIX B

BET of Chalk

Gemini 2375 V4.01
 Instrument ID: 1089
 Setup Group: 9 - Clay

Sample ID: 9238-9 Started: 09/03/04 10:32:40
 Sample Weight: 2.0737 g Completed: 09/03/04 11:07:02
 Evacuation Rate: 300.0 mmHg/min Evacuation Time: 1.0 min
 Measured Free Space: -2.660 cc STP Saturation Pressure: 790.05 mmHg
 Analysis Mode: Equilibration Equilibration Time: 5 sec

BET Multipoint Surface Area Report

Surface Area: 8.6097 sq. m/g
 Slope: 0.498666
 Y-Intercept: 0.006951
 C: 72.744942
 Vm: 1.977782
 Correlation Coefficient: 9.9992e-001

BET Single Point Surface Area: 8.3586 sq. m/g

t-Method Micropore Report

Micropore Volume: -0.000375 cc/g
 Micropore Area: -0.5326 sq. m/g
 External Surface Area: 9.1423 sq. m/g
 Slope: 0.591044
 Y-Intercept: -0.242689
 Correlation Coefficient: 9.9984e-001
 Thickness Values Between: 3.500 and 5.000 A
 Area Correction Factor: 1.000
 0.5000
 $t = [13.9900 / (0.0340 - \log(P/P_0))]$

Analysis Log

Relative Pressure	Pressure (mmHg)	Vol. Adsorbed (cc/g STP)	Elapsed Time, (h:m)	Statistical Thickness, (A)	Surface Area Point
0.0499	39.39	1.691	0:22	3.236	*
0.1122	88.67	1.989	0:25	3.771	*
0.1746	137.95	2.236	0:28	4.203	*
0.2370	187.28	2.483	0:30	4.607	*
0.2995	236.60	2.743	0:33	5.009	*

Gemini 2375 V4.01
Instrument ID: 1089
Setup Group: 9 - Clay

Sample ID: 9242-8	Started: 09/03/04 12:21:36
Sample Weight: 2.0776 g	Completed: 09/03/04 12:55:17
Evacuation Rate: 300.0 mmHg/min	Evacuation Time: 1.0 min
Measured Free Space: -2.677 cc STP	Saturation Pressure: 790.05 mmHg
Analysis Mode: Equilibration	Equilibration Time: 5 sec

BET Multipoint Surface Area Report

Surface Area:	11.7433	sq. m/g
Slope:	0.366206	
Y-Intercept:	0.004491	
C:	82.550835	
Vm:	2.697625	
Correlation Coefficient:	9.9993e-001	

BET Single Point Surface Area: 11.4406 sq. m/g

t-Method Micropore Report

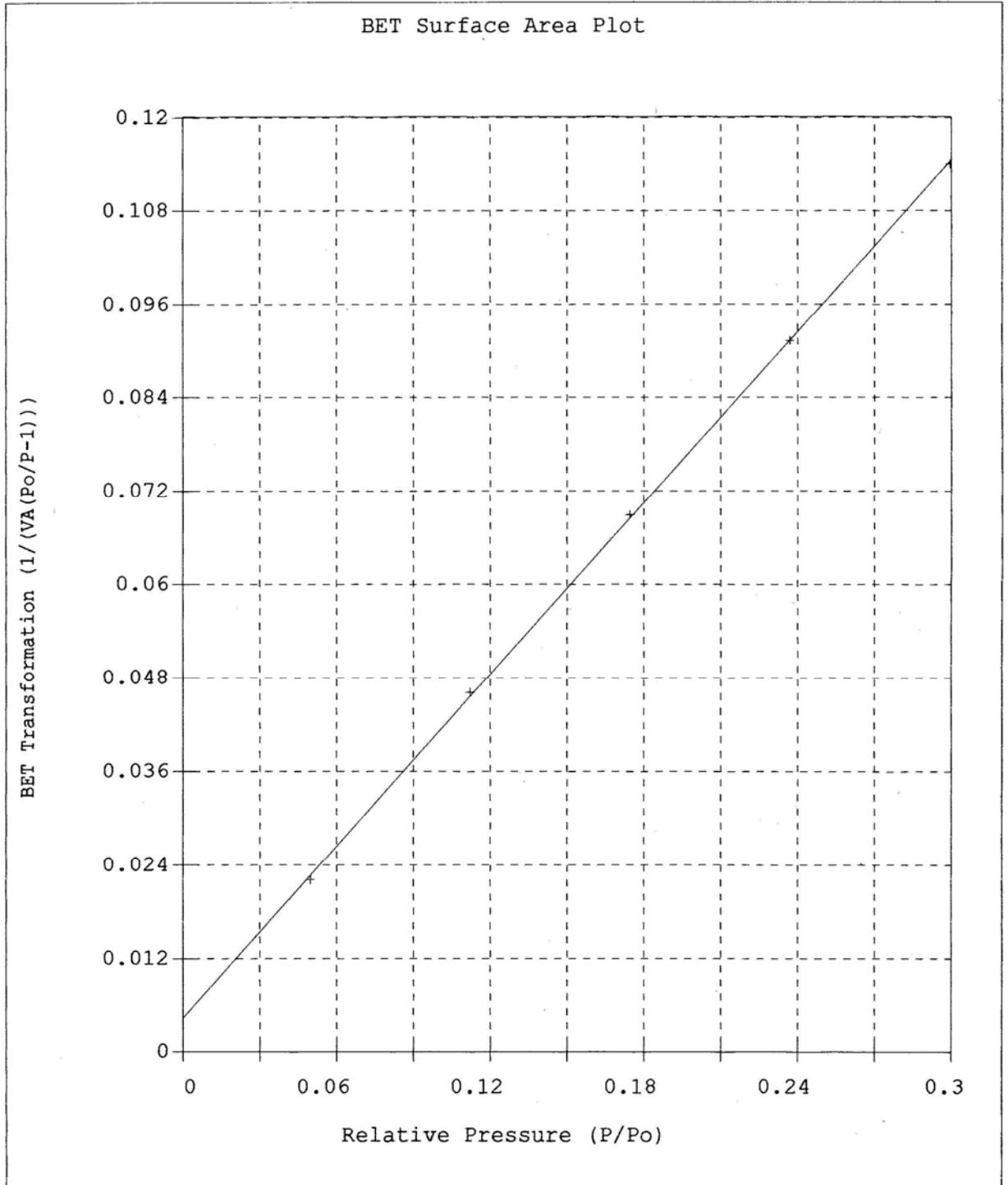
Micropore Volume:	-0.000361	cc/g
Micropore Area:	-0.4554	sq. m/g
External Surface Area:	12.1987	sq. m/g
Slope:	0.788639	
Y-Intercept:	-0.233143	
Correlation Coefficient:	9.9975e-001	
Thickness Values Between:	3.500 and	5.000 A
Area Correction Factor:	1.000	
		0.5000
t = [13.9900/(0.0340 - log(P/Po))]	

Analysis Log

Relative Pressure	Pressure (mmHg)	Vol. Adsorbed (cc/g STP)	Elapsed Time, (h:m)	Statistical Thickness, (A)	Surface Area Point
0.0499	39.38	2.363	0:20	3.236	*
0.1122	88.67	2.745	0:23	3.771	*
0.1746	137.97	3.073	0:26	4.203	*
0.2371	187.29	3.405	0:30	4.607	*
0.2995	236.60	3.754	0:33	5.009	*

Micromeritics Instrument Corporation
Gemini 2375 V4.01 Instrument ID: 1089

Sample ID: 9242-8 File: 9242-8.MGD
Sample Weight: 2.077600
Start Date & Time: 09/03/04 12:21:36
End Date & Time: 09/03/04 12:55:17



Gemini 2375 V4.01
Instrument ID: 1089
Setup Group: 9 - Clay

Sample ID: 9251-2	Started: 09/03/04 12:59:17
Sample Weight: 2.1735 g	Completed: 09/03/04 13:32:44
Evacuation Rate: 300.0 mmHg/min	Evacuation Time: 1.0 min
Measured Free Space: -2.827 cc STP	Saturation Pressure: 790.05 mmHg
Analysis Mode: Equilibration	Equilibration Time: 5 sec

BET Multipoint Surface Area Report

Surface Area:	8.5688	sq. m/g
Slope:	0.500828	
Y-Intercept:	0.007200	
C:	70.559479	
Vm:	1.968397	
Correlation Coefficient:	9.9990e-001	

BET Single Point Surface Area: 8.3134 sq. m/g

t-Method Micropore Report

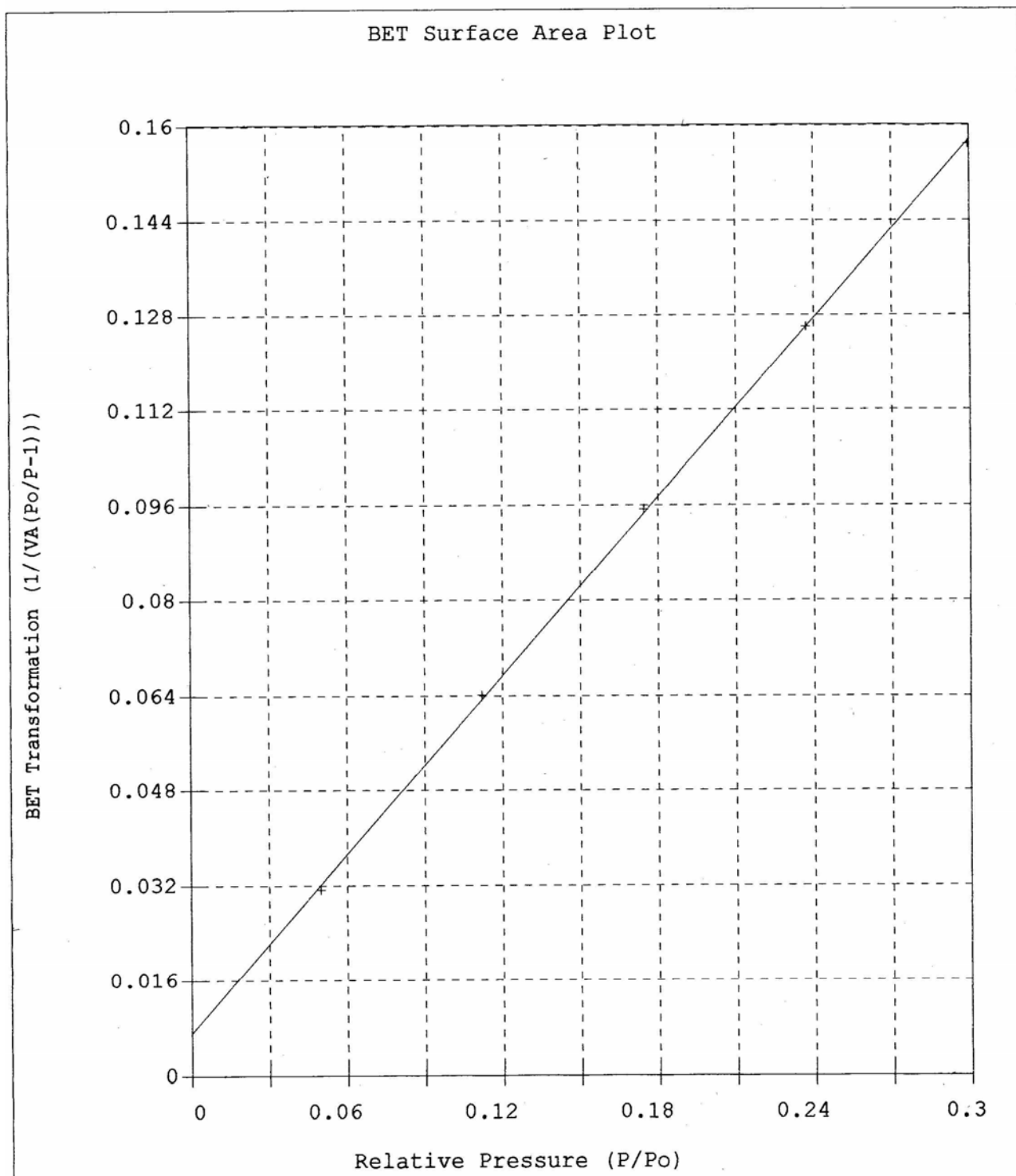
Micropore Volume:	-0.000414	cc/g
Micropore Area:	-0.6067	sq. m/g
External Surface Area:	9.1755	sq. m/g
Slope:	0.593194	
Y-Intercept:	-0.267815	
Correlation Coefficient:	9.9980e-001	
Thickness Values Between:	3.500 and	5.000 A
Area Correction Factor:	1.000	
		0.5000
t = [13.9900 / (0.0340 - log(P/Po))]

Analysis Log

Relative Pressure	Pressure (mmHg)	Vol. Adsorbed (cc/g STP)	Elapsed Time, (h:m)	Statistical Thickness, (A)	Surface Area Point
0.0499	39.39	1.675	0:20	3.236	*
0.1122	88.67	1.972	0:23	3.771	*
0.1746	137.95	2.220	0:26	4.203	*
0.2371	187.31	2.468	0:29	4.607	*
0.2995	236.62	2.728	0:33	5.009	*

Micromeritics Instrument Corporation
Gemini 2375 V4.01 Instrument ID: 1089

Sample ID: 9251-2 File: 9251-2.MGD
Sample Weight: 2.173500
Start Date & Time: 09/03/04 12:59:17
End Date & Time: 09/03/04 13:32:44



Gemini 2375 V4.01
Instrument ID: 1089
Setup Group: 9 - Clay

Sample ID: 9254-6	Started: 09/03/04 08:25:25
Sample Weight: 1.5339 g	Completed: 09/03/04 08:58:32
Evacuation Rate: 300.0 mmHg/min	Evacuation Time: 1.0 min
Measured Free Space: -1.996 cc STP	Saturation Pressure: 790.05 mmHg
Analysis Mode: Equilibration	Equilibration Time: 5 sec

BET Multipoint Surface Area Report

Surface Area:	8.6772	sq. m/g
Slope:	0.494434	
Y-Intercept:	0.007251	
C:	69.185760	
Vm:	1.993283	
Correlation Coefficient:	9.9992e-001	

BET Single Point Surface Area: 8.4093 sq. m/g

t-Method Micropore Report

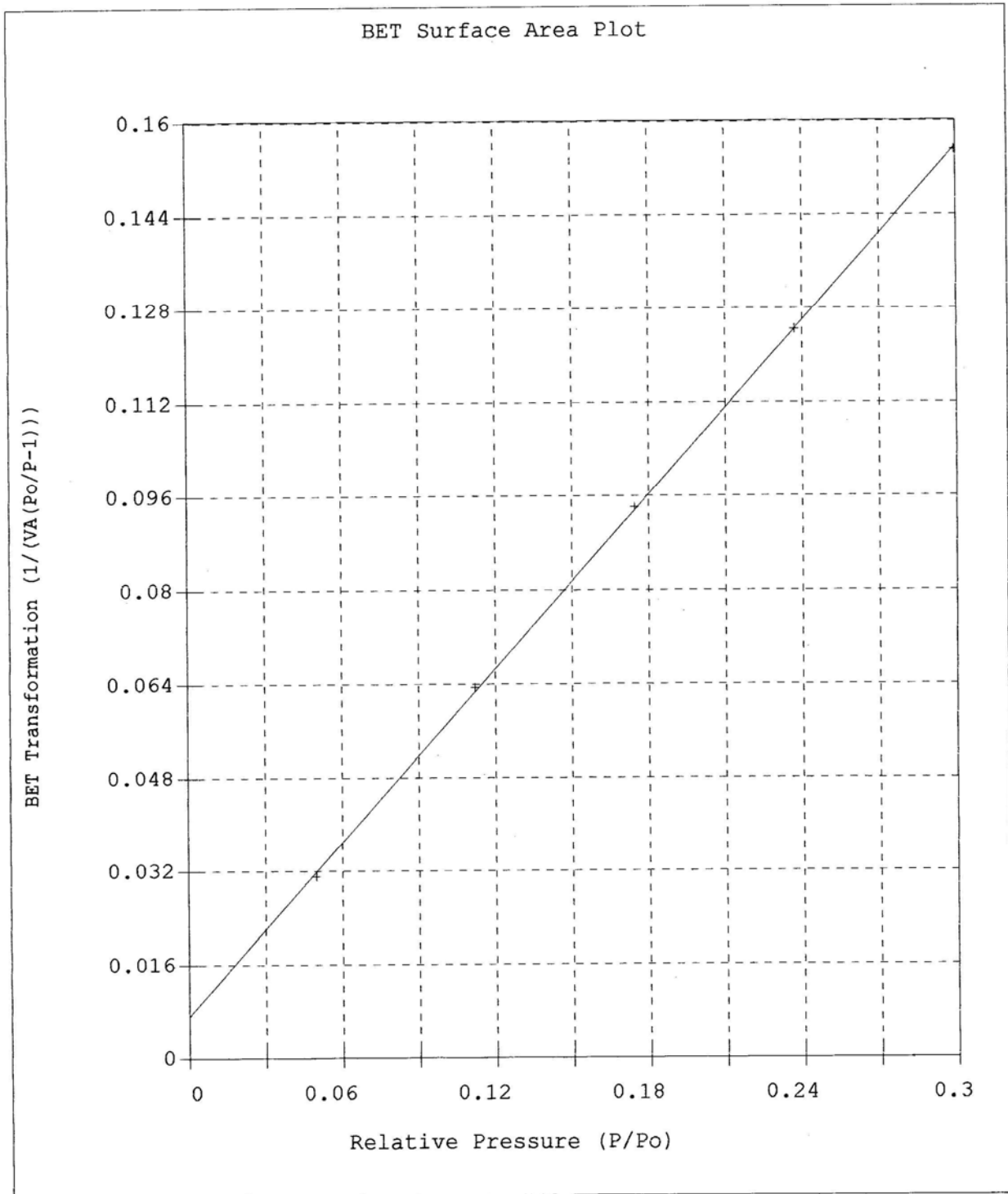
Micropore Volume:	-0.000434	cc/g
Micropore Area:	-0.6424	sq. m/g
External Surface Area:	9.3196	sq. m/g
Slope:	0.602506	
Y-Intercept:	-0.280618	
Correlation Coefficient:	9.9987e-001	
Thickness Values Between:	3.500 and	5.000 A
Area Correction Factor:	1.000	
		0.5000
t = [13.9900 / (0.0340 - log(P/Po))]

Analysis Log

Relative Pressure	Pressure (mmHg)	Vol. Adsorbed (cc/g STP)	Elapsed Time, (h:m)	Statistical Thickness, (A)	Surface Area Point
0.0499	39.38	1.685	0:21	3.236	*
0.1122	88.67	1.994	0:25	3.771	*
0.1746	137.94	2.247	0:27	4.203	*
0.2371	187.29	2.498	0:30	4.607	*
0.2995	236.63	2.760	0:32	5.009	*

Micromeritics Instrument Corporation
Gemini 2375 V4.01 Instrument ID: 1089

Sample ID: 9254-6 File: 9254-6.MGD
Sample Weight: 1.533900
Start Date & Time: 09/03/04 08:25:25
End Date & Time: 09/03/04 08:58:32



Gemini 2375 V4.01
Instrument ID: 1089
Setup Group: 9 - Clay

Sample ID: 9256-1	Started: 09/03/04 09:45:48
Sample Weight: 2.0511 g	Completed: 09/03/04 10:19:44
Evacuation Rate: 300.0 mmHg/min	Evacuation Time: 1.0 min
Measured Free Space: -2.623 cc STP	Saturation Pressure: 790.05 mmHg
Analysis Mode: Equilibration	Equilibration Time: 5 sec

BET Multipoint Surface Area Report

Surface Area:	9.4904	sq. m/g
Slope:	0.452013	
Y-Intercept:	0.006681	
C:	68.659637	
Vm:	2.180102	
Correlation Coefficient:	9.9990e-001	

BET Single Point Surface Area: 9.1999 sq. m/g

t-Method Micropore Report

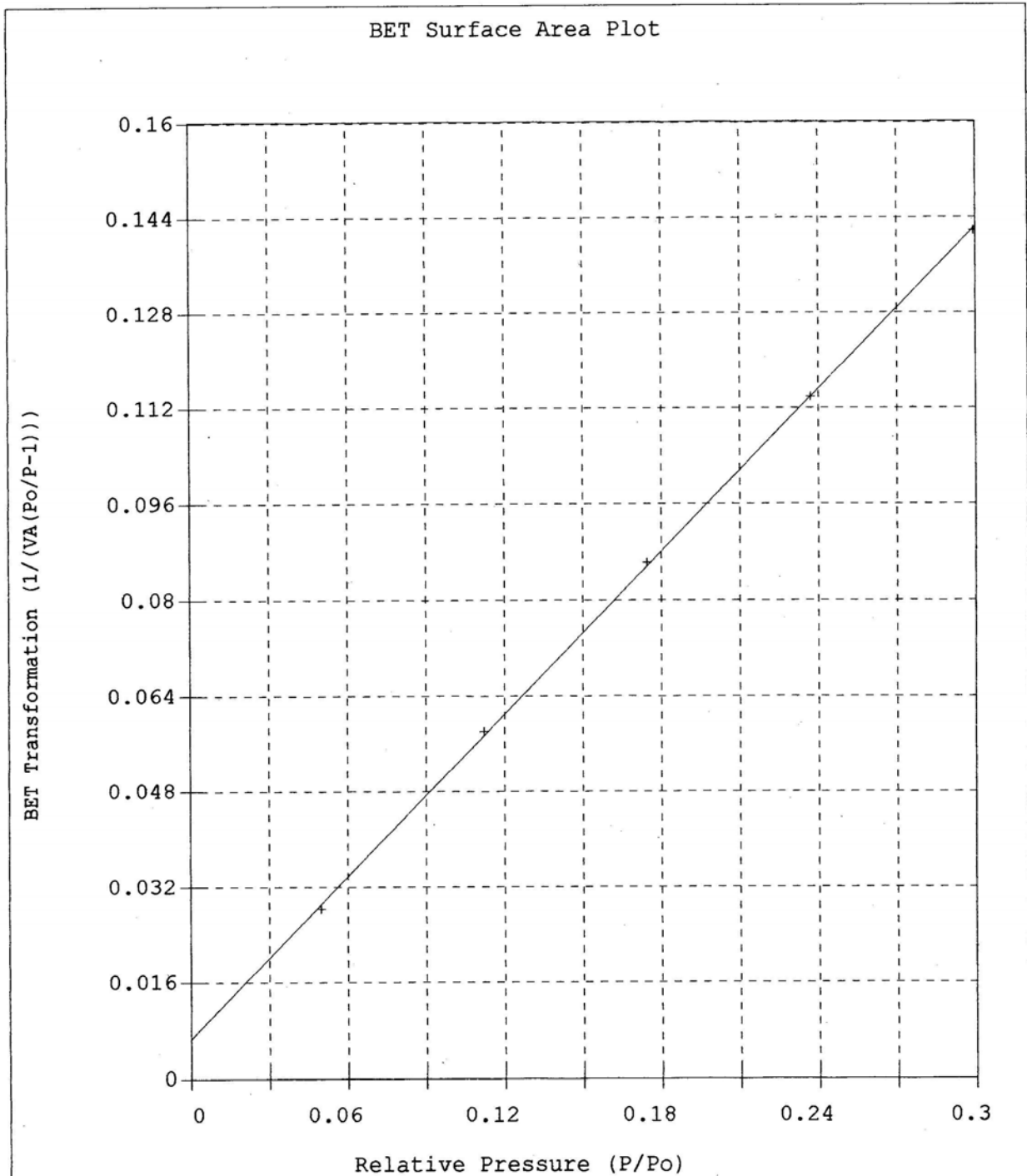
Micropore Volume:	-0.000495	cc/g
Micropore Area:	-0.7401	sq. m/g
External Surface Area:	10.2305	sq. m/g
Slope:	0.661398	
Y-Intercept:	-0.319968	
Correlation Coefficient:	9.9985e-001	
Thickness Values Between:	3.500 and	5.000 A
Area Correction Factor:	1.000	
		0.5000
t = [13.9900 / (0.0340 - log(P/Po))]

Analysis Log

Relative Pressure	Pressure (mmHg)	Vol. Adsorbed (cc/g STP)	Elapsed Time, (h:m)	Statistical Thickness, (A)	Surface Area Point
0.0499	39.40	1.846	0:20	3.236	*
0.1122	88.68	2.177	0:23	3.771	*
0.1746	137.96	2.454	0:27	4.203	*
0.2371	187.29	2.730	0:30	4.607	*
0.2995	236.59	3.019	0:33	5.009	*

Micromeritics Instrument Corporation
Gemini 2375 V4.01 Instrument ID: 1089

Sample ID: 9256-1 File: 9256-1.MGD
Sample Weight: 2.051100
Start Date & Time: 09/03/04 09:45:48
End Date & Time: 09/03/04 10:19:44



Gemini 2375 V4.01
Instrument ID: 1089
Setup Group: 9 - Clay

Sample ID: 9329-2 Started: 09/03/04 13:36:10
Sample Weight: 1.5896 g Completed: 09/03/04 14:10:20
Evacuation Rate: 300.0 mmHg/min Evacuation Time: 1.0 min
Measured Free Space: -2.041 cc STP Saturation Pressure: 790.05 mmHg
Analysis Mode: Equilibration Equilibration Time: 5 sec

BET Multipoint Surface Area Report

Surface Area: 11.5740 sq. m/g
Slope: 0.371204
Y-Intercept: 0.004913
C: 76.553864
Vm: 2.658743
Correlation Coefficient: 9.9992e-001

BET Single Point Surface Area: 11.2570 sq. m/g

t-Method Micropore Report

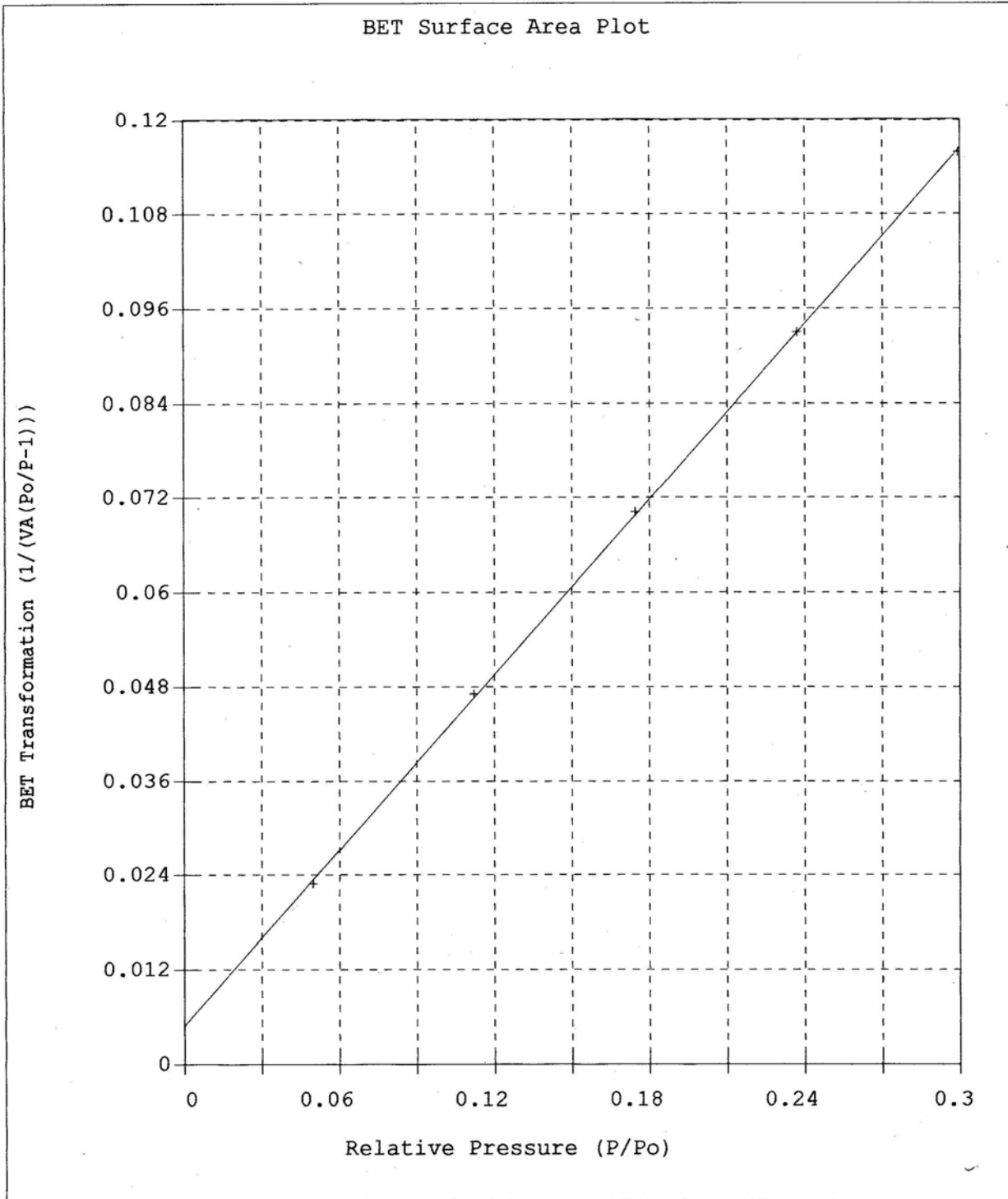
Micropore Volume: -0.000430 cc/g
Micropore Area: -0.5728 sq. m/g
External Surface Area: 12.1468 sq. m/g
Slope: 0.785286
Y-Intercept: -0.278149
Correlation Coefficient: 9.9985e-001
Thickness Values Between: 3.500 and 5.000 A
Area Correction Factor: 1.000
0.5000
 $t = [13.9900 / (0.0340 - \log(P/P_0))]$

Analysis Log

Relative Pressure	Pressure (mmHg)	Vol. Adsorbed (cc/g STP)	Elapsed Time, (h:m)	Statistical Thickness, (A)	Surface Area Point
0.0499	39.40	2.298	0:19	3.236	*
0.1122	88.67	2.686	0:23	3.771	*
0.1746	137.97	3.016	0:27	4.203	*
0.2371	187.29	3.343	0:30	4.607	*
0.2995	236.59	3.694	0:33	5.009	*

Micromeritics Instrument Corporation
Gemini 2375 V4.01 Instrument ID: 1089

Sample ID: 9329-2 File: 9329-2.MGD
Sample Weight: 1.589600
Start Date & Time: 09/03/04 13:36:10
End Date & Time: 09/03/04 14:10:20



Gemini 2375 V4.01
 Instrument ID: 1089
 Setup Group: 9 - Clay

Sample ID: 9351-1	Started: 09/03/04 07:49:16
Sample Weight: 1.2799 g	Completed: 09/03/04 08:21:44
Evacuation Rate: 300.0 mmHg/min	Evacuation Time: 1.0 min
Measured Free Space: -1.655 cc STP	Saturation Pressure: 790.05 mmHg
Analysis Mode: Equilibration	Equilibration Time: 5 sec

BET Multipoint Surface Area Report

Surface Area:	7.7070	sq. m/g
Slope:	0.555154	
Y-Intercept:	0.009683	
C:	58.334728	
Vm:	1.770423	
Correlation Coefficient:	9.9989e-001	

BET Single Point Surface Area: 7.4264 sq. m/g

t-Method Micropore Report

Micropore Volume:	-0.000566	cc/g
Micropore Area:	-0.9045	sq. m/g
External Surface Area:	8.6115	sq. m/g
Slope:	0.556728	
Y-Intercept:	-0.365994	
Correlation Coefficient:	9.9993e-001	
Thickness Values Between:	3.500 and	5.000 A
Area Correction Factor:	1.000	0.5000
t = [13.9900 / (0.0340 - log(P/Po))]		

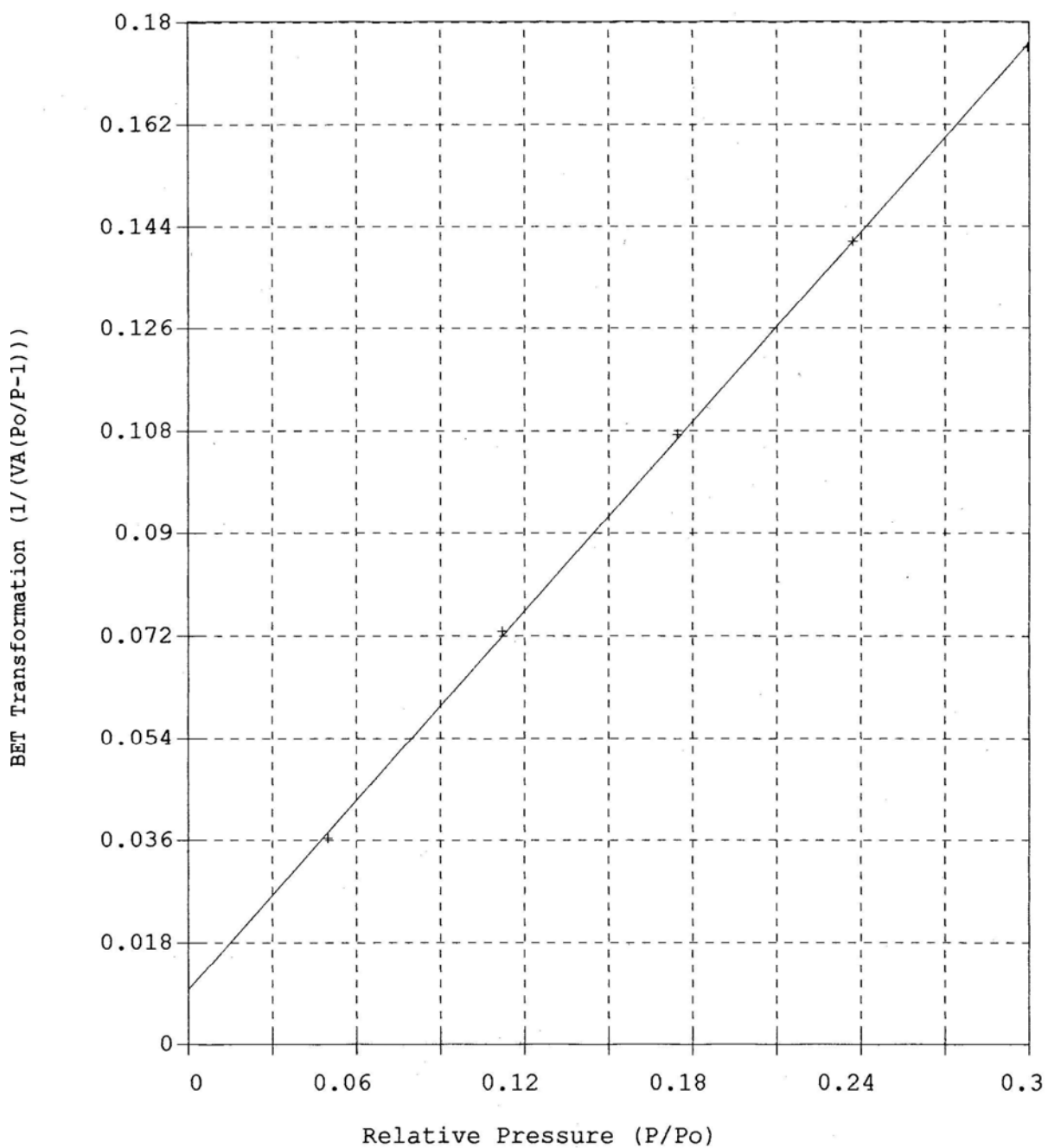
Analysis Log

Relative Pressure	Pressure (mmHg)	Vol. Adsorbed (cc/g STP)	Elapsed Time, (h:m)	Statistical Thickness, (A)	Surface Area Point
0.0499	39.38	1.443	0:21	3.236	*
0.1122	88.67	1.735	0:24	3.771	*
0.1746	137.95	1.971	0:26	4.203	*
0.2371	187.30	2.201	0:29	4.607	*
0.2995	236.65	2.437	0:32	5.009	*

Micromeritics Instrument Corporation
Gemini 2375 V4.01 Instrument ID: 1089

Sample ID: 9351-1 File: 9351-1.MGD
Sample Weight: 1.279900
Start Date & Time: 09/03/04 07:49:16
End Date & Time: 09/03/04 08:21:44

BET Surface Area Plot



Gemini 2375 V4.01
Instrument ID: 1089
Setup Group: 9 - Clay

Sample ID: 9352-1	Started: 09/03/04 07:11:38
Sample Weight: 1.8131 g	Completed: 09/03/04 07:44:31
Evacuation Rate: 300.0 mmHg/min	Evacuation Time: 1.0 min
Measured Free Space: -2.352 cc STP	Saturation Pressure: 790.05 mmHg
Analysis Mode: Equilibration	Equilibration Time: 5 sec

BET Multipoint Surface Area Report

Surface Area:	5.5286	sq. m/g
Slope:	0.771152	
Y-Intercept:	0.016247	
C:	48.463703	
Vm:	1.270004	
Correlation Coefficient:	9.9995e-001	

BET Single Point Surface Area: 5.2708 sq. m/g

t-Method Micropore Report

Micropore Volume:	-0.000546	cc/g
Micropore Area:	-0.9143	sq. m/g
External Surface Area:	6.4429	sq. m/g
Slope:	0.416528	
Y-Intercept:	-0.353093	
Correlation Coefficient:	9.9998e-001	
Thickness Values Between:	3.500 and	5.000 A
Area Correction Factor:	1.000	
		0.5000
t = [13.9900/(0.0340 - log(P/Po))]	

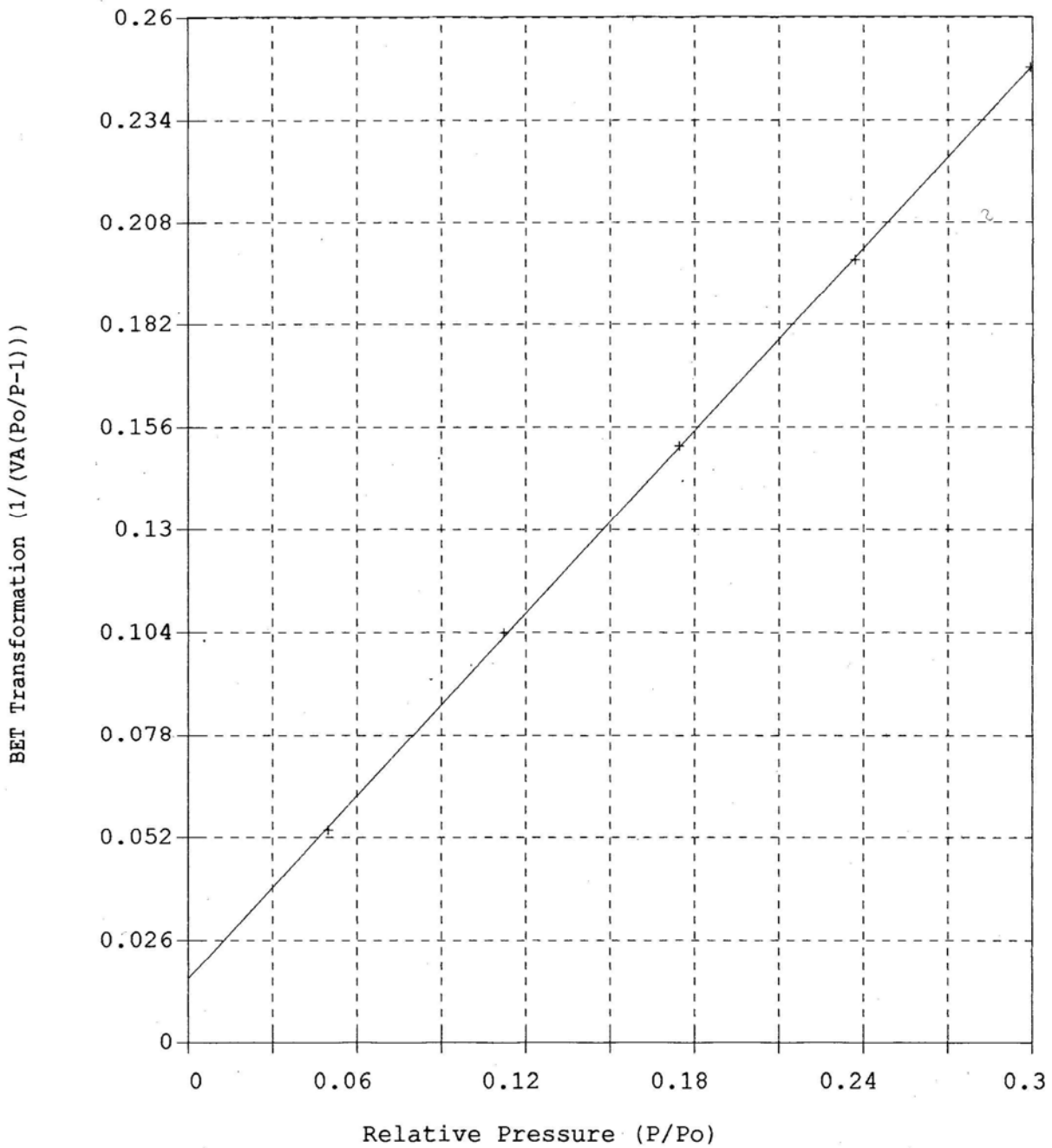
Analysis Log

Relative Pressure	Pressure (mmHg)	Vol. Adsorbed (cc/g STP)	Elapsed Time, (h:m)	Statistical Thickness, (A)	Surface Area Point
0.0498	39.38	0.974	0:21	3.236	*
0.1122	88.68	1.217	0:24	3.771	*
0.1746	137.93	1.399	0:27	4.203	*
0.2371	187.29	1.565	0:29	4.607	*
0.2995	236.60	1.730	0:32	5.009	*

Micromeritics Instrument Corporation
Gemini 2375 V4.01 Instrument ID: 1089

Sample ID: 9352-1 File: 9352-1.MGD
Sample Weight: 1.813100
Start Date & Time: 09/03/04 07:11:38
End Date & Time: 09/03/04 07:44:31

BET Surface Area Plot



Gemini 2375 V4.01
 Instrument ID: 1089
 Setup Group: 9 - Clay

Sample ID: 9368-9	Started: 09/03/04 11:10:52
Sample Weight: 1.7824 g	Completed: 09/03/04 11:41:44
Evacuation Rate: 300.0 mmHg/min	Evacuation Time: 1.0 min
Measured Free Space: -2.348 cc STP	Saturation Pressure: 790.05 mmHg
Analysis Mode: Equilibration	Equilibration Time: 5 sec

BET Multipoint Surface Area Report

Surface Area:	5.7361	sq. m/g
Slope:	0.744581	
Y-Intercept:	0.014337	
C:	52.935905	
Vm:	1.317667	
Correlation Coefficient:	9.9994e-001	

BET Single Point Surface Area: 5.4931 sq. m/g

t-Method Micropore Report

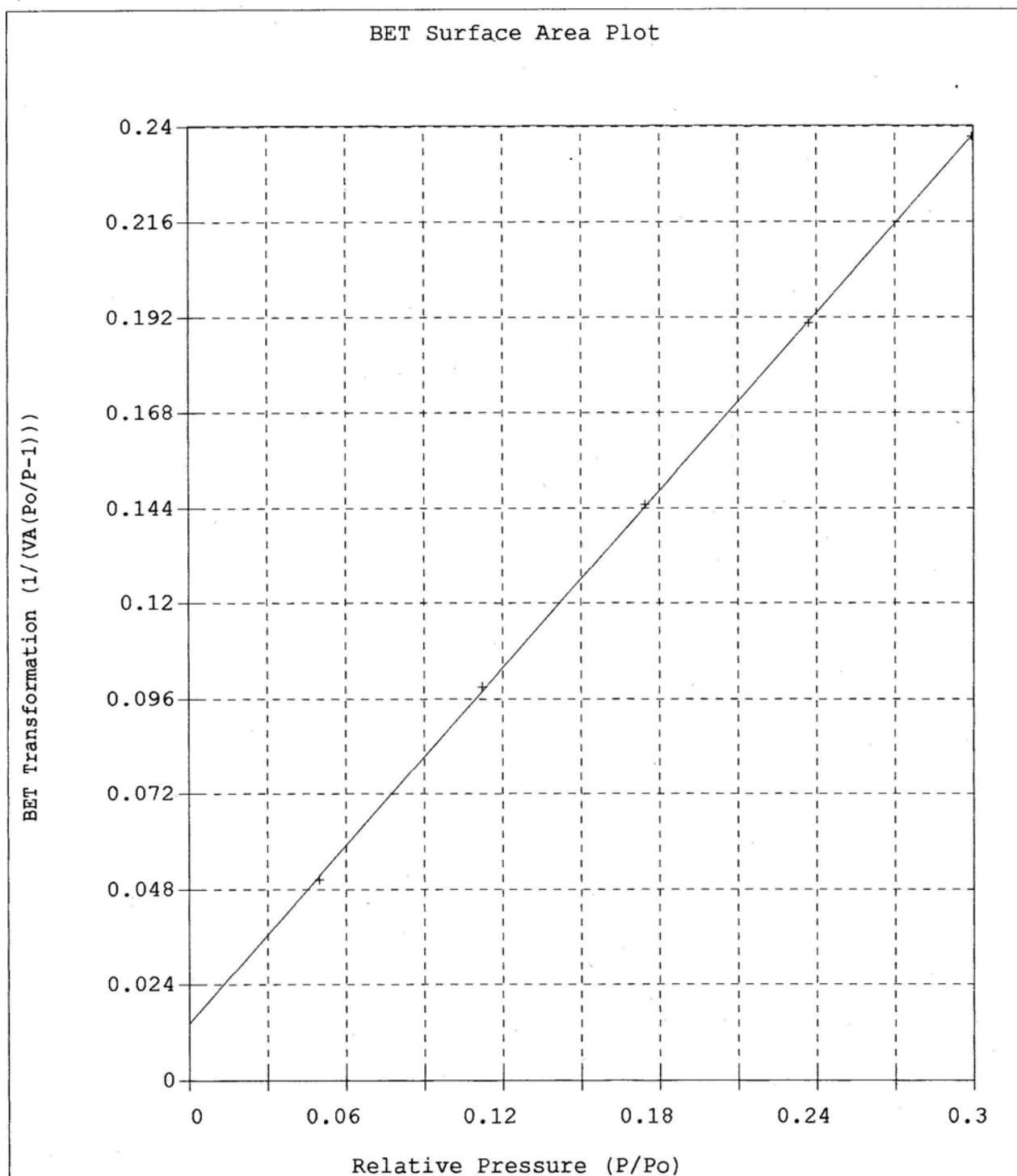
Micropore Volume:	-0.000503	cc/g
Micropore Area:	-0.8348	sq. m/g
External Surface Area:	6.5708	sq. m/g
Slope:	0.424802	
Y-Intercept:	-0.324885	
Correlation Coefficient:	1.0000e+000	
Thickness Values Between:	3.500 and	5.000 A
Area Correction Factor:	1.000	
		0.5000
t = [13.9900/(0.0340 - log(P/Po))]	

Analysis Log

Relative Pressure	Pressure (mmHg)	Vol. Adsorbed (cc/g STP)	Elapsed Time, (h:m)	Statistical Thickness, (A)	Surface Area Point
0.0499	39.40	1.039	0:20	3.236	*
0.1122	88.68	1.277	0:22	3.771	*
0.1746	137.96	1.461	0:25	4.203	*
0.2371	187.30	1.632	0:27	4.607	*
0.2995	236.63	1.803	0:30	5.009	*

Micromeritics Instrument Corporation
Gemini 2375 V4.01 Instrument ID: 1089

Sample ID: 9368-9 File: 9368-9.MGD
Sample Weight: 1.782400
Start Date & Time: 09/03/04 11:10:52
End Date & Time: 09/03/04 11:41:44



Gemini 2375 V4.01
 Instrument ID: 1089
 Setup Group: 9 - Clay

Sample ID: 9370-2	Started: 09/03/04 09:09:07
Sample Weight: 1.2331 g	Completed: 09/03/04 09:41:55
Evacuation Rate: 300.0 mmHg/min	Evacuation Time: 1.0 min
Measured Free Space: -1.634 cc STP	Saturation Pressure: 790.05 mmHg
Analysis Mode: Equilibration	Equilibration Time: 5 sec

BET Multipoint Surface Area Report

Surface Area:	6.1001	sq. m/g
Slope:	0.698601	
Y-Intercept:	0.015028	
C:	47.486156	
Vm:	1.401288	
Correlation Coefficient:	9.9995e-001	

BET Single Point Surface Area: 5.8070 sq. m/g

t-Method Micropore Report

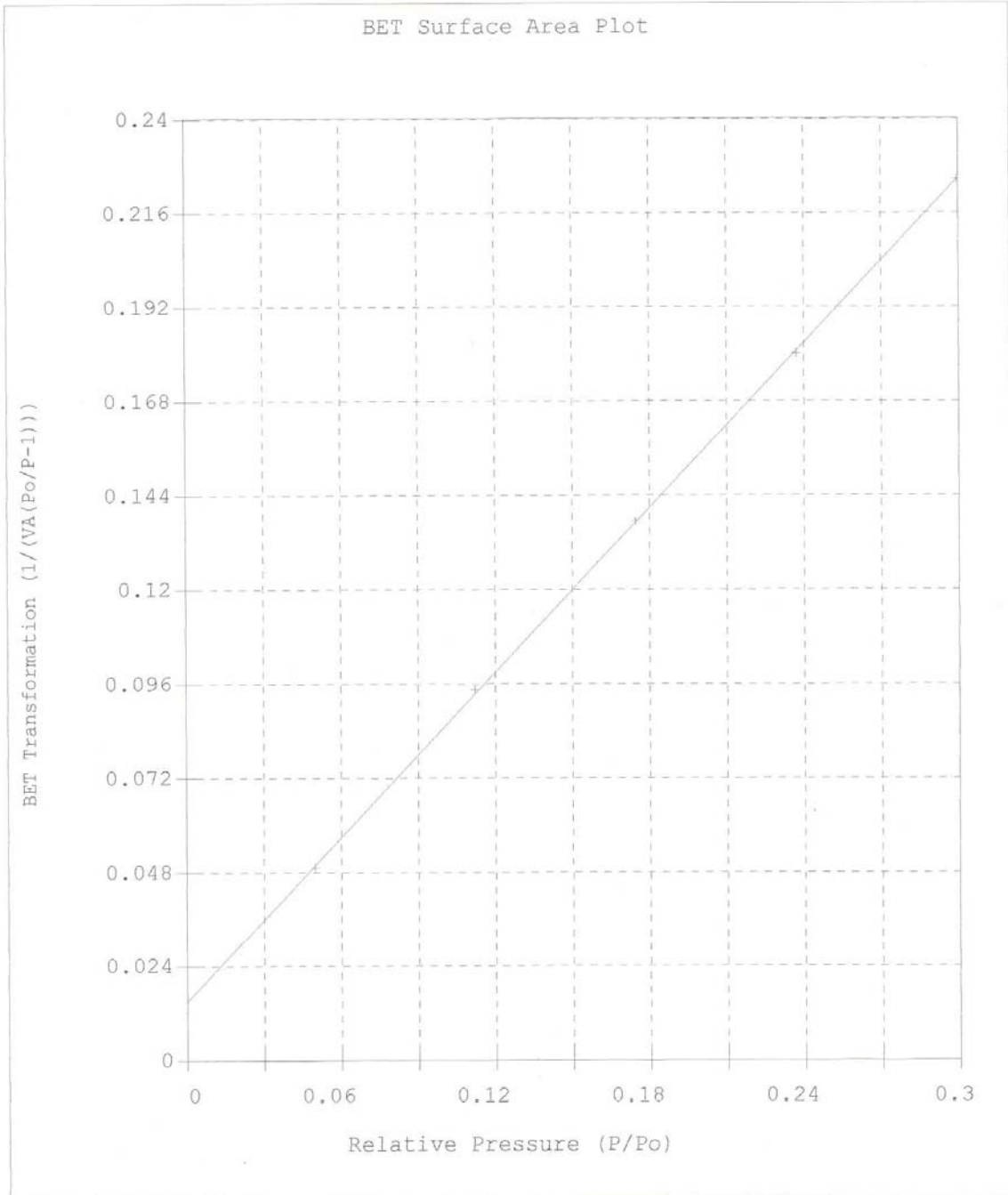
Micropore Volume:	-0.000627	cc/g
Micropore Area:	-1.0594	sq. m/g
External Surface Area:	7.1594	sq. m/g
Slope:	0.462855	
Y-Intercept:	-0.405611	
Correlation Coefficient:	9.9997e-001	
Thickness Values Between:	3.500 and	5.000 A
Area Correction Factor:	1.000	
		0.5000
t = [13.9900/(0.0340 - log(P/Po))]	

Analysis Log

Relative Pressure	Pressure (mmHg)	Vol. Adsorbed (cc/g STP)	Elapsed Time, (h:m)	Statistical Thickness, (A)	Surface Area Point
0.0499	39.40	1.068	0:21	3.236	*
0.1122	88.67	1.339	0:24	3.771	*
0.1746	137.95	1.542	0:26	4.203	*
0.2371	187.29	1.726	0:29	4.607	*
0.2995	236.62	1.906	0:32	5.009	*

Micromeritics Instrument Corporation
Gemini 2375 V4.01 Instrument ID: 1089

Sample ID: 9370-2 File: 9370-2.MGD
Sample Weight: 1.233100
Start Date & Time: 09/03/04 09:09:07
End Date & Time: 09/03/04 09:41:55



APPENDIX C

BET of IR

Gemini 2375 V4.01
Instrument ID: 1089
Setup Group: 9 - Clay

Sample ID: R-9238-9 Started: 05/04/04 06:04:15
Sample Weight: 0.5928 g Completed: 05/04/04 06:49:52
Evacuation Rate: 300.0 mmHg/min Evacuation Time: 1.0 min
Measured Free Space: -0.820 cc STP Saturation Pressure: 771.93 mmHg
Analysis Mode: Equilibration Equilibration Time: 5 sec

BET Multipoint Surface Area Report

Surface Area: 32.0319 sq. m/g
Slope: 0.133403
Y-Intercept: 0.002499
C: 54.382511
Vm: 7.358243
Correlation Coefficient: 9.9985e-001

BET Single Point Surface Area: 30.7851 sq. m/g

t-Method Micropore Report

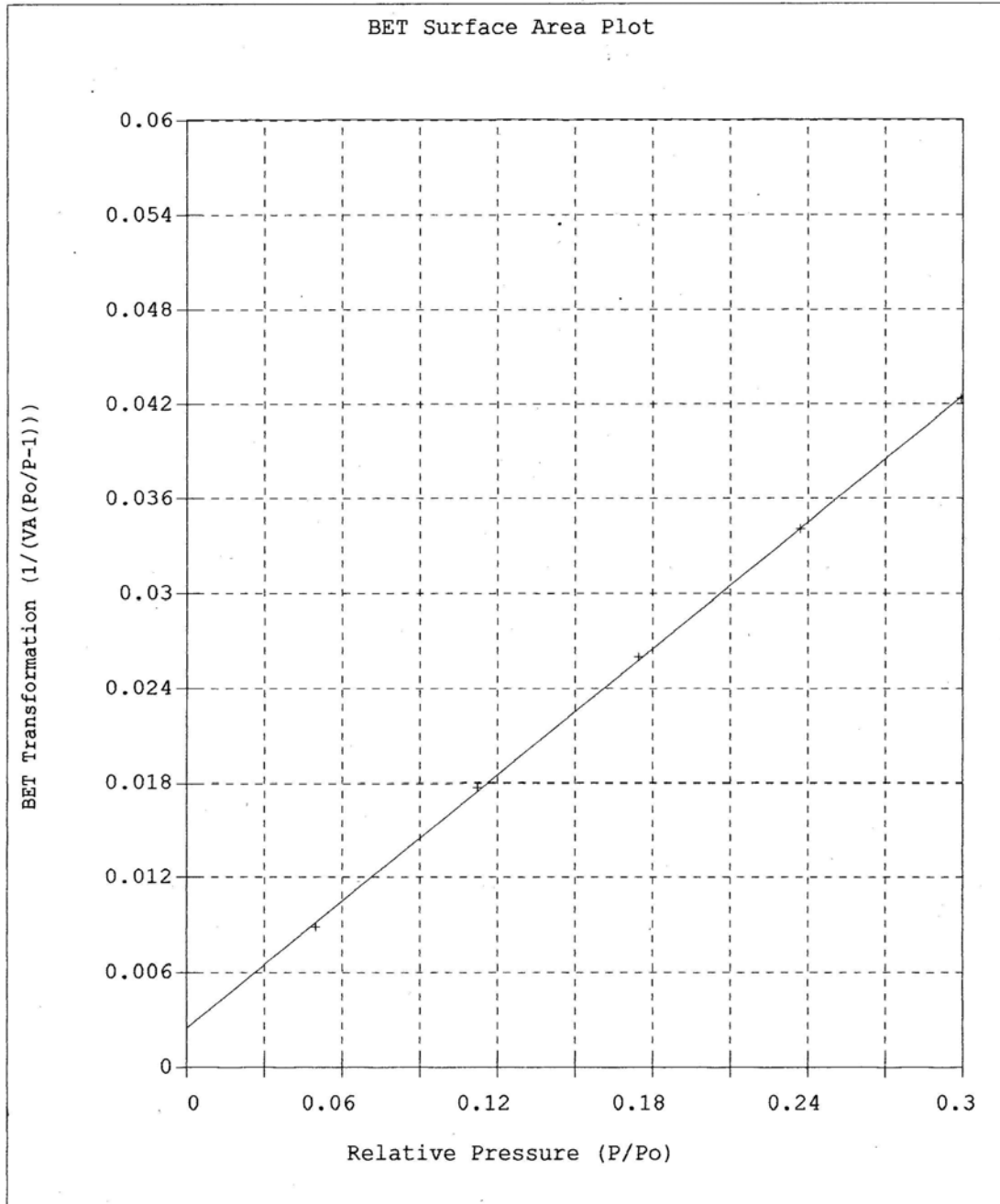
Micropore Volume: -0.002790 cc/g
Micropore Area: -4.6079 sq. m/g
External Surface Area: 36.6398 sq. m/g
Slope: 2.368746
Y-Intercept: -1.803970
Correlation Coefficient: 9.9990e-001
Thickness Values Between: 3.500 and 5.000 A
Area Correction Factor: 1.000
0.5000
 $t = [13.9900 / (0.0340 - \log(P/P_0))]$

Analysis Log

Relative Pressure	Pressure (mmHg)	Vol. Adsorbed (cc/g STP)	Elapsed Time, (h:m)	Statistical Thickness, (A)	Surface Area Point
0.0499	38.49	5.914	0:25	3.236	*
0.1123	86.65	7.137	0:32	3.771	*
0.1746	134.79	8.136	0:36	4.203	*
0.2370	182.96	9.117	0:41	4.607	*
0.2995	231.15	10.102	0:45	5.009	*

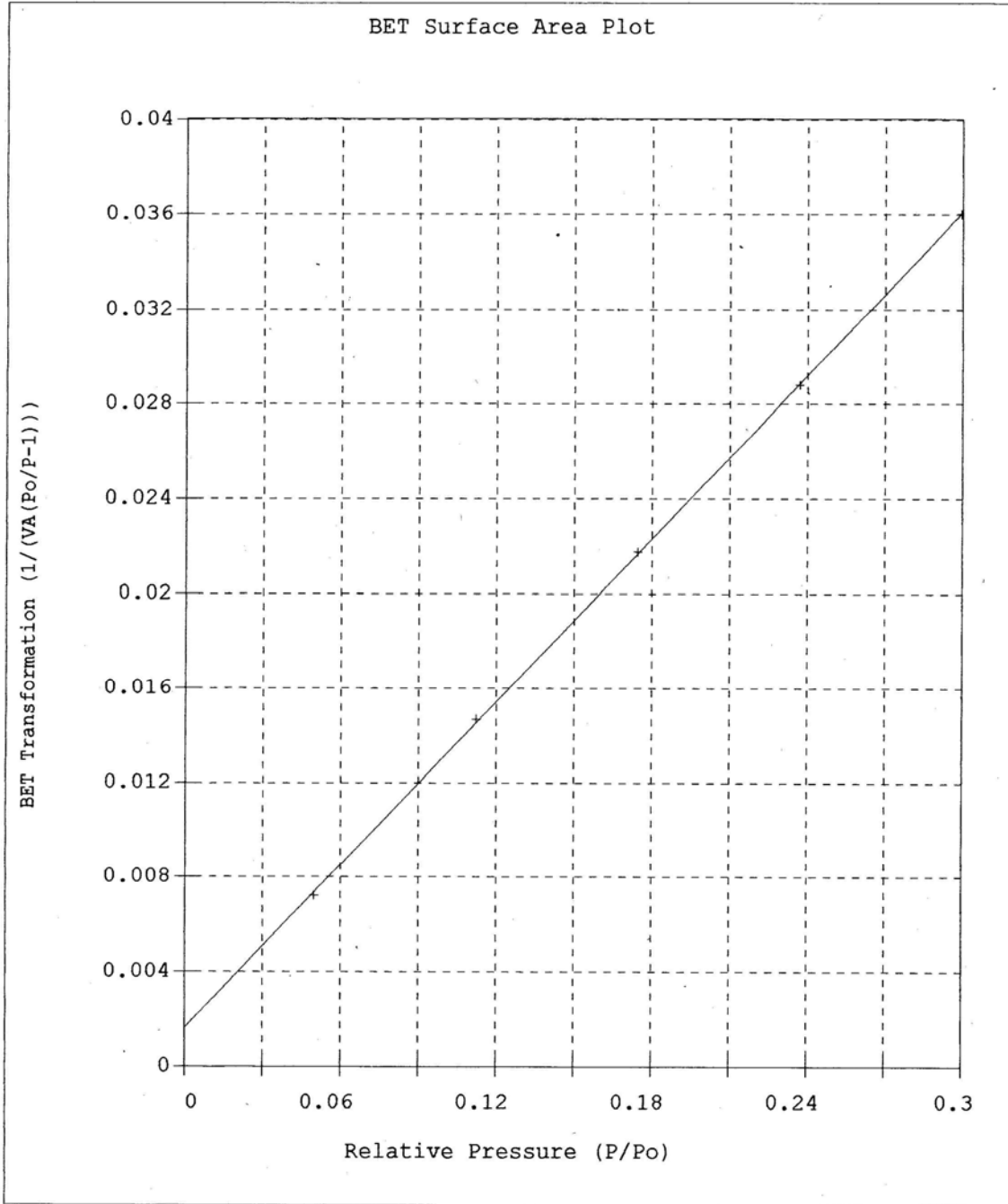
Micromeritics Instrument Corporation
Gemini 2375 V4.01 Instrument ID: 1089

Sample ID: R-9238-9 File: R-9238-9.MGD
Sample Weight: 0.592800
Start Date & Time: 05/04/04 06:04:15
End Date & Time: 05/04/04 06:49:52



Micromeritics Instrument Corporation
Gemini 2375 V4.01 Instrument ID: 1089

Sample ID: R-9242-8 File: R-9242-8.MGD
Sample Weight: 0.583400
Start Date & Time: 05/04/04 10:20:10
End Date & Time: 05/04/04 11:00:44



Gemini 2375 V4.01
Instrument ID: 1089
Setup Group: 9 - Clay

Sample ID: R-9251-2 Started: 05/04/04 08:41:07
Sample Weight: 0.7280 g Completed: 05/04/04 09:23:30
Evacuation Rate: 300.0 mmHg/min Evacuation Time: 1.0 min
Measured Free Space: -1.010 cc STP Saturation Pressure: 771.93 mmHg
Analysis Mode: Equilibration Equilibration Time: 5 sec

BET Multipoint Surface Area Report

Surface Area: 30.6189 sq. m/g
Slope: 0.139758
Y-Intercept: 0.002415
C: 58.865849
Vm: 7.033653
Correlation Coefficient: 9.9987e-001

BET Single Point Surface Area: 29.5175 sq. m/g

t-Method Micropore Report

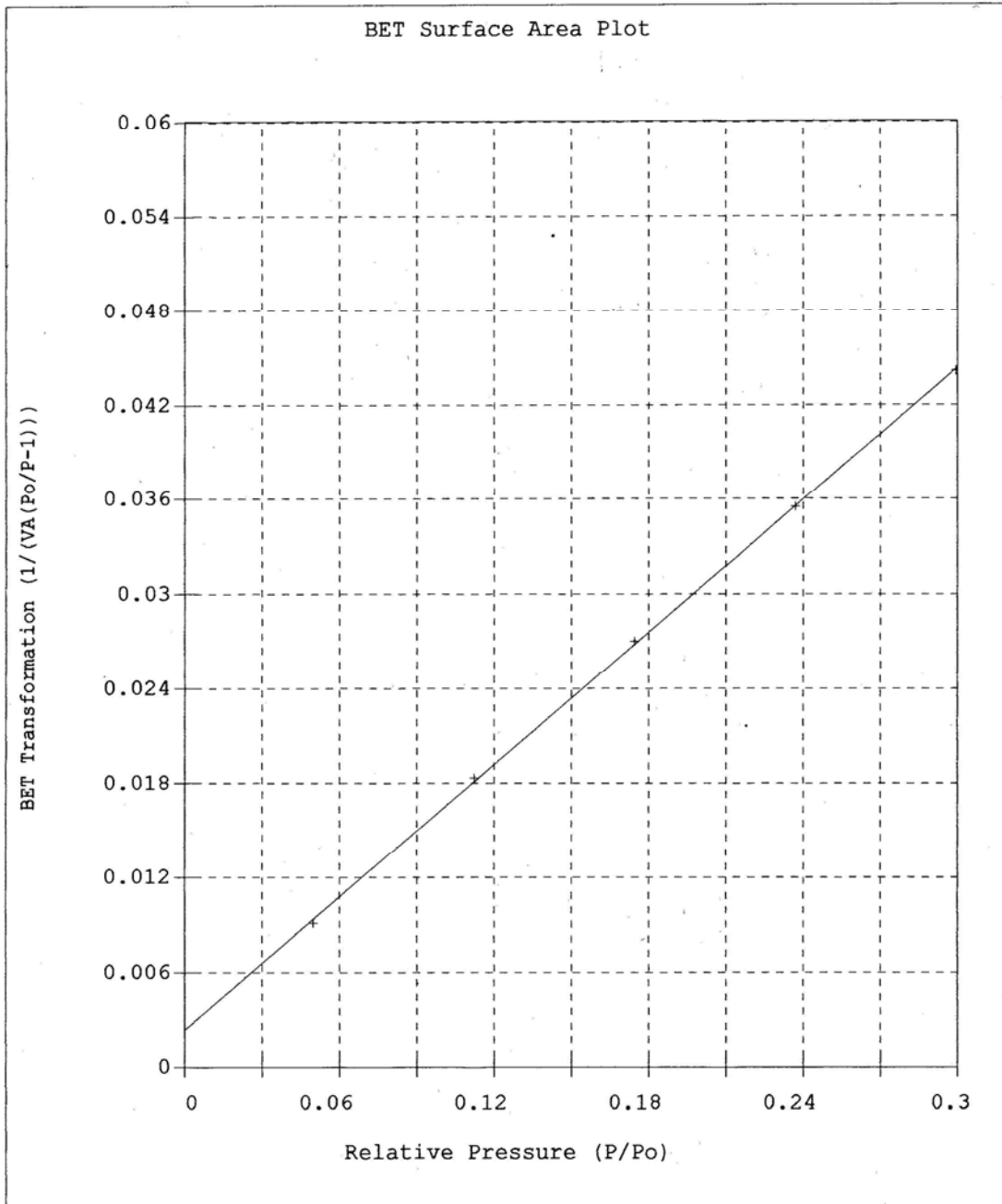
Micropore Volume: -0.002324 cc/g
Micropore Area: -3.7794 sq. m/g
External Surface Area: 34.3983 sq. m/g
Slope: 2.223837
Y-Intercept: -1.502775
Correlation Coefficient: 9.9989e-001
Thickness Values Between: 3.500 and 5.000 A
Area Correction Factor: 1.000
0.5000
 $t = [13.9900 / (0.0340 - \log(P/P_0))]$

Analysis Log

Relative Pressure	Pressure (mmHg)	Vol. Adsorbed (cc/g STP)	Elapsed Time, (h:m)	Statistical Thickness, (A)	Surface Area Point
0.0499	38.49	5.763	0:23	3.236	*
0.1123	86.66	6.891	0:28	3.771	*
0.1746	134.79	7.828	0:32	4.203	*
0.2370	182.97	8.750	0:37	4.607	*
0.2995	231.20	9.687	0:41	5.009	*

Micromeritics Instrument Corporation
Gemini 2375 V4.01 Instrument ID: 1089

Sample ID: R-9251-2 File: R-9251-2.MGD
Sample Weight: 0.728000
Start Date & Time: 05/04/04 08:41:07
End Date & Time: 05/04/04 09:23:30



Gemini 2375 V4.01
Instrument ID: 1089
Setup Group: 9 - Clay

Sample ID: R-9254-6 Started: 05/04/04 12:01:29
Sample Weight: 0.5635 g Completed: 05/04/04 12:38:46
Evacuation Rate: 300.0 mmHg/min Evacuation Time: 1.0 min
Measured Free Space: -0.773 cc STP Saturation Pressure: 771.93 mmHg
Analysis Mode: Equilibration Equilibration Time: 5 sec

BET Multipoint Surface Area Report

Surface Area: 34.0953 sq. m/g
Slope: 0.125478
Y-Intercept: 0.002199
C: 58.056629
Vm: 7.832233
Correlation Coefficient: 9.9986e-001

BET Single Point Surface Area: 32.8529 sq. m/g

t-Method Micropore Report

Micropore Volume: -0.002675 cc/g
Micropore Area: -4.3746 sq. m/g
External Surface Area: 38.4699 sq. m/g
Slope: 2.487061
Y-Intercept: -1.729095
Correlation Coefficient: 9.9992e-001
Thickness Values Between: 3.500 and 5.000 A
Area Correction Factor: 1.000
0.5000
 $t = [13.9900 / (0.0340 - \log(P/P_0))]$

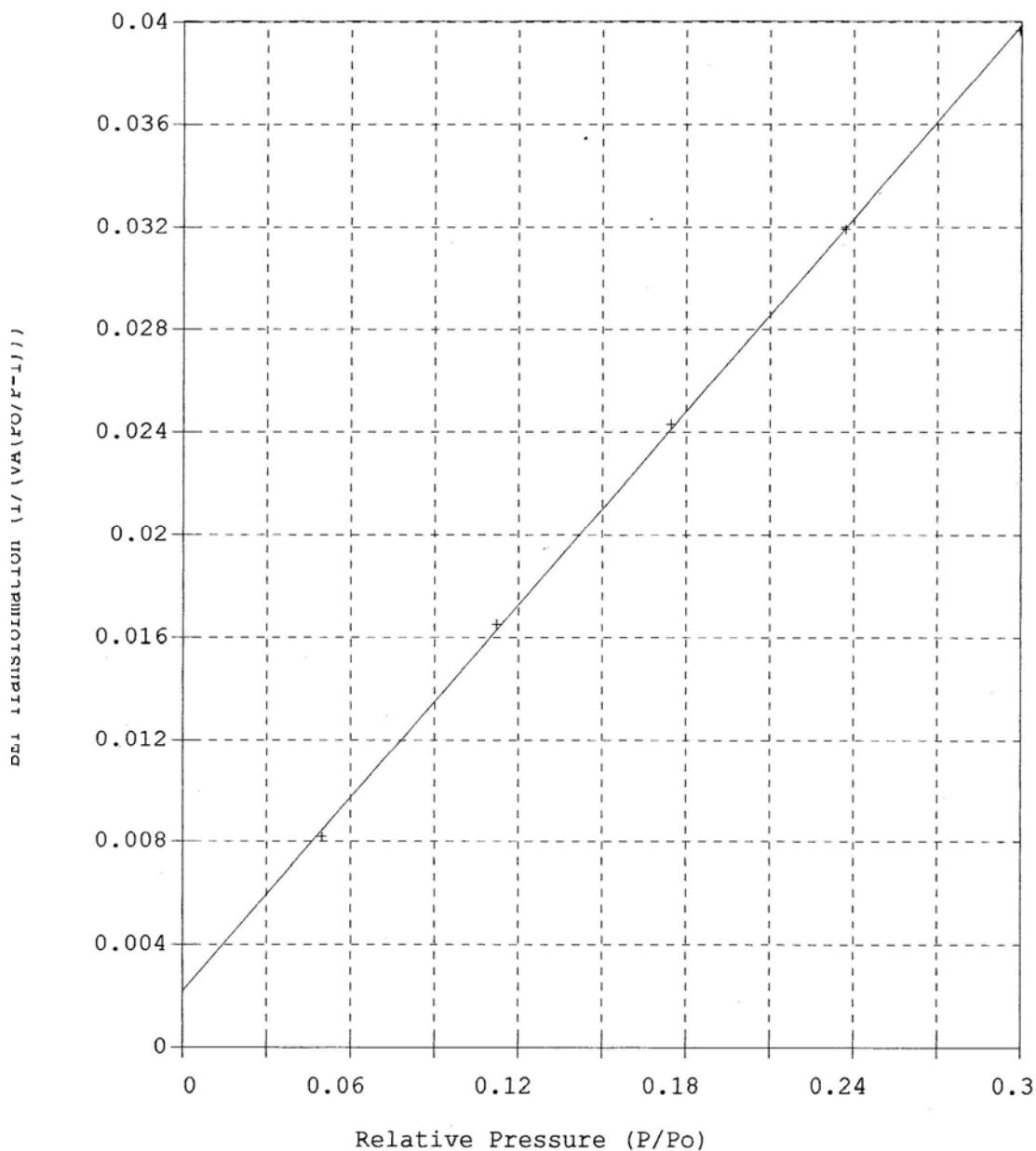
Analysis Log

Relative Pressure	Pressure (mmHg)	Vol. Adsorbed (cc/g STP)	Elapsed Time, (h:m)	Statistical Thickness, (A)	Surface Area Point
0.0499	38.49	6.399	0:21	3.236	*
0.1123	86.65	7.657	0:25	3.771	*
0.1746	134.79	8.709	0:29	4.203	*
0.2370	182.97	9.736	0:33	4.607	*
0.2995	231.18	10.781	0:36	5.009	*

Micromeritics Instrument Corporation
Gemini 2375 V4.01 Instrument ID: 1089

Sample ID: R-9254-6 File: R-9254-6.MGD
Sample Weight: 0.563500
Start Date & Time: 05/04/04 12:01:29
End Date & Time: 05/04/04 12:38:46

BET Surface Area Plot



Gemini 2375 V4.01
 Instrument ID: 1089
 Setup Group: 9 - Clay

Sample ID: R-9256-1 Started: 05/04/04 07:36:44
 Sample Weight: 0.5985 g Completed: 05/04/04 08:19:27
 Evacuation Rate: 300.0 mmHg/min Evacuation Time: 1.0 min
 Measured Free Space: -0.785 cc STP Saturation Pressure: 771.93 mmHg
 Analysis Mode: Equilibration Equilibration Time: 5 sec

BET Multipoint Surface Area Report

Surface Area: 33.4579 sq. m/g
 Slope: 0.127776
 Y-Intercept: 0.002334
 C: 55.743214
 Vm: 7.685826
 Correlation Coefficient: 9.9984e-001

BET Single Point Surface Area: 32.2028 sq. m/g

t-Method Micropore Report

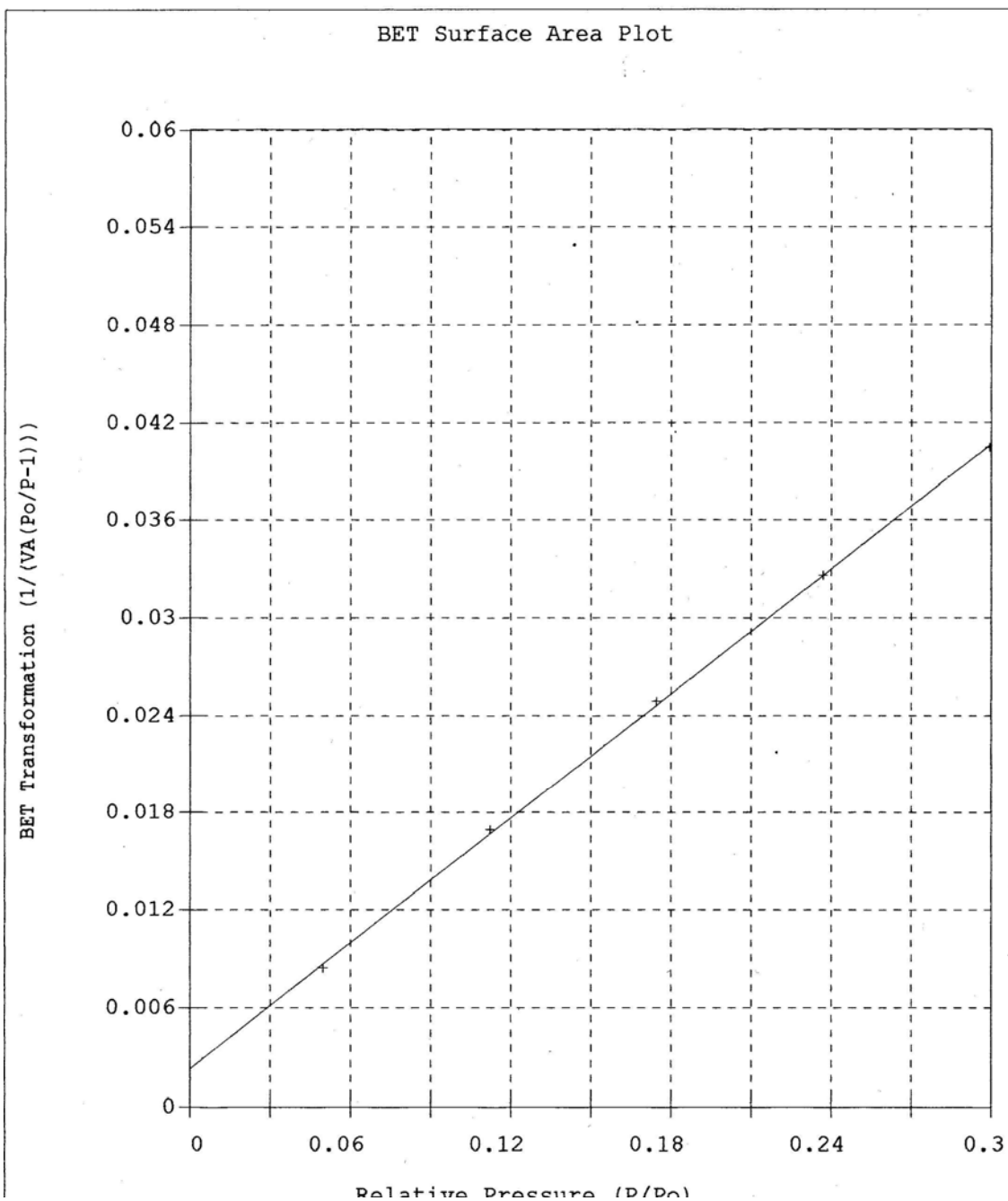
Micropore Volume: -0.002793 cc/g
 Micropore Area: -4.5754 sq. m/g
 External Surface Area: 38.0334 sq. m/g
 Slope: 2.458842
 Y-Intercept: -1.805691
 Correlation Coefficient: 9.9991e-001
 Thickness Values Between: 3.500 and 5.000 A
 Area Correction Factor: 1.000
 0.5000
 $t = [13.9900 / (0.0340 - \log(P/P_0))]$

Analysis Log

Relative Pressure	Pressure (mmHg)	Vol. Adsorbed (cc/g STP)	Elapsed Time, (h:m)	Statistical Thickness, (A)	Surface Area Point
0.0499	38.50	6.227	0:25	3.236	*
0.1123	86.65	7.475	0:30	3.771	*
0.1746	134.79	8.513	0:34	4.203	*
0.2370	182.98	9.530	0:38	4.607	*
0.2995	231.18	10.568	0:42	5.009	*

Micromeritics Instrument Corporation
Gemini 2375 V4.01 Instrument ID: 1089

Sample ID: R-9256-1 File: R-9256-1.MGD
Sample Weight: 0.598500
Start Date & Time: 05/04/04 07:36:44
End Date & Time: 05/04/04 08:19:27



Gemini 2375 V4.01
Instrument ID: 1089
Setup Group: 9 - Clay

Sample ID: R-9329-2 Started: 05/04/04 09:27:08
Sample Weight: 0.8574 g Completed: 05/04/04 10:15:20
Evacuation Rate: 300.0 mmHg/min Evacuation Time: 1.0 min
Measured Free Space: -1.105 cc STP Saturation Pressure: 771.93 mmHg
Analysis Mode: Equilibration Equilibration Time: 5 sec

BET Multipoint Surface Area Report

Surface Area: 34.0363 sq. m/g
Slope: 0.125999
Y-Intercept: 0.001900
C: 67.308662
Vm: 7.818679
Correlation Coefficient: 9.9992e-001

BET Single Point Surface Area: 32.9156 sq. m/g

t-Method Micropore Report

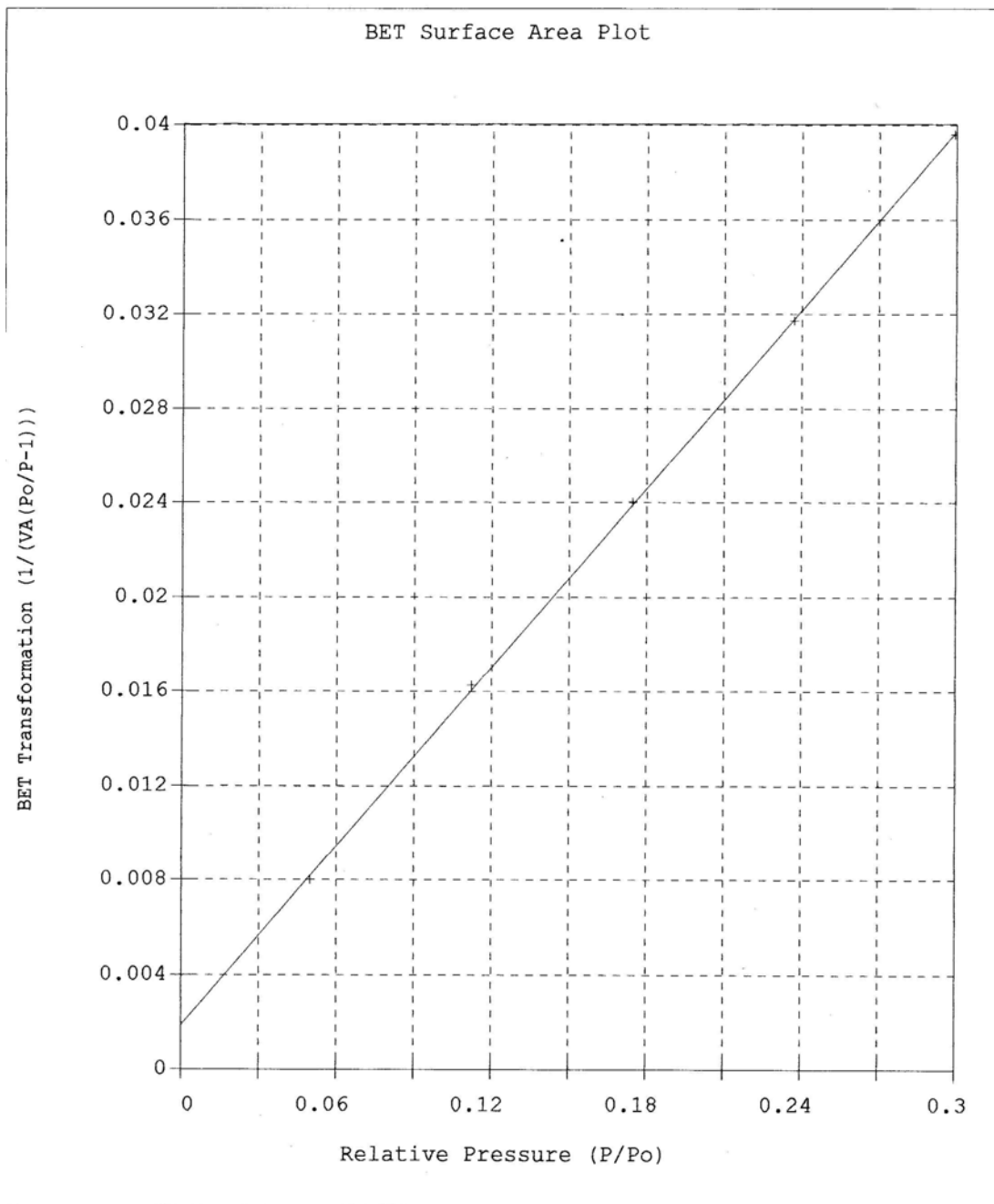
Micropore Volume: -0.002048 cc/g
Micropore Area: -3.2982 sq. m/g
External Surface Area: 37.3344 sq. m/g
Slope: 2.413656
Y-Intercept: -1.323949
Correlation Coefficient: 9.9999e-001
Thickness Values Between: 3.500 and 5.000 A
Area Correction Factor: 1.000
0.5000
 $t = [13.9900 / (0.0340 - \log(P/P_0))]$

Analysis Log

Relative Pressure	Pressure (mmHg)	Vol. Adsorbed (cc/g STP)	Elapsed Time, (h:m)	Statistical Thickness, (A)	Surface Area Point
0.0499	38.49	6.565	0:28	3.236	*
0.1123	86.65	7.781	0:33	3.771	*
0.1746	134.79	8.815	0:40	4.203	*
0.2370	182.97	9.798	0:43	4.607	*
0.2995	231.16	10.801	0:47	5.009	*

Micromeritics Instrument Corporation
Gemini 2375 V4.01 Instrument ID: 1089

Sample ID: R-9329-2 File: R-9329-2.MGD
Sample Weight: 0.857400
Start Date & Time: 05/04/04 09:27:08
End Date & Time: 05/04/04 10:15:20



Gemini 2375 V4.01
Instrument ID: 1089
Setup Group: 9 - Clay

Sample ID: R-9351-1	Started: 05/04/04 13:17:09
Sample Weight: 0.6878 g	Completed: 05/04/04 13:56:56
Evacuation Rate: 300.0 mmHg/min	Evacuation Time: 1.0 min
Measured Free Space: -0.934 cc STP	Saturation Pressure: 771.93 mmHg
Analysis Mode: Equilibration	Equilibration Time: 5 sec

BET Multipoint Surface Area Report

Surface Area:	30.3447	sq. m/g
Slope:	0.140819	
Y-Intercept:	0.002639	
C:	54.363335	
Vm:	6.970672	
Correlation Coefficient:	9.9982e-001	

BET Single Point Surface Area: 29.1951 sq. m/g

t-Method Micropore Report

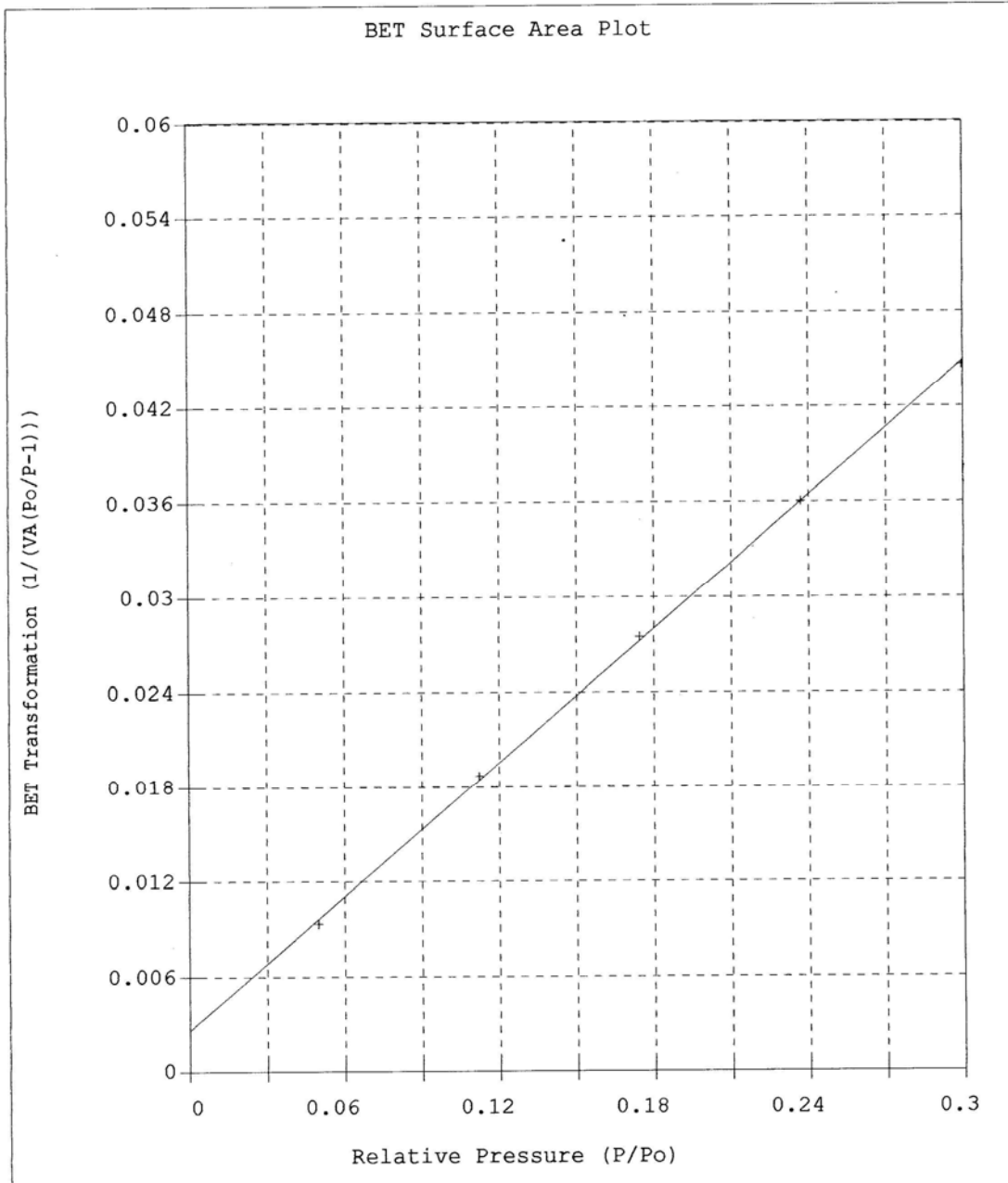
Micropore Volume:	-0.002600	cc/g
Micropore Area:	-4.2345	sq. m/g
External Surface Area:	34.5792	sq. m/g
Slope:	2.235532	
Y-Intercept:	-1.680835	
Correlation Coefficient:	9.9991e-001	
Thickness Values Between:	3.500 and	5.000 A
Area Correction Factor:	1.000	0.5000
t = [13.9900 / (0.0340 - log(P/Po))]		

Analysis Log

Relative Pressure	Pressure (mmHg)	Vol. Adsorbed (cc/g STP)	Elapsed Time, (h:m)	Statistical Thickness, (A)	Surface Area Point
0.0499	38.49	5.621	0:24	3.236	*
0.1123	86.67	6.757	0:27	3.771	*
0.1746	134.79	7.700	0:31	4.203	*
0.2370	182.97	8.626	0:35	4.607	*
0.2995	231.18	9.581	0:39	5.009	*

Micromeritics Instrument Corporation
Gemini 2375 V4.01 Instrument ID: 1089

Sample ID: R-9351-1 File: R-9351-1.MGD
Sample Weight: 0.687800
Start Date & Time: 05/04/04 13:17:09
End Date & Time: 05/04/04 13:56:56



Gemini 2375 V4.01
 Instrument ID: 1089
 Setup Group: 9 - Clay

Sample ID: R-9352-1 Started: 05/04/04 12:42:04
 Sample Weight: 0.2574 g Completed: 05/04/04 13:13:44
 Evacuation Rate: 300.0 mmHg/min Evacuation Time: 1.0 min
 Measured Free Space: -0.387 cc STP Saturation Pressure: 771.93 mmHg
 Analysis Mode: Equilibration Equilibration Time: 5 sec

BET Multipoint Surface Area Report

Surface Area: 18.3290 sq. m/g
 Slope: 0.233190
 Y-Intercept: 0.004313
 C: 55.070301
 Vm: 4.210474
 Correlation Coefficient: 9.9996e-001

BET Single Point Surface Area: 17.5738 sq. m/g

t-Method Micropore Report

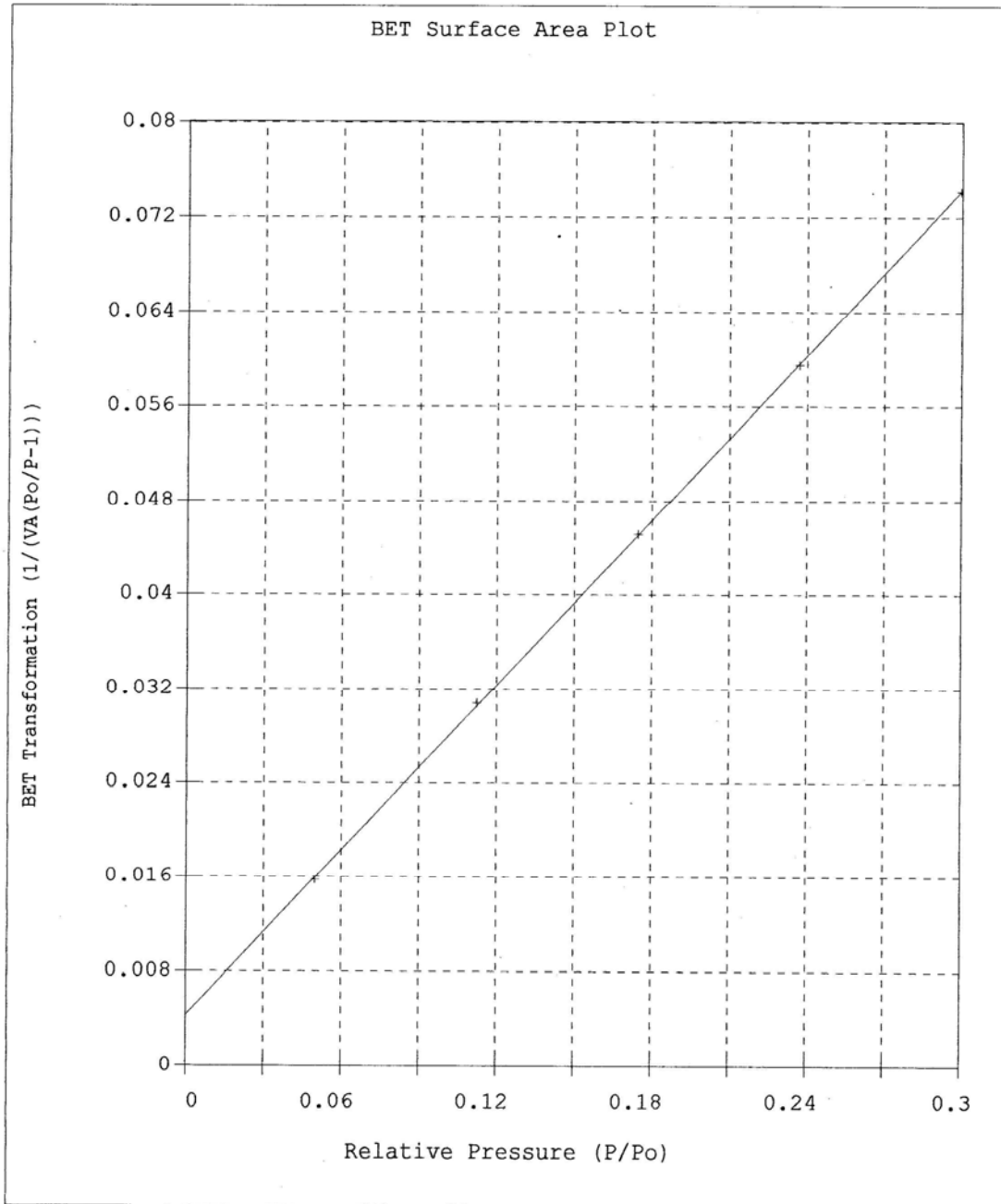
Micropore Volume: -0.001439 cc/g
 Micropore Area: -2.3431 sq. m/g
 External Surface Area: 20.6721 sq. m/g
 Slope: 1.336445
 Y-Intercept: -0.930422
 Correlation Coefficient: 9.9998e-001
 Thickness Values Between: 3.500 and 5.000 A
 Area Correction Factor: 1.000
 0.5000
 $t = [13.9900 / (0.0340 - \log(P/P_0))]$

Analysis Log

Relative Pressure	Pressure (mmHg)	Vol. Adsorbed (cc/g STP)	Elapsed Time, (h:m)	Statistical Thickness, (A)	Surface Area Point
0.0499	38.54	3.341	0:20	3.236	*
0.1123	86.68	4.108	0:23	3.771	*
0.1746	134.79	4.690	0:26	4.203	*
0.2370	182.99	5.225	0:28	4.607	*
0.2995	231.21	5.767	0:31	5.009	*

Micromeritics Instrument Corporation
Gemini 2375 V4.01 Instrument ID: 1089

Sample ID: R-9352-1 File: R-9352-1.MGD
Sample Weight: 0.257400
Start Date & Time: 05/04/04 12:42:04
End Date & Time: 05/04/04 13:13:44



Gemini 2375 V4.01
Instrument ID: 1089
Setup Group: 9 - Clay

Sample ID: R-9368-9 Started: 05/04/04 06:56:24
Sample Weight: 0.3041 g Completed: 05/04/04 07:33:18
Evacuation Rate: 300.0 mmHg/min Evacuation Time: 1.0 min
Measured Free Space: -0.458 cc STP Saturation Pressure: 771.93 mmHg
Analysis Mode: Equilibration Equilibration Time: 5 sec

BET Multipoint Surface Area Report

Surface Area: 24.2282 sq. m/g
Slope: 0.176152
Y-Intercept: 0.003522
C: 51.010719
Vm: 5.565619
Correlation Coefficient: 9.9993e-001

BET Single Point Surface Area: 23.1763 sq. m/g

t-Method Micropore Report

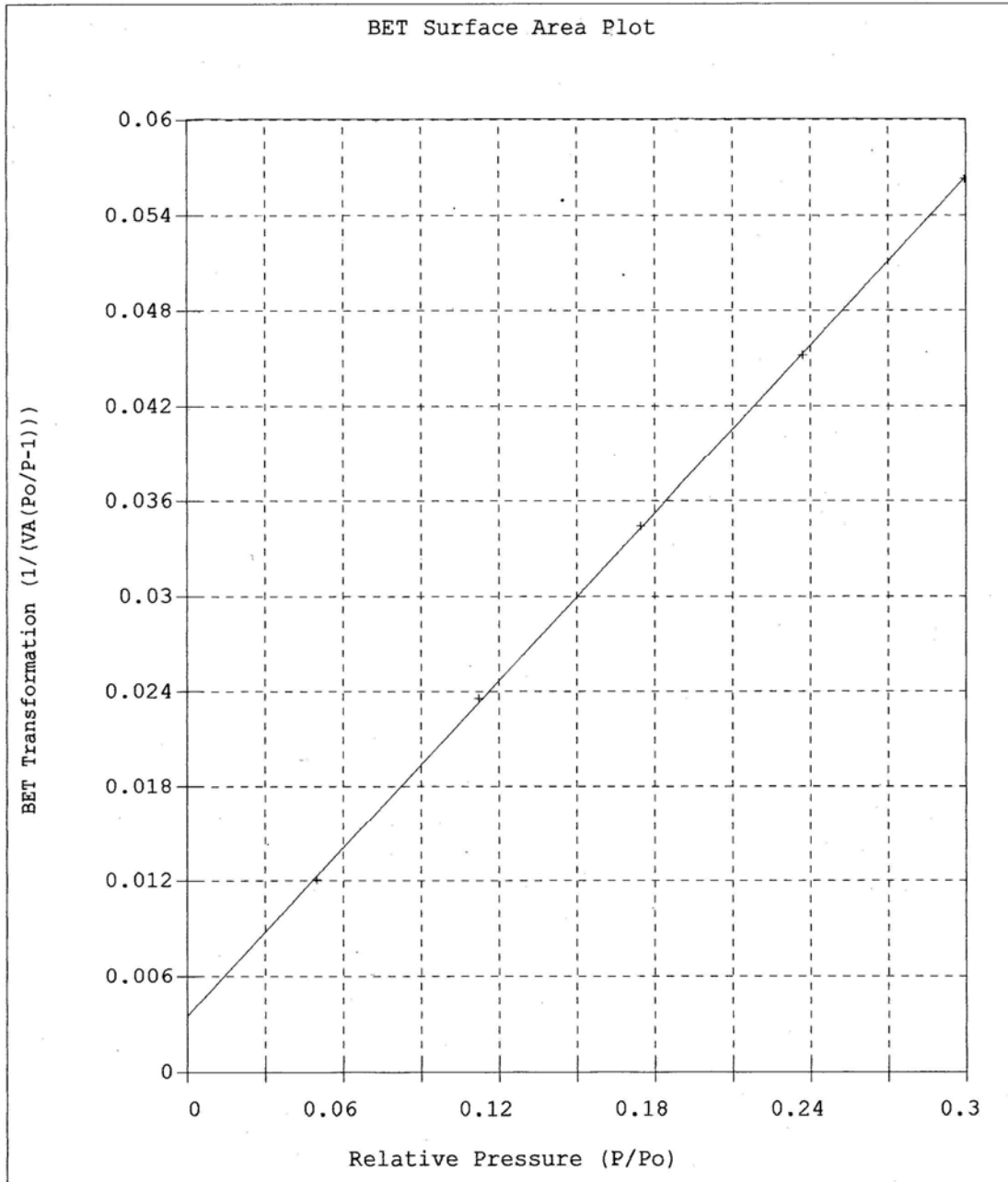
Micropore Volume: -0.002248 cc/g
Micropore Area: -3.7391 sq. m/g
External Surface Area: 27.9673 sq. m/g
Slope: 1.808077
Y-Intercept: -1.453283
Correlation Coefficient: 1.0000e+000
Thickness Values Between: 3.500 and 5.000 A
Area Correction Factor: 1.000
0.5000
 $t = [13.9900 / (0.0340 - \log(P/P_0))]$

Analysis Log

Relative Pressure	Pressure (mmHg)	Vol. Adsorbed (cc/g STP)	Elapsed Time, (h:m)	Statistical Thickness, (A)	Surface Area Point
0.0499	38.51	4.354	0:23	3.236	*
0.1123	86.67	5.365	0:26	3.771	*
0.1746	134.79	6.146	0:29	4.203	*
0.2370	182.97	6.876	0:33	4.607	*
0.2995	231.19	7.606	0:36	5.009	*

Micromeritics Instrument Corporation
Gemini 2375 V4.01 Instrument ID: 1089

Sample ID: R-9368-9 File: R-9368-9.MGD
Sample Weight: 0.304100
Start Date & Time: 05/04/04 06:56:24
End Date & Time: 05/04/04 07:33:18



Gemini 2375 V4.01
Instrument ID: 1089
Setup Group: 9 - Clay

Sample ID: R-9370-2 Started: 05/04/04 11:22:26
Sample Weight: 0.4323 g Completed: 05/04/04 11:57:32
Evacuation Rate: 300.0 mmHg/min Evacuation Time: 1.0 min
Measured Free Space: -0.322 cc STP Saturation Pressure: 771.93 mmHg
Analysis Mode: Equilibration Equilibration Time: 5 sec

BET Multipoint Surface Area Report

Surface Area: 22.5782 sq. m/g
Slope: 0.189295
Y-Intercept: 0.003511
C: 54.920433
Vm: 5.186572
Correlation Coefficient: 9.9996e-001

BET Single Point Surface Area: 21.6213 sq. m/g

t-Method Micropore Report

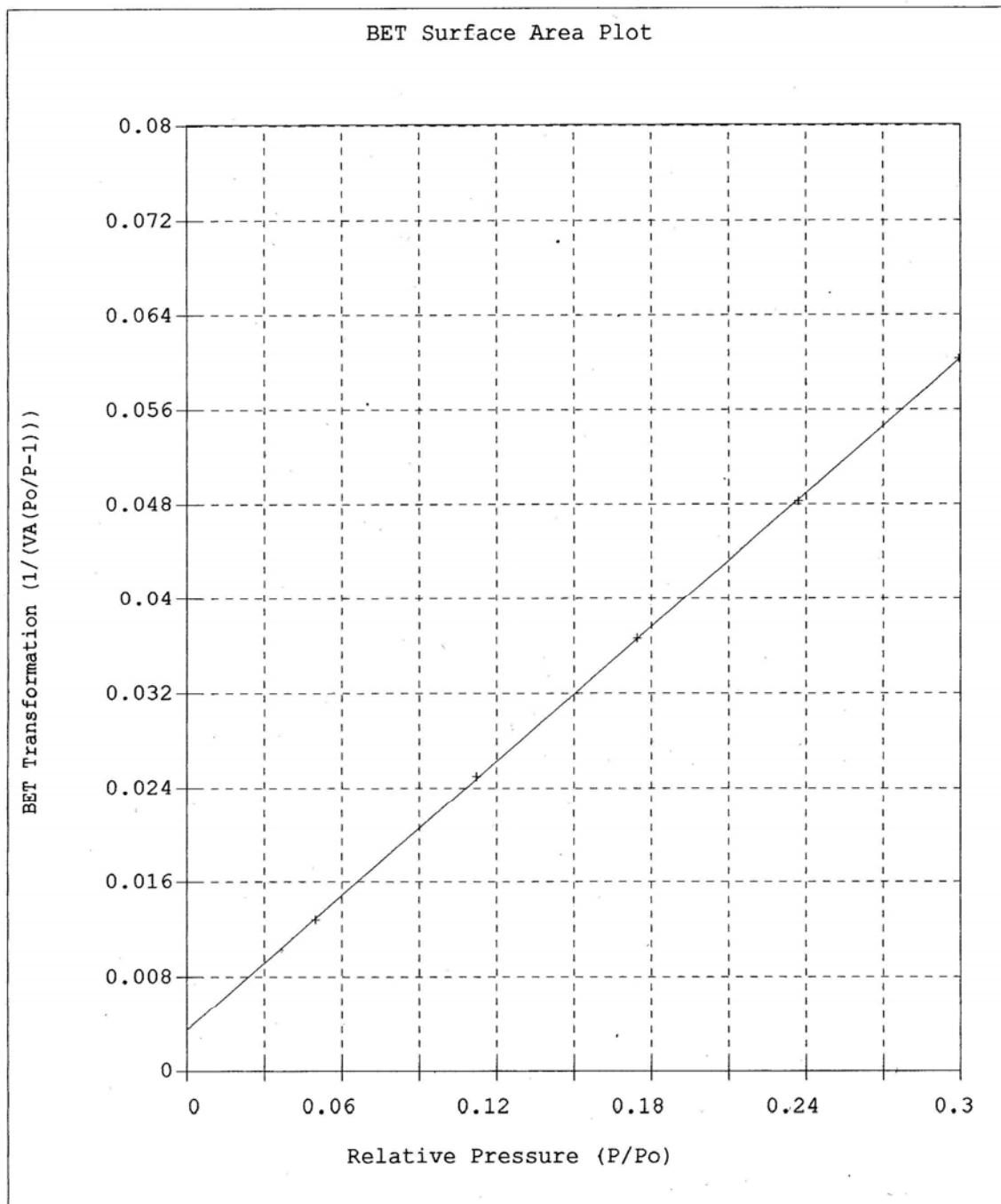
Micropore Volume: -0.001818 cc/g
Micropore Area: -3.0101 sq. m/g
External Surface Area: 25.5883 sq. m/g
Slope: 1.654273
Y-Intercept: -1.175558
Correlation Coefficient: 9.9997e-001
Thickness Values Between: 3.500 and 5.000 A
Area Correction Factor: 1.000
0.5000
 $t = [13.9900 / (0.0340 - \log(P/P_0))]$

Analysis Log

Relative Pressure	Pressure (mmHg)	Vol. Adsorbed (cc/g STP)	Elapsed Time, (h:m)	Statistical Thickness, (A)	Surface Area Point
0.0499	38.49	4.098	0:21	3.236	*
0.1123	86.67	5.060	0:24	3.771	*
0.1746	134.80	5.784	0:27	4.203	*
0.2370	182.98	6.442	0:31	4.607	*
0.2995	231.18	7.095	0:34	5.009	*

Micromeritics Instrument Corporation
Gemini 2375 V4.01 Instrument ID: 1089

Sample ID: R-9370-2 File: R-9370-2.MGD
Sample Weight: 0.432300
Start Date & Time: 05/04/04 11:22:26
End Date & Time: 05/04/04 11:57:32



APPENDIX D

CEC

Cation Exchange Capacity Calculations

The exchange solution with concentration C_1 diluted to concentration C_2 in the selected standard concentration range. Before running the sample ASS was calibrated by running the standard for each element desired to be measured.

Concentration of exchange solution was determined by correction factor for dilution.

$C_1 = d * C_2$ exchange solution

C_3 = contamination of same ion in test IM NaCl solution.

C_4 is the actual concentration of exchangeable cation in extracted solution

$$C_5 = \frac{C_4 \times m_{liq}}{998.3}$$

The density of water at 20 °C

m_{liq} = mass of exchangeable solution

$$mMg = \sum C_{5i}$$

$mMg = 0.6980mg$

mMg is the mass of magnesium

As the mole weight is 24.305 g/mol, and one mole weight is half the equivalent mass the latter becomes:

$$meq = \frac{mMg \times 2eq / mmol}{MMg} = \frac{0.6980mg \times 2eq / mmol}{24.305mg / mmol} = 0.058082$$

The calcium exchange capacity per gram

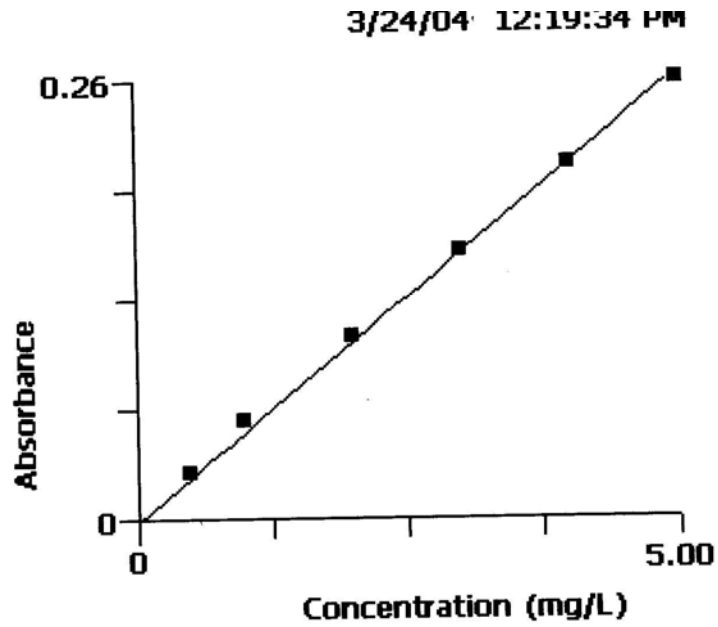
$CEC = 0.019361 meq/g$

$MEC = meq \times 100 / \text{weight of sample}$

$= 0.058082 meq \times 100 / 3.000g = 1.9361 meq/100g$

Ca Standards			
mg/l	Mean abs	SD	RSD (%)
0	-0.001	0.0003	61.4
0.5	0.030	0.0003	1.0
1	0.061	0.0006	1.0
2	0.111	0.0004	0.3
3	0.162	0.0016	1.0
4	0.214	0.0001	0
5	0.264	0.0013	0.5

Ca



Calibration Type Linear Through Zero

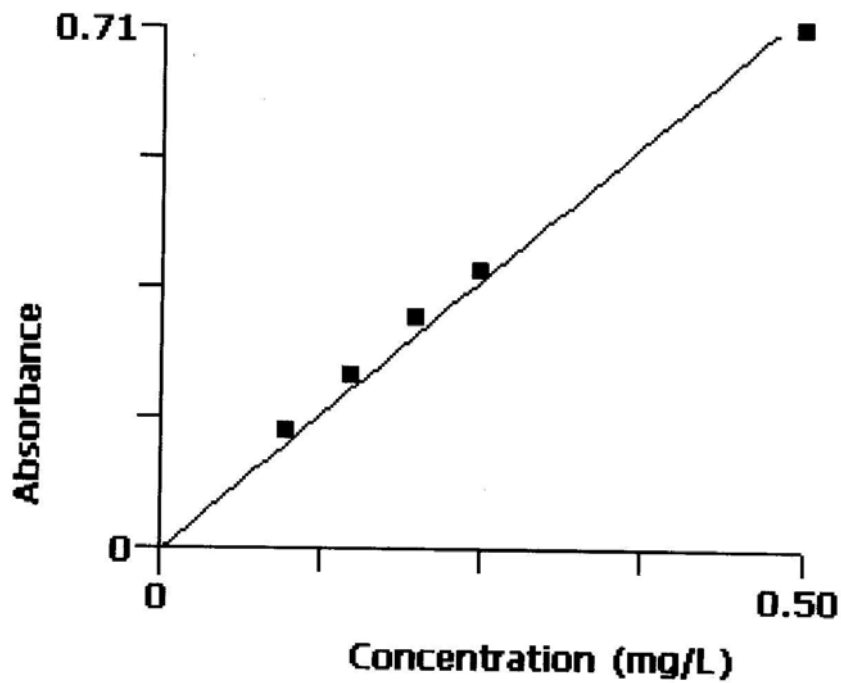
Slope 0.05358

Correlation Coefficient 0.998820

Mg Standards			
mg/l	Mean abs	SD	RSD (%)
0	0.000	0.0011	794.6
0.1	0.154	0.0011	0.7
0.15	0.229	0.0018	0.8
0.20	0.298	0.0023	0.8
0.25	0.375	0.0036	1.0
0.5	.699	0.0041	0.6

Mg

3/22/04 5:25:25 PM

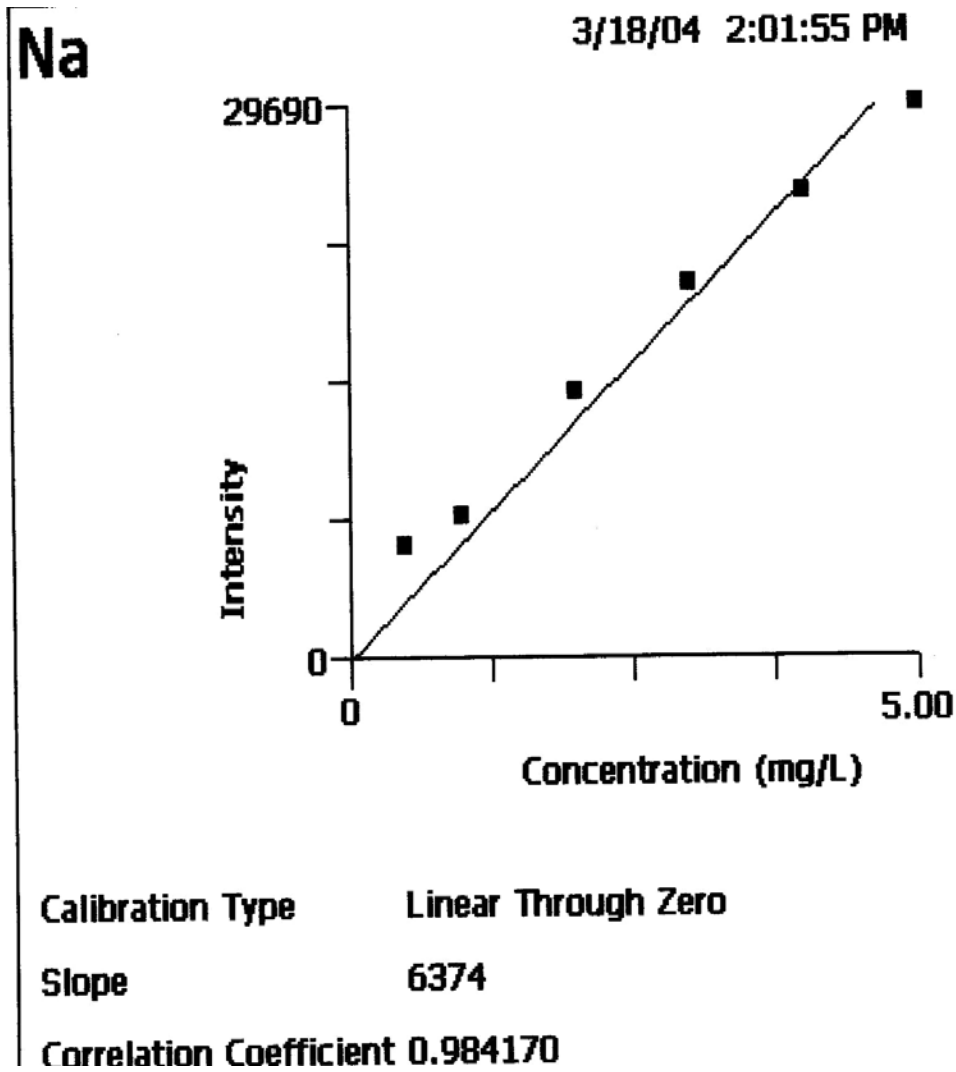


Calibration Type **Linear Through Zero**

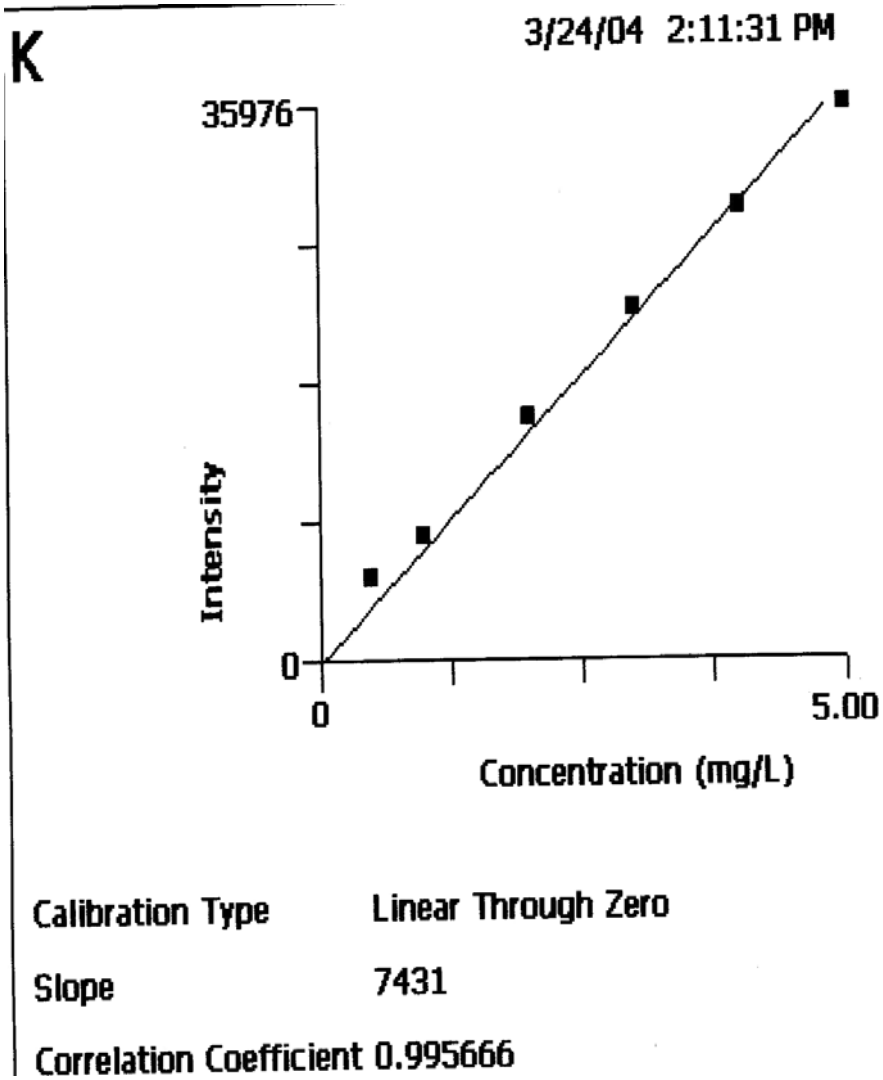
Slope **1.46431**

Correlation Coefficient **0.995335**

Na Standards			
mg/l	Mean abs	SD	RSD (%)
0	53	5.6773	10.8
0,5	4100	17.3020	0.4
1	6601	9.760	0.1
2	12271	64.1144	0.5
3	17330	25.1420	0.1
4	21446	113.0201	0.5
5	2554	142.5010	0.6



K Standards			
mg/l	Mean abs	SD	RSD (%)
0	1	2.0874	247.7
0,5	4295	31.9628	0.7
1	8325	19.8770	0.2
2	15940	46.4468	0.3
3	22999	83.6332	0.4
4	29437	61.7869	0.2
5	35976	97.1512	0.3



Calcium

1st Extraction

Sample No	m _{liquid} = NaCl added mg/l	C ₂ mg /l	Dilution =d	C ₁ = d *C ₂ mg /l	C ₃ = contamination in NaCl	C ₄ =C ₁ -C ₃	C ₃ * m _{liquid}	m _{liquid} * C ₃ C ₅ = ----- 998,3
9238-9	26,14	2,034	50	101,7	1,124	100,576	2629	2,633534
9368-9	26,13	1,545	50	77,25	1,124	76,126	1989	1,99256
9256-1	26,12	2,86	50	143	1,124	141,876	3705	3,712112
9352-1	26	2,032	200	406,4	1,124	405,276	10537	10,55512
9254-6	25,95	1,832	50	91,6	1,124	90,476	2347	2,35185
9329-2	26,06	2,746	50	137,3	1,124	136,176	3548	3,55479
9251-2	26	1,882	50	94,1	1,124	92,976	2417	2,421493
9242-8	25,92	3,318	50	165,9	1,124	164,776	4270	4,278267
9351-1	25,96	2,554	50	127,7	1,124	126,576	3285	3,291509
9370-2	26,02	1,826	50	91,3	1,124	90,176	2346	2,350375

2nd Extraction

9238-9	25,43	3,083	10	30,83	1,124	29,706	755	0,75671
9368-9	25,68	3,16	10	31,6	1,124	30,476	782	0,783956
9256-1	30,48	2,885	10	28,85	1,124	27,726	845	0,846528
9352-1	23,29	4,028	10	40,28	1,124	39,156	911	0,913496
9254-6	25,18	3,185	10	31,85	1,124	30,726	773	0,774998
9329-2	24,92	4,491	10	44,91	1,124	43,786	1091	1,093005
9251-2	31,8	4,084	10	40,84	1,124	39,716	1262	1,26512
9242-8	24,78	4,979	10	49,79	1,124	48,666	1205	1,207997
9351-1	25,15	3,931	10	39,31	1,124	38,186	96079	0,962013

3rd Extraction

9238-9	38,27	3,017	10	30,17	1,124	29,046	1111	1,113483
9368-9	31,79	3,168	10	31,68	1,124	30,556	971	0,973029
9256-1	37,09	2,839	10	28,39	1,124	27,266	1011	1,013018
9352-1	30,97	3,384	10	33,84	1,124	32,716	1013	1,01494
9254-6	31,2	2,972	10	29,72	1,124	28,596	892	0,893715
9329-2	35,72	3,619	10	36,19	1,124	35,066	1252	1,25469
9251-2	37,26	2,677	10	26,77	1,124	25,646	955	0,957197
9242-8	31,25	3,6	10	36	1,124	34,876	1089	1,091731
9351-1	33,96	2,023	10	20,23	1,124	19,106	648	0,649945
9370-2	34,07	3,515	10	35,15	1,124	34,026	1159	1,16124

Calcium

4th Extraction

Sample No	m _{liquid} = NaCl added mg/l	C ₂ mg /l	Dilution =d	C ₁ = d *C ₂ mg /l	C ₃ = contamination in NaCl	C ₄ =C ₁ -C ₃	C ₃ * m _{liquid}	m _{liquid} * C ₃ C ₅ =----- 998,3
9238-9	37,83	5,07	5	25,35	1,124	24,226	916	0,91803
9368-9	30,1	4,708	5	23,54	1,124	22,416	674	0,675871
9256-1	37,47	4,662	5	23,31	1,124	22,186	831	0,832725
9352-1	29,15	2,54	20	50,8	1,124	49,676	1448	1,450521
9254-6	29,63	4,548	5	22,74	1,124	21,616	6401	0,641573
9329-2	35,13	2,352	10	23,52	1,124	22,396	786	0,788111
9251-2	36,81	4,991	5	24,955	1,124	23,831	877	0,878713
9242-8	31,1	4,688	5	23,44	1,124	22,316	694	0,695209
9351-1	32,1	4,373	5	21,865	1,124	20,741	665	0,66692
9370-2	33,51	4,113	5	20,565	1,124	19,441	651	0,652577

5th Extraction

9238-9	38,03	4,93	5	24,65	1,124	23,526	894	0,896217
9368-9	31,89	5,279	5	26,395	1,124	25,271	805	0,807265
9256-1	36,89	4,948	5	24,74	1,124	23,616	871	0,872678
9352-1	30,47	3,835	10	38,35				
9254-6	29,13	5,135	5	25,675	1,124	24,551	715	0,716388
9329-2	38,59	5,33	5	26,65	1,124	25,526	9853	0,986726
9251-2	35,66	4,77	5	23,85	1,124	22,726	810	0,811789
9242-8	34,27	5,493	5	27,465	1,124	26,341	902	0,904243
9351-1	32,26	5,409	5	27,045	1,124	25,921	8365	0,837635
9370-2	33,6	4,719	5	23,595	1,124	22,471	755	0,756311

6th Extraction

9238-9	36,49	1,295	20	25,9	1,124	24,776	904	0,905616
9368-9	27,63	4,787	5	23,935	1,124	22,811	630	0,631341
9256-1	35,01	4,728	5	23,64	1,124	22,516	788	0,789628
9352-1	27,66	5,007	5	25,035	1,124	23,911	661	0,662505
9254-6	28,99	4,661	5	23,305	1,124	22,181	643	0,644122
9329-2	35,83	4,727	5	23,635	1,124	22,511	806	0,807943
9251-2	34,35	4,88	5	24,4	1,124	23,276	7996	0,800892
9242-8	28,51	5,319	5	26,595	1,124	25,471	726	0,727415
9351-1	31,27	4,489	5	22,445	1,124	21,321	666	0,667843
9370-2	32,11	3,009	5	15,045	1,124	13,921	447	0,447765

Calcium

7th Extraction

9238-9	32,88	4,013	5	20,065	1,124	18,941	622	0,623841
9368-9	30,19	3,737	5	18,685	1,124	17,561	530	0,531069
9256-1	36,31	3,737	5	18,685	1,124	17,561	637	0,638726
9352-1	28,9	3,31	5	16,55	1,124	15,426	445	0,446571
9254-6	28,2	4,056	5	20,28	1,124	19,156	5402	0,541119
9329-2	35,9	4,103	5	20,515	1,124	19,391	696	0,697322
9251-2	36,58	3,324	5	16,62	1,124	15,496	566	0,567809
9242-8	29,32	4,104	5	20,52	1,124	19,396	568	0,569659
9351-1	32,21	4,034	5	20,17	1,124	19,046	613	0,614516
9370-2	29,69	3,767	5	18,835	1,124	17,711	525	0,526735

8th Extraction

9238-9	31	3,807	5	19,035	1,124	17,911	555	0,556187
9368-9	28,34	3,788	5	18,94	1,124	17,816	504	0,505765
9256-1	35,29	3,707	5	18,535	1,124	17,411	614	0,615481
9352-1	29,56	3,562	5	17,81	1,124	16,686	4932	0,494078
9254-6	27,97	3,804	5	19,02	1,124	17,896	500	0,501404
9329-2	35,47	3,736	5	18,68	1,124	17,556	622	0,623772
9251-2	35,38	3,721	5	18,605	1,124	17,481	618	0,619531
9242-8	30,18	3,886	5	19,43	1,124	18,306	552	0,553416
9351-1	31,11	3,65	5	18,25	1,124	17,126	532	0,533697
9370-2	32,66	3,644	5	18,22	1,124	17,096	558	0,559306

9th Extraction

9238-9	28	3,549	5	17,745	1,124	16,621	465	0,466181
9368-9	25,34	3,5	5	17,5	1,124	16,376	414	0,415674
9256-1	31,29	3,571	5	17,855	1,124	16,731	523	0,524404
9352-1	26,56	3,497	5	17,485	1,124	16,361	434	0,435288
9254-6	22,97	3,526	5	17,63	1,124	16,506	379	0,379788
9329-2	32,47	3,808	5	19,04	1,124	17,916	581	0,582723
9251-2	32,38	4,211	5	21,055	1,124	19,931	645	0,646465
9242-8	27,18	4,857	5	24,285	1,124	23,161	629	0,630588
9351-1	28,11	4,2	5	21	1,124	19,876	558	0,559666
9370-2	29	4,2	5	21	1,124	19,876	576	0,577386

Calcium

10th Extraction

238-9	28	1,8	5	9	1,124	7,876	220	0,220904
9368-9	25,34	1,75	5	8,75	1,124	7,626	193	0,193572
9256-1	31,29	1,43	5	7,15	1,124	6,026	188	0,188875
9352-1	26,56	1,3	5	6,5	1,124	5,376	142	0,14303
9254-6	22,97	1,5	5	7,5	1,124	6,376	146	0,146706
9329-2	32,47	1,6	5	8	1,124	6,876	223	0,223644
9251-2	32,38	1,45	5	7,25	1,124	6,126	198	0,198698
9242-8	27,18	1,47	5	7,35	1,124	6,226	169	0,169511
9351-1	28,11	1,53	5	7,65	1,124	6,526	183	0,183758
9370-2	29	1,42	5	7,1	1,124	5,976	173	0,173599

Sample No	Total mg of Ca	Atomic weight of Ca	mg Ca 2 eq /m mol meq= ----- Atomic weight of Ca	Weight of sample in g	CEC per 100 g
9238-9		40	9,626398	3,05	15,75027
9368-9		40	7,986148	3,04	13,10955
9256-1		40	10,61304	3,03	17,47919
9352-1		40	17,72635	3,04	29,09844
9254-6		40	8,01466	3,03	13,19977
9329-2		40	11,26304	3,02	18,61112
9251-2		40	9,871833	3,21	15,34676
9242-8		40	11,50812	4,09	14,04122
9351-1		40	9,58173	3,41	14,02212
9370-2		40	7,92107	3,16	12,50888

Magnesium

1st Extraction

Sample No	m _{liquid} = NaCl added mg/l	C ₂ mg /l	Dilution =d	C ₁ = d *C ₂ mg /l	C ₃ = contamination in NaCl	C ₄ =C ₁ -C ₃	C ₃ * m _{liquid}	m _{liquid} * C ₃ C ₅ = ----- 998,3
9238-9	26,14	0,261	0,4	50	13,05	12,65	330	0,331234
9368-9	26,13	0,089	0,4	50	4,45	4,05	105	0,106007
9256-1	26,12	0,228	0,4	50	11,4	11	287	0,287809
9352-1	26	0,224	0,4	50	11,2	10,8	280	0,281278
9254-6	25,95	0,215	0,4	50	10,75	10,35	268	0,26904
9329-2	26,06	0,297	0,4	50	14,85	14,45	376	0,377208
9251-2	26	0,277	0,4	50	13,85	13,45	349	0,350296
9242-8	25,92	0,34	0,4	50	17	16,6	430	0,431005
9351-1	25,96	0,157	0,4	50	7,85	7,45	193	0,193731
9370-2	26,02	0,093	0,4	50	4,65	4,25	110	0,110773

2nd Extraction

9238-9	25,43	0,491	0,4	10	4,91	4,51	114	0,114885
9368-9	25,68	0,18	0,4	10	1,8	1,4	35	0,036013
9256-1	30,48	0,361	0,4	10	3,61	3,21	97	0,098007
9352-1	23,29	0,26	0,4	10	2,6	2,2	51	0,051325
9254-6	25,18	0,382	0,4	10	3,82	3,42	86	0,086262
9329-2	24,92	0,9	0,4	10	9	8,6	214	0,214677
9251-2	31,8	0,547	0,4	10	5,47	5,07	161	0,161501
9242-8	24,78	0,65	0,4	10	6,5	6,1	151	0,151415
9351-1	25,15	0,35	0,4	10	3,5	3,1	77	0,078098
9370-2	25,46	0,147	0,4	10	1,47	1,07	27	0,027289

3rd Extraction

9238-9	38,27	0,101	0,4	10	1,01	0,61	23	0,023384
9368-9	31,79	0,049	0,4	10	0,49	0,09	2,	0,002866
9256-1	37,09	0,094	0,4	10	0,94	0,54	20	0,020063
9352-1	30,97	0,7	0,4	10	7	6,6	204	0,20475
9254-6	31,2	0,105	0,4	10	1,05	0,65	20	0,020315
9329-2	35,72	0,165	0,4	10	1,65	1,25	44	0,044726
9251-2	37,26	0,097	0,4	10	0,97	0,57	21	0,021274
9242-8	31,25	0,07	0,4	10	0,7	0,3	9,	0,009391
9351-1	33,96	0,086	0,4	10	0,86	0,46	15	0,015648
9370-2	34,07	0,052	0,4	10	0,52	0,12	4	0,004095

Magnesium

4th Extraction

Sample No	$m_{\text{liquid}} = \text{NaCl added mg/l}$	C_2 mg /l	Dilution =d	$C_1 = d * C_2$ mg /l	$C_3 =$ contamination in NaCl	$C_4 = C_1 - C_3$	$C_3 * m_{\text{liquid}}$	$m_{\text{liquid}} * C_3$ $C_5 = \frac{\quad}{998,3}$
9238-9	37,83	0,106	0,4	5	0,53	0,13	4	0,004926
9368-9	30,1	0,065	0,4	5	0,325	0	0	0
9256-1	37,47	0,097	0,4	5	0,485	0,085	3	0,00319
9352-1	29,15	0,107	0,4	5	0,535	0,135	3	0,003942
9254-6	29,63	0,103	0,4	5	0,515	0,115	3	0,003413
9329-2	35,13	0,183	0,4	5	0,915	0,515	18	0,018123
9251-2	36,81	0,112	0,4	5	0,56	0,16	5	0,0059
9242-8	31,1	0,094	0,4	5	0,47	0,07	2	0,002181
9351-1	32,1	0,052	0,4	5	0,26	0	0	0
9370-2	33,51	0,003	0,4	5	0,015	0	0	0

5th Extraction

9238-9	38,03	0,538	0,4	5	2,69	2,29	87	0,087237
9368-9	31,89	0,252	0,4	5	1,26	0,86	27	0,027472
9256-1	36,89	0,252	0,4	10	2,52	2,12	78	0,07834
9352-1	30,47	0,473	0,4	5	2,365	1,965	59	0,059976
9254-6	29,13	0,09	0,4	5	0,45	0,05	1	0,001459
9329-2	38,59	0,31	0,4	10	3,1	2,7	104	0,10437
9251-2	35,66	0,235	0,4	5	10	9,6	342	0,342919
9242-8	34,27	0,268	0,4	10	2,68	2,28	78	0,078269
9351-1	32,26	0,521	0,4	5	2,605	2,205	71	0,071254
9370-2	33,6	0,222	0,4	5	1,11	0,71	23	0,023897

Sample No	Total mg of Mg	atomic weight of Mg	$\text{mg ca } 2 \text{ eq / m mol}$ $\text{meq} = \frac{\quad}{\text{atomic weigh of Mg}}$	weight of samples in g	CEC per 100 g
9238-9	0,573729	24,305	0,047211	3,05	1,547893
9368-9	0,198561	24,305	0,016339	3,04	0,537472
9256-1	0,504769	24,305	0,041536	3,03	1,370833
9352-1	0,609029	24,305	0,050116	3,04	1,648537
9254-6	0,38528	24,305	0,031704	3,03	1,04633
9329-2	0,803609	24,305	0,066127	3,02	2,189638
9251-2	0,906491	24,305	0,074593	3,21	2,323769
9242-8	0,699677	24,305	0,057575	4,09	1,407695
9351-1	0,371888	24,305	0,030602	3,41	0,897411
9370-2	0,16927	24,305	0,013929	3,16	0,440786

Sodium

1st Extraction

Sample No	*m _{liquid} =NH ₄ Cl added mg/l	C ₂ mg /l from AAs	Dilutio n =d	C ₁ = d *C ₂ mg /l	C ₃ Contaminatio n in solution	C ₄ =C ₁ - C ₃	C ₃ *m _{liquid}	C ₅ =C ₃ * mquid ----- 998,3
9238-9	25,55	0,576	10	5,76	0,4	5,36	136	0,137181
9368-9	25,38	0,247	10	2,47	0,4	2,07	52	0,052626
9256-1	25,5	0,602	10	6,02	0,4	5,62	143	0,143554
9352-1	25,46	0,366	10	3,66	0,4	3,26	82	0,083141
9254-6	25,57	0,62	10	6,2	0,4	5,8	148	0,148559
9329-2	25,85	2,45	10	24,5	0,4	24,1	622	0,624046
9251-2	25,66	0,56	10	5,6	0,4	5,2	133	0,133659
9242-8	25,54	0,852	10	8,52	0,4	8,12	2078	0,207738
9351-1	25,36	0,423	10	4,23	0,4	3,83	97	0,097294
9370-2	25,31	0,266	10	2,66	0,4	2,26	57	0,057298

2nd Extraction

9238-9	23,91	0,506	10	5,06	0,4	4,66	111	0,11161
9368-9	34,05	0,377	10	3,77	0,4	3,37	114	0,114944
9256-1	26,02	0,184	10	1,84	0,4	1,44	37	0,037533
9352-1	20,3	0,896	10	8,96	0,4	8,56	173	0,174064
9254-6	32,55	0,2	10	2	0,4	1,6	52	0,052169
9329-2	27,05	0,577	10	5,77	0,4	5,37	145	0,145506
9251-2	30,43	0,183	10	1,83	0,4	1,43	43	0,043589
9242-8	27,46	0,225	10	2,25	0,4	1,85	50	0,050888
9351-1	27,38	0,154	10	1,54	0,4	1,14	31	0,031266
9370-2	26,01	0,148	10	1,48	0,4	1,08	28	0,028139

3rd Extraction

9238-9	30,96	0,246	5	1,23	0,4	0,83	25	0,025741
9368-9	36,85	0,137	5	0,685	0,4	0,285	10	0,01052
9256-1	23,81	0,331	5	1,655	0,4	1,255	295	0,029932
9352-1	28,08	0,404	5	2,02	0,4	1,62	45	0,045567
9254-6	36,81	0,158	5	0,79	0,4	0,39	14	0,01438
9329-2	31,66	0,564	5	2,82	0,4	2,42	76	0,076748
9251-2	34,48	0,318	5	1,59	0,4	1,19	41	0,041101
9242-8	29,75	0,213	5	1,065	0,4	0,665	19	0,019817
9351-1	30,66	0,184	5	0,92	0,4	0,52	15	0,01597
9370-2	30,21	0,274	5	1,37	0,4	0,97	29	0,029354

Sodium

4th Extraction

Sample No	*m _{liquid} =NH ₄ Cl added mg/l	C ₂ mg /l	Dilution =d	C ₁ = d *C ₂ mg /l		C ₄ =C ₁ -C ₃		C ₃ * m _{liquid} C ₅ = ----- 998,3
9238-9	30,01	0,172	5	0,86	0,4	0,46	13	0,013828
9368-9	36,06	0,133	5	0,665	0,4	0,265	9	0,009572
9256-1	26,85	0,387	5	1,935	0,4	1,535	41	0,041285
9352-1	31,33	0,218	5	1,09	0,4	0,69	21	0,021655
9254-6	35,84	0,409	5	2,045	0,4	1,645	58	0,059057
9329-2	31,76	0,144	5	0,72	0,4	0,32	10	0,010181
9251-2	36,1	0,185	5	0,925	0,4	0,525	18	0,018985
9242-8	29,46	0,213	5	1,065	0,4	0,665	19	0,019624
9351-1	30,84	0,394	5	1,97	0,4	1,57	48	0,048501
9370-2	30,48	0,351	5	1,755	0,4	1,355	41	0,041371

5th Extraction

9238-9	27,47	0,41	5	2,05	0,4	1,65	45	0,045403
9368-9	35,96	0,338	5	1,69	0,4	1,29	46	0,046467
9256-1	32,04	0,399	5	1,995	0,4	1,595	51	0,051191
9352-1	30,59	0,416	5	2,08	0,4	1,68	51	0,051479
9254-6	34,14	0,317	5	1,585	0,4	1,185	40	0,040525
9329-2	32,28	1,17	5	0,86	0,4	0,46	14	0,014874
9251-2	33,96	0,172	5	5,85	0,4	5,45	185	0,185397
9242-8	29,42	0,208	5	1,04	0,4	0,64	18	0,018861
9351-1	31,09	0,168	5	0,84	0,4	0,44	13	0,013703
9370-2	31,7	0,351	5	1,755	0,4	1,355	42	0,043027

6th Extraction

9238-9	28,44	0,612	2	1,224	0,4	0,824	23	0,023474
9368-9	34,09	0,367	2	0,734	0,4	0,334	11	0,011405
9256-1	29,32	0,835	2	1,67	0,4	1,27	37	0,0373
9352-1	29,51	0,412	2	0,824	0,4	0,424	12	0,012534
9254-6	35,15	1,148	2	2,296	0,4	1,896	66	0,066758
9329-2	32,49	0,576	2	1,152	0,4	0,752	24	0,024474
9251-2	34,22	0,356	2	0,712	0,4	0,312	10	0,010695
9242-8	29,2	0,377	2	0,754	0,4	0,354	10	0,010354
9351-1	31,22	0,965	2	1,93	0,4	1,53	47	0,047848
9370-2	33,16	0,351	2	0,702	0,4	0,302	102	0,010031

Sodium

Sample No	Total mg of Na	atomic weight of Na	mg Na eq /m mol meq= ----- atomic weigh of Na	weight of sample in g	CEC per 100 g
9238-9	0,331609	22,98978	0,014424	3	0,472924
9368-9	0,23513	22,98978	0,010228	3	0,336434
9256-1	0,3109	22,98978	0,013523	3,02	0,446317
9352-1	0,343046	22,98978	0,014922	3,05	0,490845
9254-6	0,367119	22,98978	0,015969	3,07	0,527023
9329-2	0,819226	22,98978	0,035634	3,02	1,179946
9251-2	0,392369	22,98978	0,017067	3,04	0,531685
9242-8	0,307516	22,98978	0,013376	4,16	0,327047
9351-1	0,238644	22,98978	0,01038	3,11	0,304412
9370-2	0,179894	22,98978	0,007825	3,09	0,247625

Potassium

1st Extraction

Sample No	m _{liquid} = NaCl added mg/l	C ₂ mg /l	Dilution =d	C ₁ = d *C ₂ mg /l	C ₃ = contamination in NaCl	C ₄ =C ₁ -C ₃	C ₃ * m _{liquid}	m _{liquid} * C ₃ C ₅ = ----- 998,3
9238-9	26,14	1,176	50	58,8	1,122	57,678	1507	1,51027
9368-9	26,13	0,904	50	45,2	1,122	44,078	1151	1,153719
9256-1	26,12	2,128	50	106,4	1,122	105,278	2749	2,754544
9352-1	26	1,057	50	52,85	1,122	51,728	1344	1,347218
9254-6	25,95	1,946	50	97,3	1,122	96,178	2495	2,500069
9329-2	26,06	2,199	50	109,95	1,122	108,828	2836	2,840887
9251-2	26	2,134	50	106,7	1,122	105,578	2745	2,749702
9242-8	25,92	3,681	50	184,05	1,122	182,928	4741	4,749568
9351-1	25,96	1,711	50	85,55	1,122	84,428	2191	2,195483
9370-2	26,02	1,249	50	62,45	1,122	61,328	1595	1,598472

2nd Extraction

9238-9	25,43	1,825	10	18,25	1,122	17,128	435	0,436307
9368-9	25,68	1,03	10	10,3	1,122	9,178	235	0,236092
9256-1	30,48	1,617	10	16,17	1,122	15,048	458	0,459444
9352-1	23,29	1,144	10	11,44	1,122	10,318	240	0,240715
9254-6	25,18	1,655	10	16,55	1,122	15,428	388	0,389139
9329-2	24,92	2,326	10	23,26	1,122	22,138	551	0,552618
9251-2	24,78	3,519	10	35,19	1,122	34,068	842	0,845643
9242-8	25,15	1,564	10	15,64	1,122	14,518	365	0,365749
9351-1	25,46	1,192	10	11,92	1,122	10,798	274	0,275385
9370-2								

3rd Extraction

9238-9	38,27	0,546	10	5,46	1,122	4,338	166	0,166298
9368-9	31,79	0,385	10	3,85	1,122	2,728	86	0,086871
9256-1	37,09	0,641	10	6,41	1,122	5,288	196	0,196466
9352-1	30,97	0,47	10	4,7	1,122	3,578	110	0,110999
9254-6	31,2	0,671	10	6,71	1,122	5,588	174	0,174642
9329-2	35,72	0,879	10	8,79	1,122	7,668	273	0,274367
9251-2	37,26	0,559	10	5,59	1,122	4,468	166	0,166761
9242-8	31,25	0,9	10	9	1,122	7,878	246	0,246607
9351-1	33,96	0,575	10	5,75	1,122	4,628	157	0,157435
9370-2	34,07	0,459	10	4,59	1,122	3,468	118	0,118356

Potassium

4th Extraction

Sample No	$m_{\text{liquid}} = \text{NaCl added mg/l}$	C_2 mg /l	Dilution =d	$C_1 = d * C_2$ mg /l	$C_3 =$ contamination in NaCl	$C_4 = C_1 - C_3$	$C_3 * m_{\text{liquid}}$	$m_{\text{liquid}} * C_3$ $C_5 = \text{-----}$ 998,3
9238-9	37,83	0,697	5	3,485	1,122	2,363	89	0,089545
9368-9	30,1	0,441	5	2,205	1,122	1,083	32	0,032654
9256-1	37,47	1,375	5	6,875	1,122	5,753	215	0,215932
9352-1	29,63	0,7	5	3,5	1,122	2,378	70	0,07058
9254-6	35,13	0,79	5	3,95	1,122	2,828	99	0,099517
9329-2	36,81	0,647	5	3,235	1,122	2,113	77	0,077912
9251-2	31,1	2,423	5	12,115	1,122	10,993	341	0,342464
9242-8	32,1	0,71	5	3,55	1,122	2,428	77	0,078072
9351-1	33,51	0,528	5	2,64	1,122	1,518	50	0,050955
9370-2								

5th Extraction

9238-9	38,03	1,493	2	2,986	1,122	1,864	70	0,071009
9368-9	31,89	1,131	2	2,262	1,122	1,14	36	0,036417
9256-1	36,89	1,523	2	3,046	1,122	1,924	70	0,071097
9352-1	30,47	1,308	2	2,616	1,122	1,494	45	0,0456
9254-6	29,13	1,635	2	3,27	1,122	2,148	62	0,062678
9329-2	38,59	1,862	2	3,724	1,122	2,602	100	0,100582
9251-2	35,66	1,461	2	2,922	1,122	1,8	64	0,064297
9242-8	34,27	2,29	2	4,58	1,122	3,458	118	0,118707
9351-1	32,26	1,578	2	3,156	1,122	2,034	65	0,065729
9370-2	33,6	1,187	5	5,935	1,122	4,813	161	0,161992

6th Extraction

9238-9	36,49	0,845	2	1,69	1,122	0,568	20	0,020762
9368-9	27,63	0,819	2	1,638	1,122	0,516	14	0,014281
9256-1	35,01	0,909	2	1,818	1,122	0,696	24	0,024408
9352-1	27,66	0,803	2	1,606	1,122	0,484	13	0,01341
9254-6	28,99	0,997	2	1,994	1,122	0,872	25	0,025322
9329-2	35,83	1,121	2	2,242	1,122	1,12	40	0,040198
9251-2	34,35	0,459	2	0,918	1,122	-0,204	-7	0
9242-8	28,51	1,342	2	2,684	1,122	1,562	44	0,044608
9351-1	31,27	0,911	5	4,555	1,122	3,433	10	0,107533
9370-2	32,11	0,754	2	1,508	1,122	0,386	12	0,012416

Sample No	Total mg of K	atomic weight of K	mg K eq /m mol meq= ----- atomic weigh of K	weight of samples in g	CEC per 100 g
9238-9	2,250871	39,083	0,057592	3,05	1,888265
9368-9	1,611895	39,083	0,041243	3,04	1,356673
9256-1	3,678217	39,083	0,094113	3,03	3,106038
9352-1	1,725457	39,083	0,044149	3,04	1,452255
9254-6	3,194794	39,083	0,081744	3,03	2,697816
9329-2	3,864434	39,083	0,098878	3,02	3,274093
9251-2	3,740586	39,083	0,095709	3,21	2,981582
9242-8	1,529682	39,083	0,039139	4,09	0,956952
9351-1	2,938647	39,083	0,07519	3,41	2,204983
9370-2	2,072825	39,083	0,053036	3,16	1,67837

APPENDIX E

Core Conductivity and Porosity

5. CORE CONDUCTIVITY

The ten clean and dry samples, selected from Suite 5, were placed in a stainless steel saturation vessel and evacuated for a minimum of 15 hours. 150,000 ppm NaCl solution was introduced at the end of this period, followed by pressurisation at 2000 psig, to assist penetration. On completion of the saturation process, gravimetric checks were made to ensure complete saturation of the pore space had been achieved.

The saturated samples were placed in individual hydrostatic core holders in a controlled environment, at a constant temperature of 70°F and a net overburden pressure of 250 psig. When the conditions were established, the samples were subjected to the following test sequence:-

- (a) Each sample was flushed with 10 pore volumes of 150,000 ppm NaCl at a maximum flow rate of 1cc per minute.
- (b) The sample was allowed to reach an equilibrium over a 3 hour period and the sample's conductivity was measured.
- (c) The sample was returned to a container of 150,00 ppm NaCl brine, immersed and allowed to stand for 24 hours.
- (d) The conductivity of the sample was re-measured.
- (e) The above procedure was repeated until the conductivity of the sample had stabilised.
- (f) On reaching equilibrium, the 150,000 ppm NaCl brine was displaced by flushing the sample with 10 pore volumes of NaCl brine having a concentration of 100,000 ppm. The effluent was monitored to ensure the conductivity matched the value for the injector at the end of the flushing cycle.

- (g) The sample was allowed to reach an equilibrium value over a 3 hour period, prior to the measurement of its conductivity.
- (h) The sample was placed in a container of 100,000 ppm NaCl brine, immersed and allowed to stand for 24 hours.
- (i) The sample was removed, mounted in the core holder and flushed with 100,000 ppm NaCl brine for 10 pore volumes.
- (j) The conductivity of the sample was re-measured.
- (k) The procedure for the brine was repeated until the conductivity of the sample was $\pm 2-3\%$.
- (l) The procedure outlined above was repeated for the remaining NaCl concentrations of 50,000 ppm, 30,000 ppm, 20,000 ppm and 10,000 ppm.

The final conductivity values, with $B.Q_v$, $F.F.^*$, and m^* are presented in Tables 5.2 to 5.4 and Figures 5.1 to 5.10. The details of the brines used are presented in Table 5.1.

Note: The value of B was taken to be 3.75 Keelan, reference 1.

TABLE 5.2
CORE CONDUCTIVITY

JOB NO: 94079B

WELL: VALDEMAR-3

COMPANY: MAERSK

SAMPLE NUMBER	DEPTH (ft)	BRINE CONCENTRATION (ppm)	BRINE+ CONDUCTIVITY (Sm ⁻¹)	CORE+ CONDUCTIVITY (Sm ⁻¹)	BQv	Q++	FF*	Ø (%)	M*
1	9238.75	150000	17.921	1.973	-0.438	0.117	9.25	34.8	2.11
		100000	13.175	1.483					
		50000	7.236	0.848					
		30000	4.543	0.525					
		20000	3.130	0.389					
3	9242.67	150000	17.921	1.595	-0.472	0.126	11.42	30.6	2.06
		100000	13.175	1.210					
		50000	7.236	0.688					
		30000	4.543	0.442					
		20000	3.130	0.318					
8	9251.17	150000	17.921	1.700	-0.271	0.072	10.66	33.6	2.17
		100000	13.175	1.267					
		50000	7.236	0.706					
		30000	4.543	0.456					
		20000	3.130	0.318					
10	9254.50	150000	17.921	2.265	-0.281	0.075	7.91	36.2	2.03
		100000	13.175	1.739					
		50000	7.236	0.990					
		30000	4.543	0.610					
		20000	3.130	0.416					
		10000	1.664	0.224					

+ All measured at 70°F
++ Assuming a value for B of 3.75, reference 1



COREX

TABLE 5.3
CORE CONDUCTIVITY

COMPANY: MAERSK

WELL: VALDEMAR-3

JOB NO: 94079B

SAMPLE NUMBER	DEPTH (ft)	BRINE CONCENTRATION (ppm)	BRINE+ CONDUCTIVITY (Sm ⁻¹)	CORE+ CONDUCTIVITY (Sm ⁻¹)	BQv	Qv++	FF*	Ø (%)	M*
12	9256.83	150000	17.921	1.936	-0.196	0.052	9.36	35.9	2.18
		100000	13.175	1.428					
		50000	7.236	0.791					
		30000	4.543	0.511					
		20000	3.130	0.356					
14	9329.17	150000	17.921	1.866	-0.261	0.070	9.69	36.4	2.24
		100000	13.175	1.404					
		50000	7.236	0.775					
		30000	4.543	0.494					
		20000	3.130	0.350					
20	9351.08	150000	17.921	2.565	-0.187	0.050	7.06	42.1	2.26
		100000	13.175	1.881					
		50000	7.236	1.071					
		30000	4.543	0.674					
		20000	3.130	0.471					
21	9352.08	150000	17.921	2.531	-0.173	0.046	7.10	40.1	2.14
		100000	13.175	1.898					
		50000	7.236	1.051					
		30000	4.543	0.669					
		20000	3.130	0.464					
		10000	1.664	0.245					

+ All measured at 70°F
 ++ Assuming a value for B of 3.75, reference 1



TABLE 5.4

CORE CONDUCTIVITY

JOB NO: 94079B

WELL: VALDEMAR-3

COMPANY: MAERSK

SAMPLE NUMBER	DEPTH (ft)	BRINE CONCENTRATION (ppm)	BRINE+ CONDUCTIVITY (Sm ⁻¹)	CORE+ CONDUCTIVITY (Sm ⁻¹)	BQv	Qv++	FF*	Ø (%)	M*
25	9368.75	150000	17.921	2.708	-0.188	0.050	6.68	45.7	2.42
		100000	13.175	2.005					
		50000	7.236	1.119					
		30000	4.543	0.705					
		20000	3.130	0.501					
26	9370.17	150000	17.921	2.594	-0.499	0.133	7.05	46.1	2.52
		100000	13.175	1.948					
		50000	7.236	1.137					
		30000	4.543	0.704					
		20000	3.130	0.521					
		10000	1.664	0.281					

+ All measured at 70°F

++ Assuming a value for B of 3.75, reference 1

COREX (UK) LTD

FIGURE 5.1

CORE CONDUCTIVITY

COMPANY: MAERSK

JOB NO: 94079B

WELL: VALDEMAR-3

SAMPLE: 1

DEPTH: 9238.75 ft

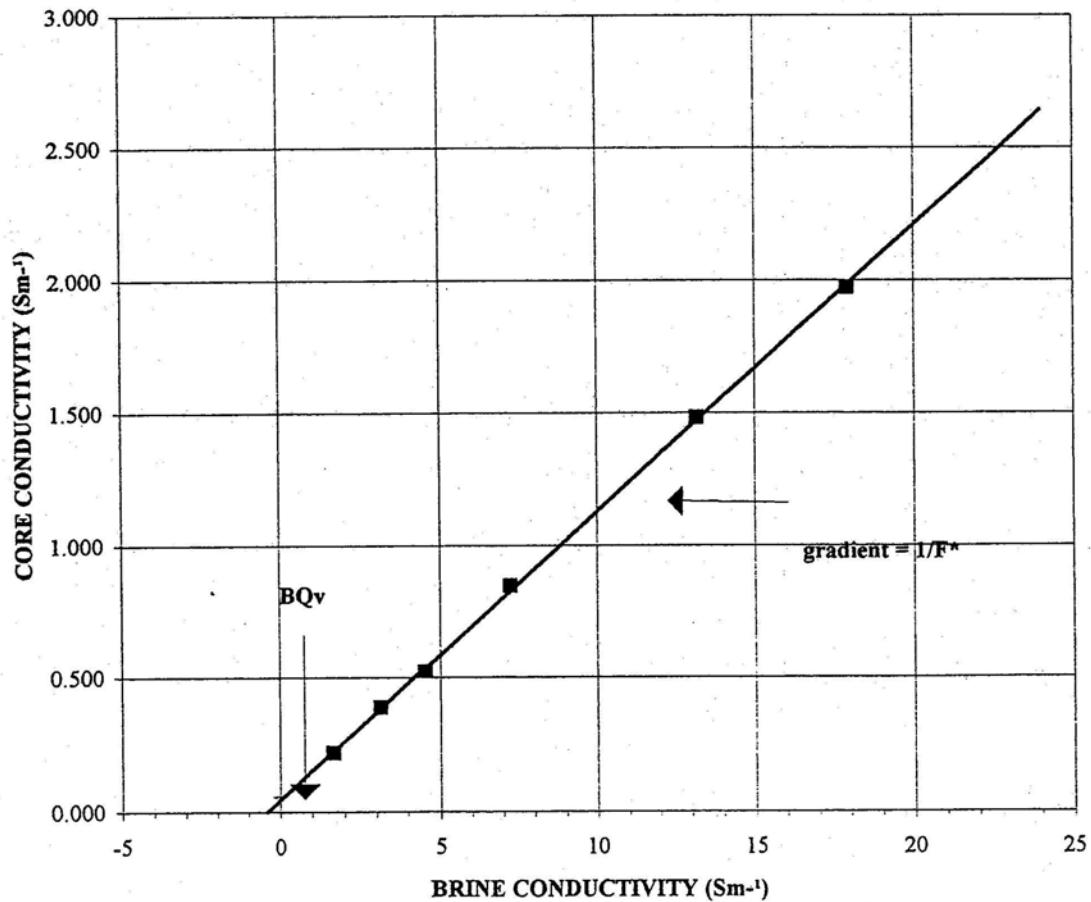
GAS PERMEABILITY: 0.382 mD

POROSITY: 34.8 %

BOv: -0.438

BRINE CONCENTRATION (ppm)	BRINE CONDUCTIVITY C_w ($S\text{m}^{-1}$)	CORE CONDUCTIVITY C_w ($S\text{m}^{-1}$)
150000	17.921	1.973
100000	13.175	1.483
50000	7.236	0.848
30000	4.543	0.525
20000	3.130	0.389
10000	1.664	0.221

Co/Cw PLOT



COREX (UK) LTD

FIGURE 5.2

CORE CONDUCTIVITY

COMPANY: MAERSK

JOB NO: 94079B

WELL: VALDEMAR-3

SAMPLE: 3

DEPTH: 9242.67 ft

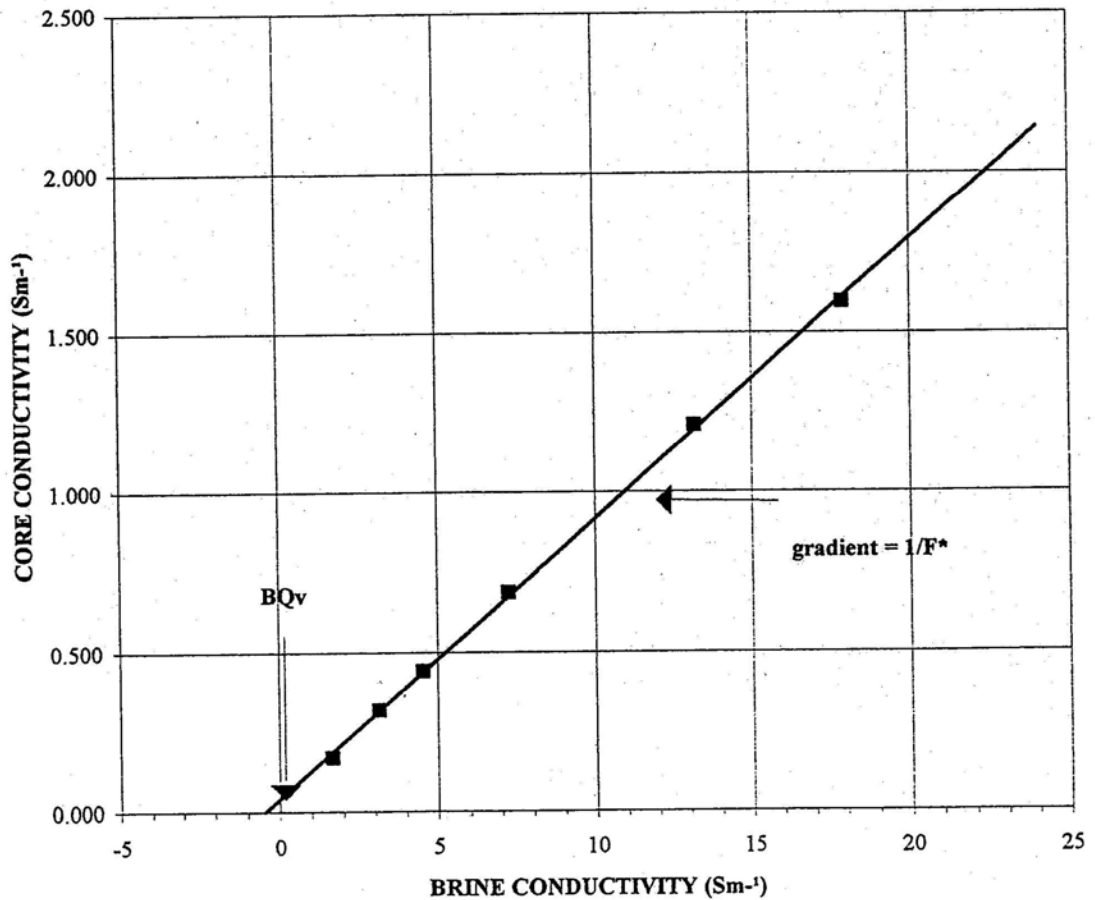
GAS PERMEABILITY: 0.222 mD

POROSITY: 30.6 %

BQv: -0.472

BRINE CONCENTRATION (ppm)	BRINE CONDUCTIVITY Cw (Sm ⁻¹)	CORE CONDUCTIVITY Cw (Sm ⁻¹)
150000	17.921	1.595
100000	13.175	1.210
50000	7.236	0.688
30000	4.543	0.442
20000	3.130	0.318
10000	1.664	0.170

Co/Cw PLOT



COREX (UK) LTD

FIGURE 5.3

CORE CONDUCTIVITY

COMPANY: MAERSK

JOB NO: 94079B

WELL: VALDEMAR-3

SAMPLE: 8

DEPTH: 9251.17 ft

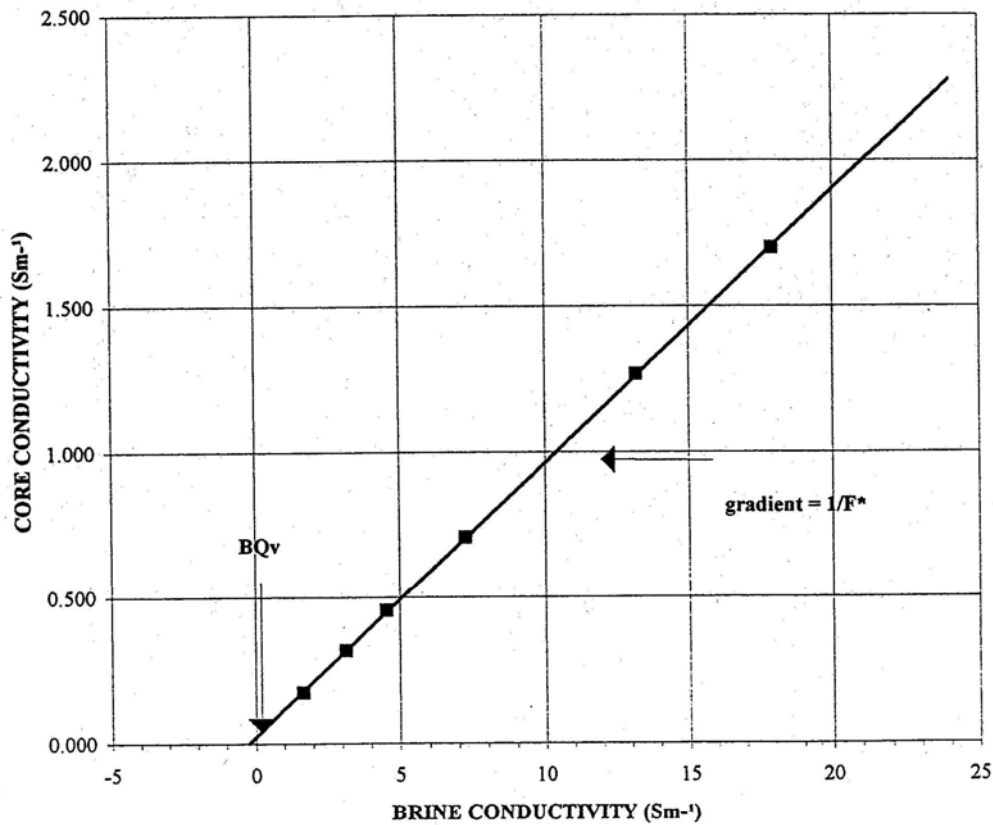
GAS PERMEABILITY: 0.335 mD

POROSITY: 33.6 %

BOv: -0.271

BRINE CONCENTRATION (ppm)	BRINE CONDUCTIVITY C_w ($S\text{m}^{-1}$)	CORE CONDUCTIVITY C_w ($S\text{m}^{-1}$)
150000	17.921	1.700
100000	13.175	1.267
50000	7.236	0.706
30000	4.543	0.456
20000	3.130	0.318
10000	1.664	0.175

Co/Cw PLOT



COREX (UK) LTD

FIGURE 5.4

CORE CONDUCTIVITY

COMPANY: MAERSK

JOB NO: 94079B

WELL: VALDEMAR-3

SAMPLE: 10

DEPTH: 9254.50 ft

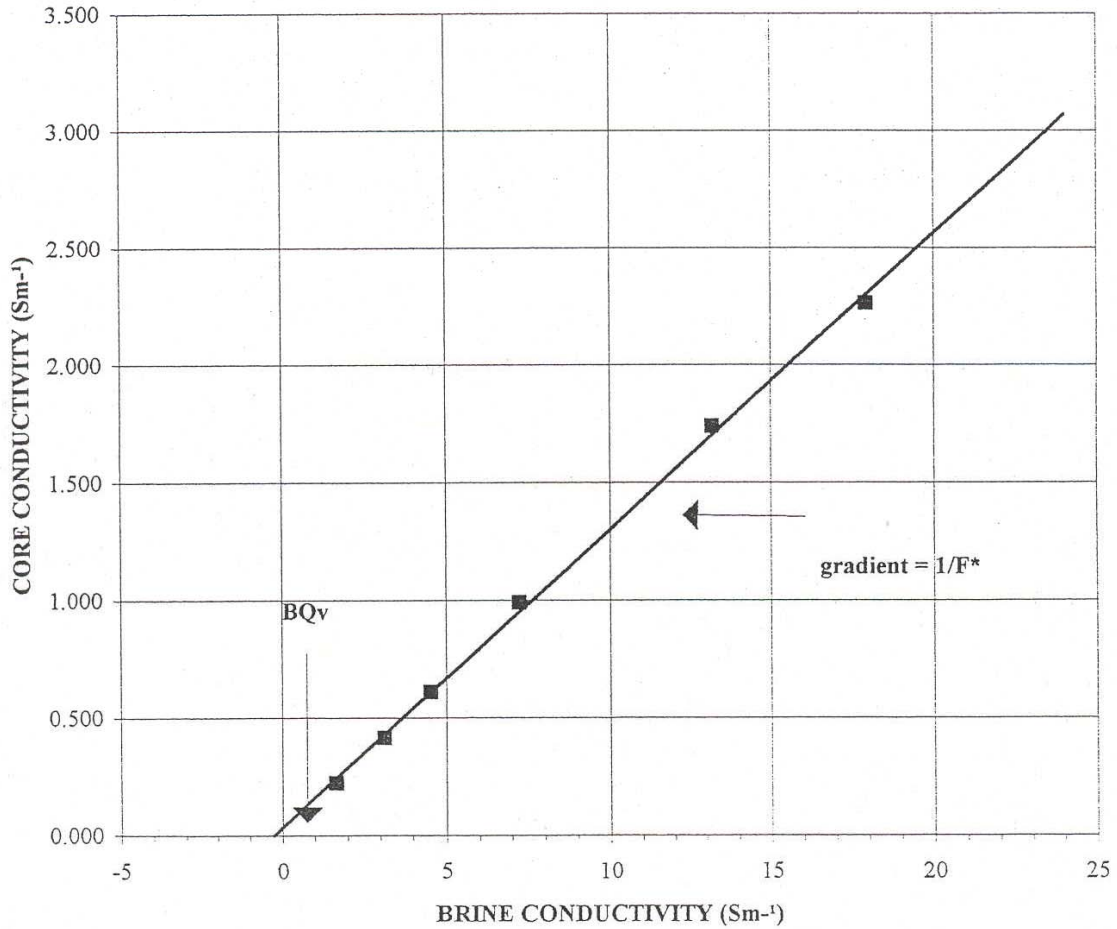
GAS PERMEABILITY: 0.544 mD

POROSITY: 36.2 %

BQv: -0.281

BRINE CONCENTRATION (ppm)	BRINE CONDUCTIVITY C_w ($S\text{m}^{-1}$)	CORE CONDUCTIVITY C_w ($S\text{m}^{-1}$)
150000	17.921	2.265
100000	13.175	1.739
50000	7.236	0.990
30000	4.543	0.610
20000	3.130	0.416
10000	1.664	0.224

Co/Cw PLOT



COREX (UK) LTD

FIGURE 5.5

CORE CONDUCTIVITY

COMPANY: MAERSK

JOB NO: 94079B

WELL: VALDEMAR-3

SAMPLE: 12

DEPTH: 9256.83 ft

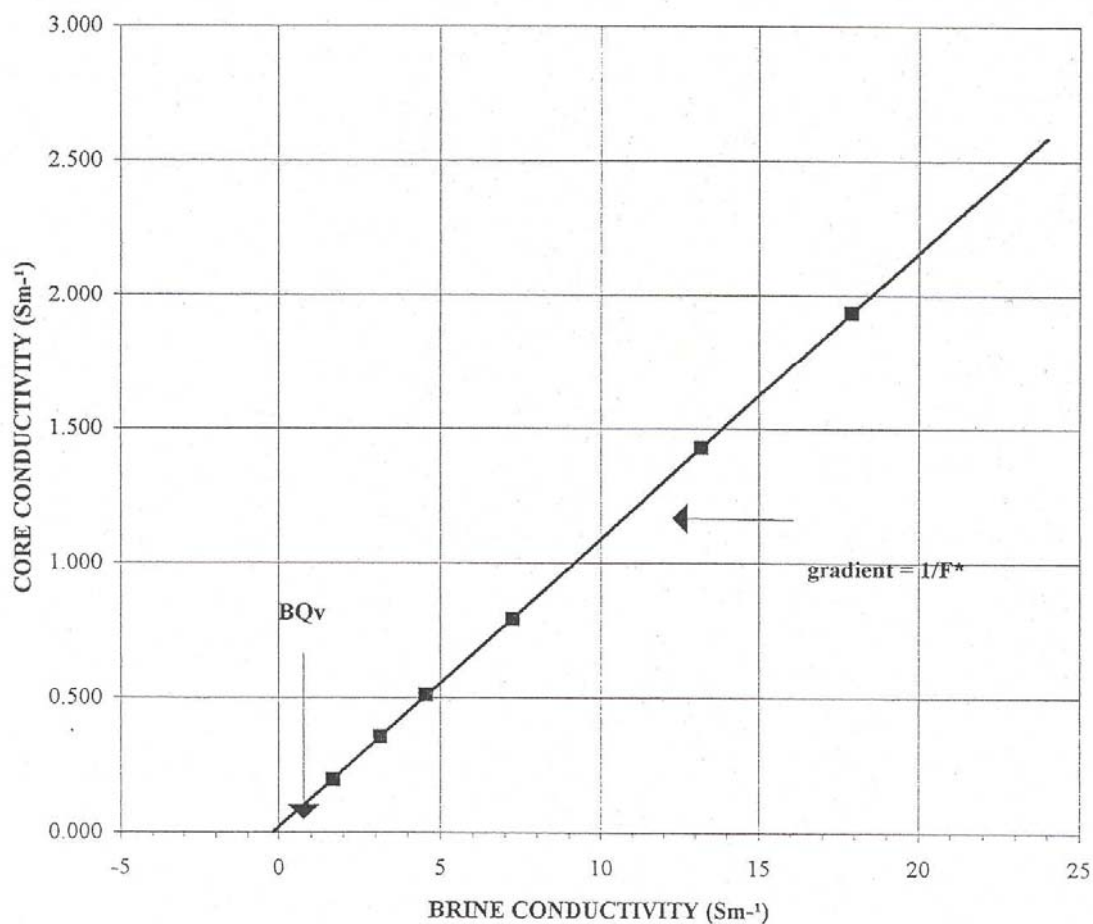
GAS PERMEABILITY: 0.344 mD

POROSITY: 35.9 %

BQv: -0.196

BRINE CONCENTRATION (ppm)	BRINE CONDUCTIVITY C_w ($S\text{m}^{-1}$)	CORE CONDUCTIVITY C_c ($S\text{m}^{-1}$)
150000	17.921	1.936
100000	13.175	1.428
50000	7.236	0.791
30000	4.543	0.511
20000	3.130	0.356
10000	1.664	0.197

Co/Cw PLOT



COREX (UK) LTD

FIGURE 5.6

CORE CONDUCTIVITY

COMPANY: MAERSK

JOB NO: 94079B

WELL: VALDEMAR-3

SAMPLE: 14

DEPTH: 9329.17 ft

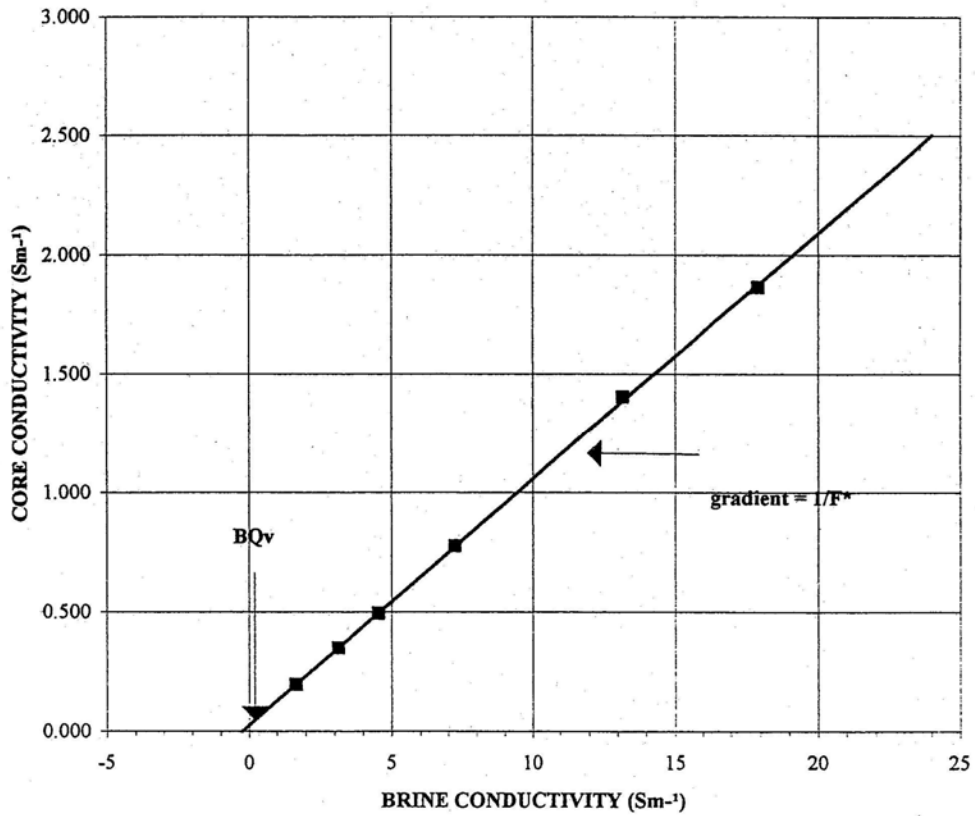
GAS PERMEABILITY: 0.351 mD

POROSITY: 36.4 %

BQv: -0.261

BRINE CONCENTRATION (ppm)	BRINE CONDUCTIVITY C_w ($S\text{m}^{-1}$)	CORE CONDUCTIVITY C_o ($S\text{m}^{-1}$)
150000	17.921	1.866
100000	13.175	1.404
50000	7.236	0.775
30000	4.543	0.494
20000	3.130	0.350
10000	1.664	0.196

Co/Cw PLOT



COREX (UK) LTD

FIGURE 5.7

CORE CONDUCTIVITY

COMPANY: MAERSK

JOB NO: 94079B

WELL: VALDEMAR-3

SAMPLE: 20

DEPTH: 9351.08 ft

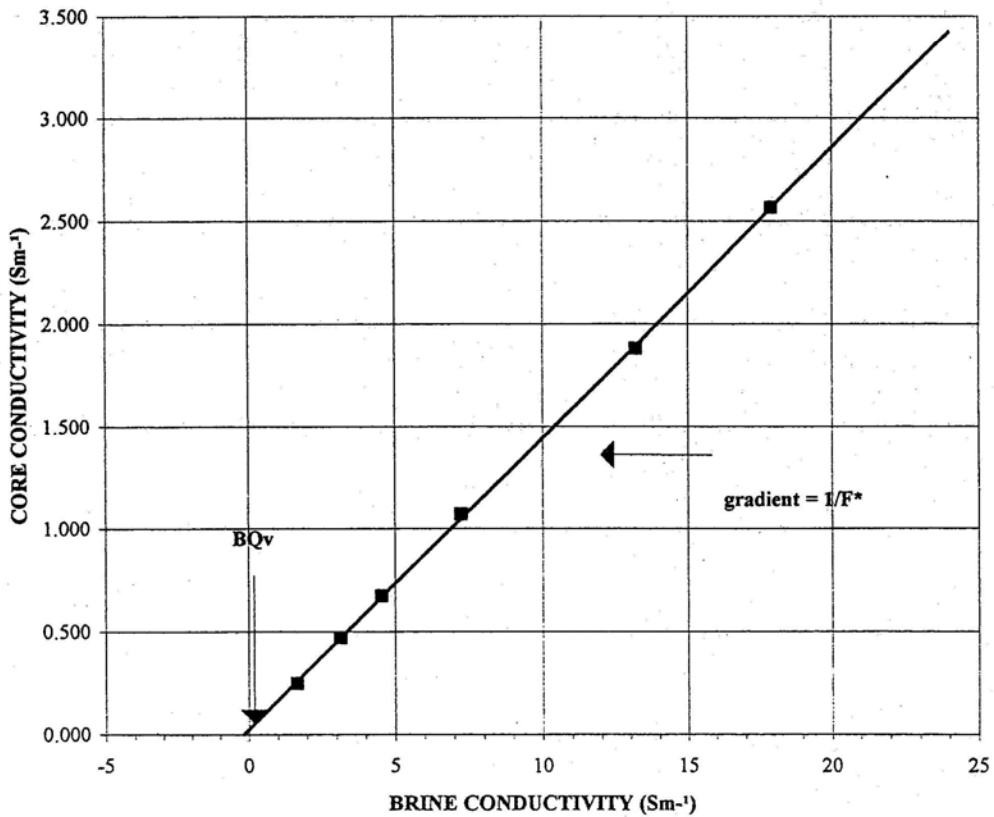
GAS PERMEABILITY: 0.970 mD

POROSITY: 42.1 %

BQv: -0.187

BRINE CONCENTRATION (ppm)	BRINE CONDUCTIVITY C_w ($S\text{m}^{-1}$)	CORE CONDUCTIVITY C_o ($S\text{m}^{-1}$)
150000	17.921	2.565
100000	13.175	1.881
50000	7.236	1.071
30000	4.543	0.674
20000	3.130	0.471
10000	1.664	0.248

Co/Cw PLOT



COREX (UK) LTD

FIGURE 5.8

CORE CONDUCTIVITY

COMPANY: MAERSK

JOB NO: 94079B

WELL: VALDEMAR-3

SAMPLE: 21

DEPTH: 9352.08 ft

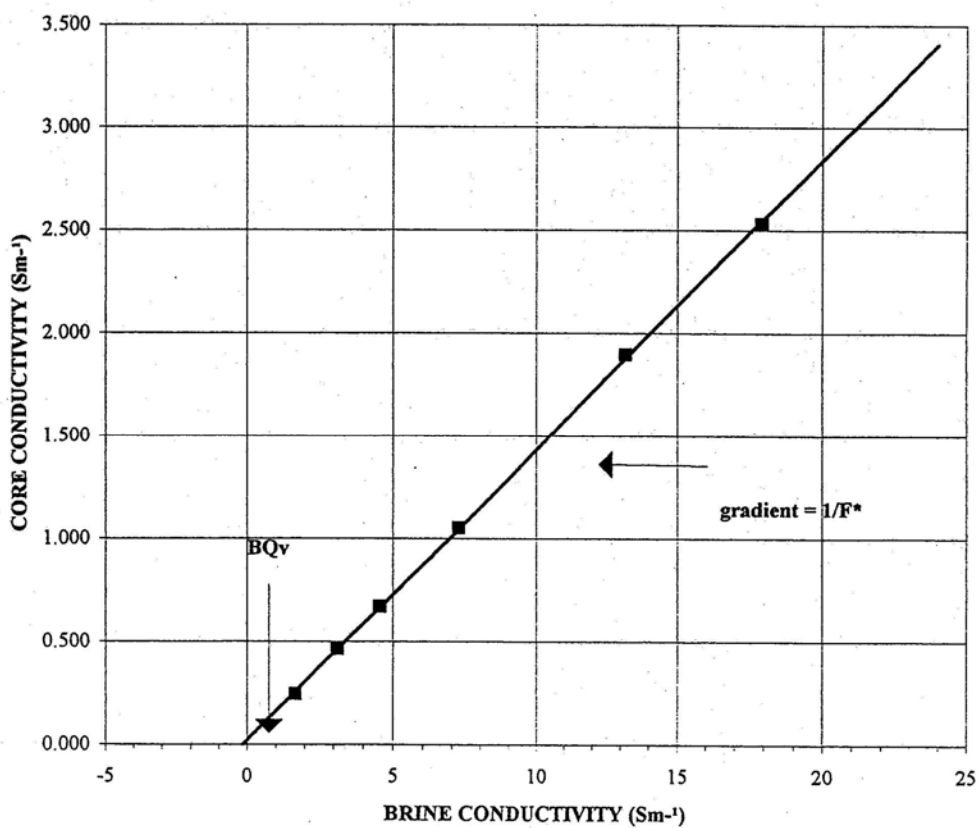
GAS PERMEABILITY: 1.16 mD

POROSITY: 40.1 %

BQv: -0.173

BRINE CONCENTRATION (ppm)	BRINE CONDUCTIVITY C_w ($S\text{m}^{-1}$)	CORE CONDUCTIVITY C_c ($S\text{m}^{-1}$)
150000	17.921	2.531
100000	13.175	1.898
50000	7.236	1.051
30000	4.543	0.669
20000	3.130	0.464
10000	1.664	0.245

Co/Cw PLOT



COREX (UK) LTD

FIGURE 5.9

CORE CONDUCTIVITY

COMPANY: MAERSK

JOB NO: 94079B

WELL: VALDEMAR-3

SAMPLE: 25

DEPTH: 9368.75 ft

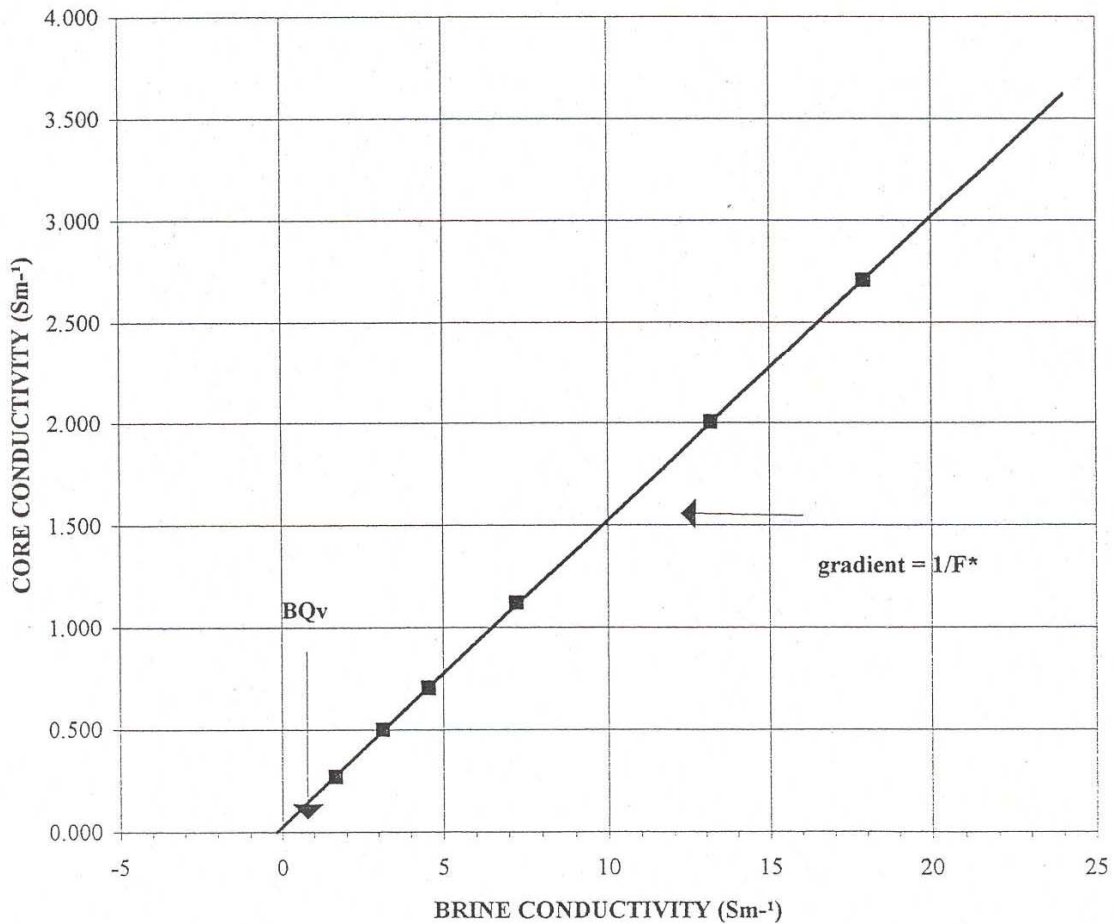
GAS PERMEABILITY: 1.93 mD

POROSITY: 45.7 %

BQv: -0.188

BRINE CONCENTRATION (ppm)	BRINE CONDUCTIVITY C_w ($S\text{m}^{-1}$)	CORE CONDUCTIVITY C_o ($S\text{m}^{-1}$)
150000	17.921	2.708
100000	13.175	2.005
50000	7.236	1.119
30000	4.543	0.705
20000	3.130	0.501
10000	1.664	0.271

Co/Cw PLOT



COREX (UK) LTD

FIGURE 5.10

CORE CONDUCTIVITY

COMPANY: MAERSK

JOB NO: 94079B

WELL: VALDEMAR-3

SAMPLE: 26

DEPTH: 9370.17 ft

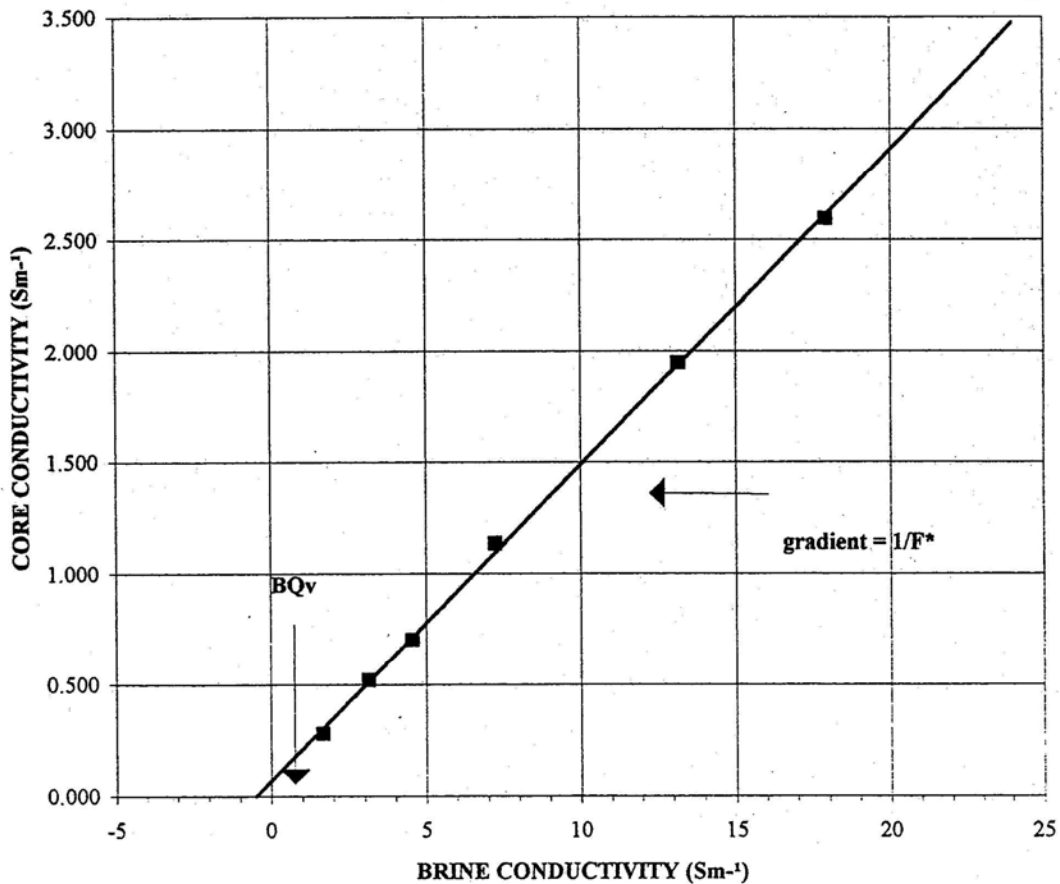
GAS PERMEABILITY: - mD

POROSITY: 46.1 %

BOv: -0.499

BRINE CONCENTRATION (ppm)	BRINE CONDUCTIVITY C_w ($S\text{m}^{-1}$)	CORE CONDUCTIVITY C_c ($S\text{m}^{-1}$)
150000	17.921	2.594
100000	13.175	1.948
50000	7.236	1.137
30000	4.543	0.704
20000	3.130	0.521
10000	1.664	0.281

Co/Cw PLOT



COREX**TABLE 6****CATION EXCHANGE CAPACITY****COMPANY:** MAERSK**JOB NO:** 94079B**WELL:** VALDEMAR-3

SAMPLE Number	DEPTH (ft)	GAS PERMEABILITY (mD)	POROSITY (%)	GRAIN DENSITY (g/cc)	CATION EXCHANGE CAPACITY	
					(MEQ/100g)	MEQ/ccP.V.
1	9238.75	0.382	34.8	2.690	1.696	0.085
4	9244.17	1.64	26.8	2.722	3.713	0.276
8	9251.17	0.335	33.5	2.689	1.352	0.072
10	9254.50	0.544	36.2	2.682	1.587	0.075
12	9256.83	0.344	35.9	2.697	1.487	0.072
14	9329.17	0.351	36.4	2.688	1.391	0.065
20	9351.08	0.970	42.1	2.698	0.661	0.025
21	9352.08	1.16	40.1	2.703	1.039	0.042
25	9368.75	1.93	45.7	2.675	0.509	0.016
26	9370.17	-	46.1	2.671	2.822	0.088

- No measurement possible

APPENDIX F

Miscellaneous

DUAL WATER MODELS

The dual water models were developed as practical solution of Waxman and Smits saturation relationship. The dual water is based on three premises.

1. The conductivity of clay is due to its CEC.
2. The CEC of pure clay is proportional to the specific surface area of clay.
3. In saline solutions, the anions are excluded from a layer of water around the surface of grain.

The thickness of layer expands as the salinity of solution (below a certain limit) decreases as shown in fig below, and the thickness is function of salinity and temperature.

Therefore, since CEC is proportional to specific area (area per unit weight), it is proportional to volume of water in the counter ion exclusion layer per unit weight of clay. Consequently, the conductivity of clay is proportional to the volume of counter ion exclusion layer, this layer being "bound" to the surface of clay grains. For clays, this very thin sheet of bound water is important to sand grains (several magnitudes greater).

Therefore in dual water model, clay is model as consisting of two components bound water and clay minerals.

The clay minerals are modelled as being electrical inert; the clay electrical conductivity is modelled as being derived from the conductivity of bound water, C_{wb} . C_{wb} is assumed to be independent of clay type (from the second postulate above). The amount of bound water varies according to clay type, being higher for finer clays (with higher specific surface area), such as montmorillonite, and lower coarse clays, such as kaolinite. Salinity also has an effect; in low salinity waters (roughly < 200,000 ppm NaCl) the diffuse layer expands.

The bound water is immovable under normal conditions; volume it occupies cannot be displaced by hydrocarbons. Since the clay minerals (dry colloids) are considered electrical inert, they may be treated just as other minerals. Schematically, shaly formations are modelled with dual model as illustrated in Table.

Table: Dual Water Model

Solids				Fluids	
Matrix	Silt	Dry Clay	Bound Water	Free Water	Hydrocarbons
Matrix	Shale			Effective Porosity	
				Total porosity	

For most rocks (except for conductivity minerals such as pyrite, which can not be treated in this way) only the porous part need to be considered when discussing electrical properties, and it is treated according to Archie water saturation equation: The equation become as:

$$C_t = \frac{\phi_t^m S_{wt}^n}{a} C_{we}$$

Where

a, m, and n have usual Archie connotations,

C_t is the conductivity of non-invaded, virgin formation,

And C_{we} is the equivalent conductivity of water in the pore space.

Note that Φ_t and S_{wt} refer to total pore volume; this includes the pore volume saturated with bound water and formation connate water (some time called the free water). The equivalent water conductivity, C_{we} , is

$$C_{we} = \frac{V_w C_w + V_{wb} C_{wb}}{V_w + V_{wb}}$$

Where V_w and V_{wb} are the bulk volume of formation water and bound water, respectively, and C_w and C_{wb} are their conductivities.

In term of saturation, above equation becomes as:

$$C_{we} = \frac{\phi_t (S_{wt} - S_{wb}) C_w + \phi_t S_{wb} C_{wb}}{\phi_t (S_{wt} - S_{wb}) + \phi_t S_{wb}}$$

Or

$$C_{we} = C_w + \left(\frac{S_{wb}}{S_{wt}} \right) (C_{wb} - C_w)$$

Where S_{wb} is bound water saturation (i.e., the fraction of total pore volume occupied by the bound water).

Equation describes the equivalent water saturation as function of formation water conductivity plus the bound water conductivity and saturation equation become as:

$$C_t = \frac{\phi_t^m S_{wt}^n}{a} \left[C_w + \left(\frac{S_{wb}}{S_{wt}} \right) (C_{wb} - C_w) \right]$$

The porosity and water saturation of sand (clean formation) phase (that is of non clay phase) of formation is obtained by subtracting the bulk-volume fraction of bound water ($\Phi_t S_{wb}$).

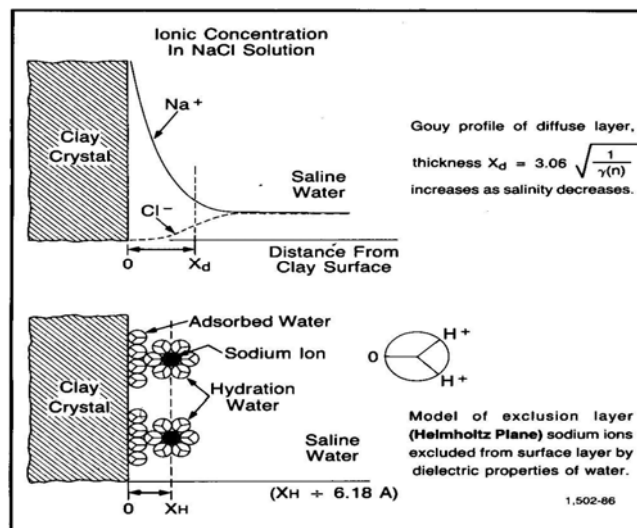


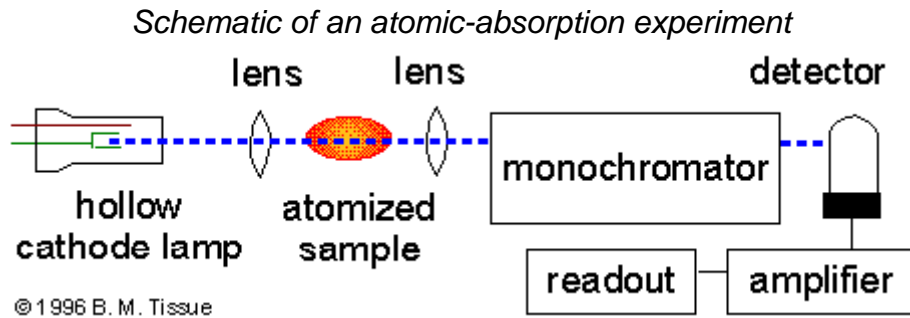
Fig: shows Different Model of diffuse layer.

Atomic Spectroscopy

Atomic absorption spectroscopy is based on the measurement of absorption of resonance radiation by free atoms in the gaseous state, i.e., of spectral lines corresponding to transition of atoms between the ground and excited states. Flame emission spectroscopy is special area of emission spectroscopy in which a flame is used to excite the atoms.

Flame Emission or Absorption

In flame emission or absorption spectroscopy, the sample, which is to be analyzed, usually an element concentration in the sample is vaporized by an air-acetylene flame which will turn the aerosol sample into atoms in the ground state. Some atoms will be excited above the ground state energy, those are minimal. Then a beam of radiant energy, a frequency which is that of some element in question, will pass through the flame and cause some of ground state atoms to absorb energy and will create the electrons of a characteristic wavelength or resonance lines. The analyte concentration is determined from the amount of absorption. Concentration measurements are usually determined from a working curve after calibrating the instrument with standards of known concentration.



Valdemar Field

Valdemar is one of 17 oil and gas fields of Denmark located in North Sea.

Review of geology

The Valdemar Field consists of a northern reservoir called North Jens and a southern reservoir called Bo, which are both anticlinal chalk structures associated with tectonic uplift.

Valdemar comprises several separate reservoirs. Oil and gas have been discovered in Danian/Upper Cretaceous chalk, and vast amounts of oil in place have been identified in Lower Cretaceous chalk. While the properties of the Upper Cretaceous reservoirs are comparable to other Danish fields like Gorm and Tyra, the Lower Cretaceous chalk possesses very difficult production properties due to its extremely low permeability. Production from the field is based on primary recovery.

Production strategy

The development of a recovery technique based on drilling long horizontal wells with numerous sand-filled, artificial fractures has made it possible to exploit the Lower Cretaceous reservoir commercially. In addition, recovery takes place from Danian/Upper Cretaceous layers.

Production facilities

The Valdemar Field (the North Jens reservoir) has been developed as a satellite to Tyra, including an unmanned production platform of the STAR type. The production is transported to Tyra East for processing and export.

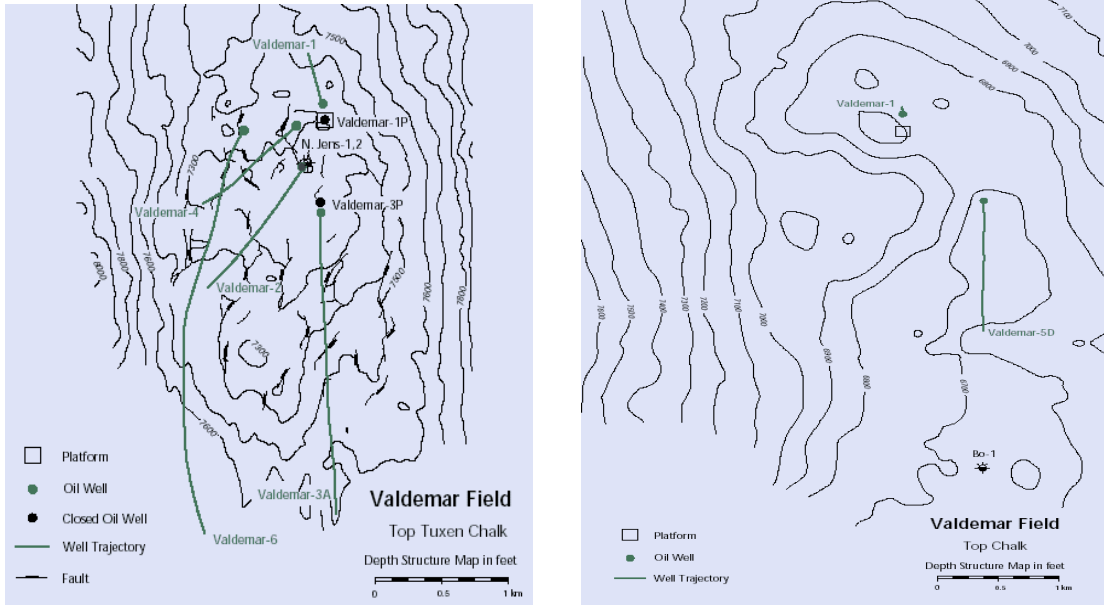


Fig: Map of Valdemar field

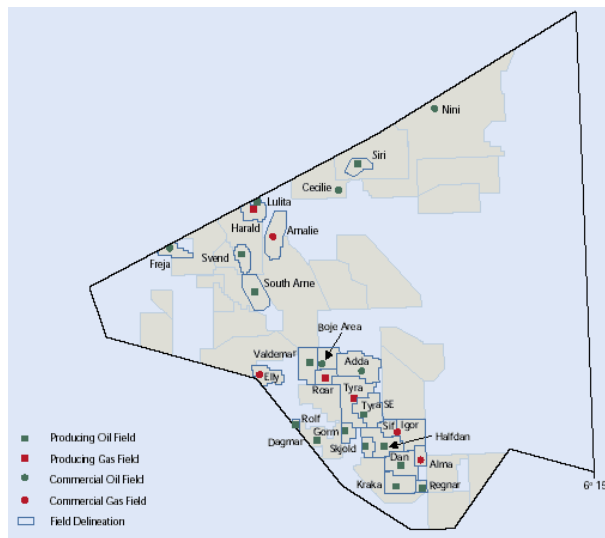


Fig shows Map of Danish Oil and Gas fields